Review

Arsenic Removal by Adsorbents from Water for Small Communities' Decentralized Systems: Performance, Characterization, and Effective Parameters

Roya Sadat Neisan [1], Noori M. Cata Saady [1,*], Carlos Bazan [2], Sohrab Zendehboudi [3], Abbas Al-nayili [4], Bassim Abbassi [5] and Pritha Chatterjee [6]

1   Faculty of Engineering and Applied Science, Memorial University, St. John's, NL A1B 3X5, Canada
2   Faculty of Business Administration, Memorial University, St. John's, NL A1B 3X5, Canada
3   Department of Process Engineering, Memorial University, St. John's, NL A1B 3X5, Canada
4   Chemistry Department, College of Education, University of Al-Qadisiyah, Al Diwaniyah 58001, Iraq
5   College of Engineering and Physical Sciences, School of Engineering, University of Guelph, Guelph, ON N1G 2W1, Canada
6   Department of Civil Engineering, Indian Institute of Technology Hyderabad, Kandi 502285, India
*   Correspondence: nsaady@mun.ca; Tel.: +1-709-864-6087

Abstract: Arsenic (As), a poisonous and carcinogenic heavy metal, affects human health and the environment. Numerous technologies can remove As from drinking water. Adsorption is the most appealing option for decentralized water treatment systems (DWTS) for small communities and household applications because it is reliable, affordable, and environmentally acceptable. Sustainable low-cost adsorbents make adsorption more appealing for DWTS to address some of the small communities' water-related issues. This review contains in-depth information on the classification and toxicity of As species and different treatment options, including ion exchange, membrane technologies, coagulation-flocculation, oxidation, and adsorption, and their effectiveness under various process parameters. Specifically, different kinetic and isotherm models were compared for As adsorption. The characterization techniques that determine various adsorbents' chemical and physical characteristics were investigated. This review discusses the parameters that impact adsorption, such as solution pH, temperature, initial As concentration, adsorbent dosage, and contact time. Finally, low-cost adsorbents application for the removal of As was discussed. Adsorption was found to be a suitable, cost-effective, and reliable technology for DWTS for small and isolated communities. New locally developed and low-cost adsorbents are promising and could support sustainable adsorption applications.

Keywords: heavy metal removal; water treatment; low-cost adsorbents; arsenic adsorption; ion-exchange; membrane technologies; coagulation-flocculation; oxidation

1. Introduction

Heavy metals such as arsenic, copper, cadmium, nickel, mercury, cobalt, lead, and chromium are a group of metals with specific densities over 5 g cm^{-3} [1]. They are widely used in industrial, agricultural, domestic, and technological applications. The most significant environmental pollution of heavy metals is from metal-based industries such as mining and metal casting [2].

Heavy metals, which are extremely soluble in water and non-degradable, occur as free ions or are bound in chemical compounds in surface and groundwater. Dissolved heavy metals can interfere with microbial processes and impair aquatic life [3]. Organisms consume heavy metals and incorporate them into the food chain, where they accumulate and impose detrimental effects on health. Short overexposure and chronic exposure to heavy metals can impair vital organs and neurological systems and kill the organism [4]. Typically, arsenic (As), cadmium (Cd), chromium (Cr), and nickel (Ni) are carcinogenic.

They cause the mutation, deletion, or oxidative damage of deoxyribonucleic acid (DNA) [2]. Figure 1 depicts a simple schematic of the consequences of exposure to heavy metals.
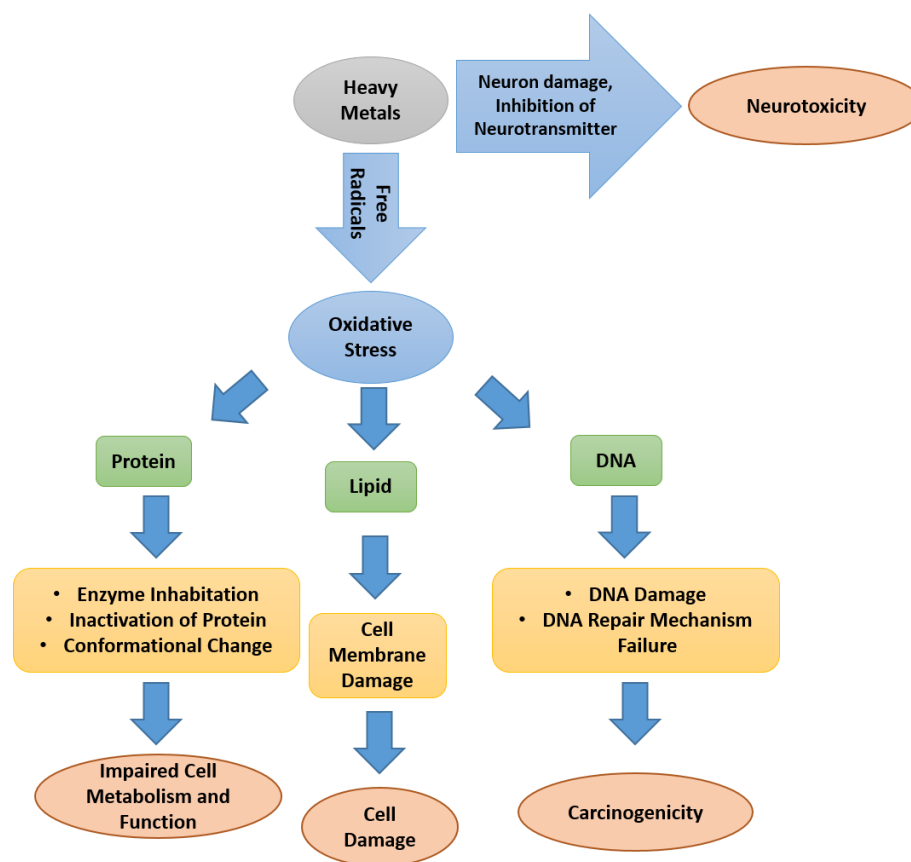
Figure 1. Toxicity mechanisms of heavy metals (modified from [3]).

Heavy metals in drinking water come from either natural geological sources or industrial activities [4]. The application of various standard methods, including chemical precipitation, evaporation, ion exchange, electrolysis, and reverse osmosis, has been investigated to remove heavy metals from drinking water. However, the search continues for cheaper, more efficient, and environmentally friendly methods [5].

1.1. Arsenic, A Toxic Metal

Among the heavy metals, As is toxic and carcinogenic; thus, its inhalation and ingestion pose a cancer risk. Arsenic poses maximum adverse effects on human health through As-contaminated drinking water and the environment since As is a significant groundwater pollutant [6]. The World Health Organization (WHO) set the maximum allowable level of arsenic in drinking water at 10 ppb. Arsenic contamination in groundwater affects roughly 108 countries, with concentrations exceeding 10 ppb. About 32 countries in Asia, 31 in Europe, 20 in Africa, and 20 in North and South America suffer from As pollution. Arsenic poisoning threatens more than 230 million people worldwide [7]. Figure 2 shows the global extent of As contamination. Due to the poor water quality in rural areas, people living in small, rural, and remote communities suffer from health problems and diseases caused by dangerous pollutants such as As [8]. Even at low concentrations, exposure to As increases the risk of cardiovascular disease and stroke [9–11]. In addition, As exposure can cause hypertension [9], and As in drinking water can also cause liver damage and skin cancer [12,13].
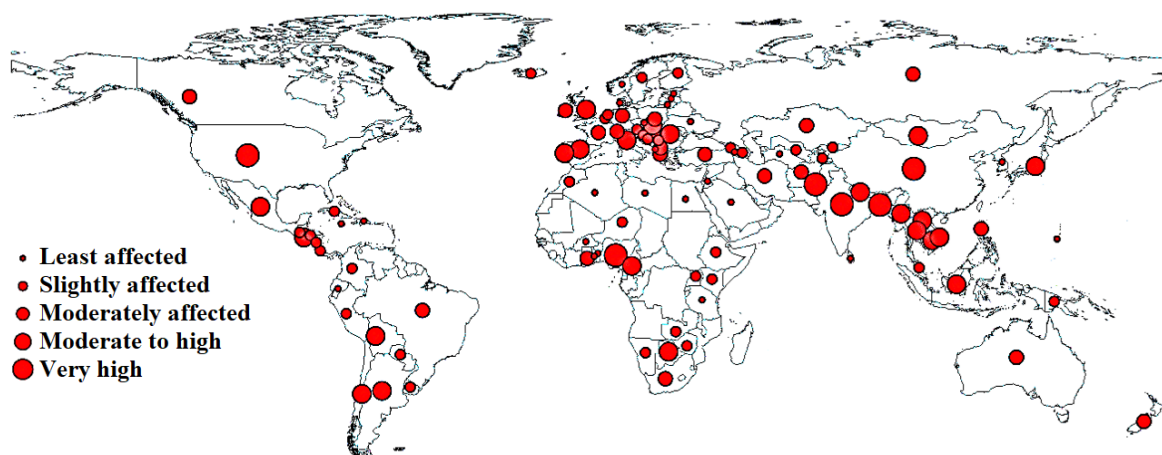
Figure 2. The global extent of arsenic contamination (modified from [7]).

1.1.1. Arsenic Occurrence

Arsenic concentrations increase in surface and groundwater because of mine and refinery wastes, wastewater sludge, agrochemicals, ceramic industries, and coal fly ash [14]. Weathering, erosion of rocks/soils, and volcanic emissions are all natural sources of As in aqueous systems. Naturally, arsenic exists in about 200 different mineral forms. The percentages of these forms are 60% as arsenates, 20% as sulfides and sulfosalts, and 20% as arsenide, arsenite, oxides, silicates and elemental arsenic [6]. Arsenic is found in water in inorganic (arsenite, arsenate) and organic (methyl and dimethyl arsenic compounds) forms [15]. Table 1 provides the most common As species in the environment.

Table 1. The most common arsenic species in the environment (adapted from [16]).

Name	Chemical Formula
Arsenous acid (arsenite)	H_3AsO_3
Arsenic acid (arsenate)	H_3AsO_4
Monomethylarsenic acid	$CH_3AsO(OH)_2$
Dimethylarsinic acid	$(CH_3)_2AsO(OH)$
Trimethylarsine oxide	$(CH_3)_2AsO$
Trimethylarsoniopropionate	$(CH_3)_3As^+CH_2CH_2COO^-$
Arsenobetaine	$(CH_3)_3As^+CH_2COOH^-$
Arsenocholine	$(CH_3)_3As^+CH_2CH_2OH^-$
Dimethylarsinyolacetic acid	$(CH_3)_2AsOCH_2COOH$
Phenylarsine oxide	C_6H_5AsO
Phenylarsonic acid	$C_6H_5AsO(OH)_2$

Dissolved As usually has an oxidation state of +III (arsenite) and +V (arsenate). Removing As(V) is easier than removing As(III) because As(III) has to be oxidized to As(V) in the early stage of the removal process [17].

1.1.2. Arsenic Structure

As is listed as the 33rd element on the periodic table and belongs to Group 15 (the nitrogen family). It has an atomic mass of 74.92 and an atomic number of 33. Arsenic-75 (75As) has 33 protons and 42 neutrons inside its nucleus; 33 electrons in various energy shells surround the nucleus. Arsenic-75 is the most stable and non-radioactive isotope of As. With an empty p orbital available for electron occupation and five valence electrons allowing As to engage in chemical bonding, the electronic configuration of the stable As form can be represented as $1s^22s^22p^63s^23p^63d^{10}4s^24p^3$ [18].

The electrons contained in the first, second and third shells of arsenic atom are 2, 8, and 18, respectively, and only five electrons occupy the fourth shell. Arsenic has four

common redox states: 3, 0, +3, and +5. Placing three more electrons in the p orbital brings the total number of electrons in this orbital up to six and creates an oxidation state of 3. The elemental arsenic forms a trigonal pyramidal structure by sharing three electrons in the 4p orbital equally with the three arsenic atoms around it [18,19].

Arsenic has a higher electronegativity than nitrogen and is similar to phosphorus. Compared to nitrogen and phosphorus, As has a greater oxidation potential, allowing it to easily show the +3 and +5 oxidation states. These variable oxidation states allow As to form covalent compounds with various elements, but in nature, it most frequently bonds to oxygen and sulfur. By sharing its valence electrons, As can display ligands characteristics and occupy electrons in bonding and antibonding orbitals. Thus, arsenic can change from an electropositive to an electronegative state (metal arsenides). It can react with methyl groups to create organic molecules in both oxidation states. Monomethylarsonic acid (MMA) and dimethylarsinic acid are two typical organic forms of As (DMA). However, compared to inorganic forms, they are less common in nature [18,20].

1.1.3. Arsenic Oxidation and Reduction

Redox potential and pH levels significantly impact the oxidation and reduction of As. When naturally occurring in water sources, As is primarily present as the oxyanions of trivalent arsenite or pentavalent arsenate [18]. An Eh-pH diagram can explain the effects of complexes, temperature, pressure, potential, and pH. The system is assumed to be in equilibrium with water, or the three components of water (H (+1), O (-2), and e (-1)), in all Eh-pH diagrams. Each of the areas in the diagrams shows a species that predominates there. While pH indicates the activity of the hydrogen ion (H+), Eh shows the electrical potential relative to the standard hydrogen potential (SHE). The thermodynamically stable water region is usually represented by two diagonal dashed lines [21].

In the system of As-O-H at 25°C and 1 bar, Figure 3 shows the dominance of As species. As(III), As(V), arsenious acids (H_3AsO_3, $H_2AsO_3^-$, and $HAsO_3^{-2}$), and As acids (H_3AsO_4, $H_2AsO_4^-$, $HAsO_4^{-2}$) are the main forms of As discovered in environmental samples. As behaves anionically in aquatic systems. Arsenate predominates under oxidizing conditions, either as the $H_2AsO_4^-$ at low pH (less than about 6.9) or as the $HAsO_4^{-2}$ at higher pH levels. At pH levels lower than about 9.2, the uncharged arsenite species H_3AsO_3 dominates in reducing conditions. As can exist as pentavalent oxyanions (arsenate) at moderate or high redox potentials (E0 (V)= 0.56 V at 25°C). These include H_3AsO_4, $H_2AsO_4^-$, $HAsO_4^{-2}$, and AsO_4^{-3} [22,23]. Below (Equations (1)–(6)) are the dissociation reactions of H_3AsO_4 and H_3AsO_3, as well as the associated equilibrium constants [18].

Arsenite (As(III))

$$H_3AsO_3 \leftrightarrow H_2AsO_3^- + H^+ \; pKa : 2.24 \tag{1}$$

$$H_2AsO_3^- \leftrightarrow HAsO_3^{-2} + H^+ \; pKa : 6.69 \tag{2}$$

$$HAsO_3^{-2} \leftrightarrow AsO_3^{-2} + H^+ \; pKa : 11.5 \tag{3}$$

Arsenate (As(V))

$$H_3AsO_4 \leftrightarrow H_2AsO_4^- + H^+ \quad pKa : 9.2 \tag{4}$$

$$H_3AsO_4^- \leftrightarrow HAsO_4^{-2} + H^+ \quad pKa : 12.1 \tag{5}$$

$$HAsO_4^{-2} \leftrightarrow AsO_4^{-3} + H^+ \quad pKa : 13.4 \tag{6}$$
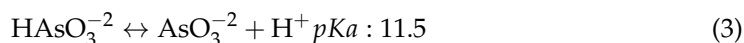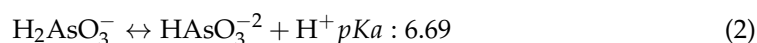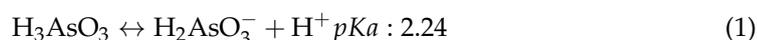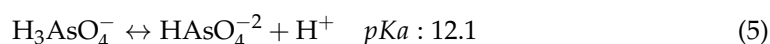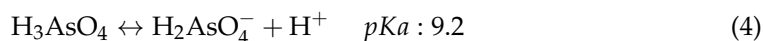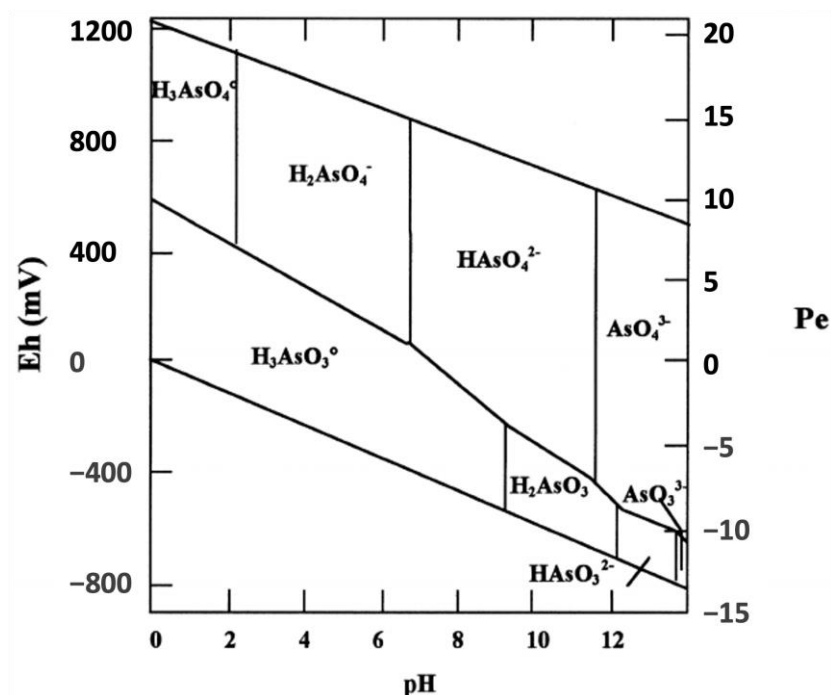
Figure 3. Eh−H diagram for aqueous arsenic species at 25 °C. (reprinted from [15] with Elsevier permission).

1.1.4. Arsenic Treatment

Adsorption, coagulation-flocculation, ion exchange, electrochemical reduction, and membrane filtration technologies are currently available to remove As. Adsorption is frequently employed because, in comparison to the alternatives, it is more affordable and easier to implement in small, rural, and remote communities, and has higher efficiency. Adsorption is defined as the adhesion of ions or molecules to the surface of solid substances (the adsorbents) [24].

Many of the conventional adsorbents such as activated carbon, activated alumina, and iron oxide-based adsorbents are economically infeasible for small communities, particularly in developing countries. Hence, locally available natural adsorptive materials provide sustainable and affordable options for removing As pollution in developing countries and rural areas [24].

Adsorption is one of the most efficient and economical methods to eliminate As from a water-based solution [25,26]. The price of the adsorbent affects how much the procedure costs. [26]. Some common As adsorbents are hydrous titanium dioxide (TiO_2) [27], iron oxides/hydroxides [28], synthetic zeolites [29], activated carbon, and activated alumina [30]. Biomass, wastes, and industrial by-products are also used for As removal. Due to the toxicity of As, researchers are working to develop more rapid and cost-effective adsorbents compared to the current adsorbents. The development of nanoparticle-based adsorbents is attracting great attention because they offer a large surface area and a high tendency to adsorb As from water [31]. Metals and metal oxides, e.g., gold [32], titanium oxide [27], cupric oxide [33], iron oxide [28], impregnated granulated activated carbon [34], and synthetic nanostructured Fe(III)–Cr(III) mixed oxides [35] have been used in As removal in different studies.

Recently, scientists have concentrated on converting waste materials into adsorbents for heavy metal removal from water because such adsorbents are low-cost and effective. However, there is still a need to develop low-cost, high-efficiency, and eco-friendly adsorbents targeting As removal based on material availability in different locations [36].

The primary goal of this work is to discuss the widely used options for removing As from drinking water and provide an appropriate starting point for new researchers who want to compare traditional heavy metal removal techniques. Despite its significance as a toxic water contaminant, few comprehensive reviews concentrate on removing As. Particularly, the number of review papers focusing on As removal in decentralized systems is very limited. This review paper aims to provide an overview of the recent development of decentralized drinking water treatment technologies and evaluate the feasibility of various methods, especially adsorption for small treatment systems. In the following sections, As removal methods (with a focus on adsorption) in decentralized water treatment systems and the most common adsorbents are explained and discussed, and their removal efficiencies are evaluated. Finally, several low-cost adsorbents are introduced as cost-effective substitutes for expensive ones.

2. Conventional Methods for Arsenic Removal from Aqueous Solutions in Decentralized Systems Other Than Adsorption

One of the problems facing community water treatment systems worldwide is the removal of pollutants, particularly pathogens and heavy metals, to provide clean drinking water; these pollutants put the local residents' health in danger [37]. The contamination of groundwater has been reported in both developed (Canada, Japan, and USA) and underdeveloped (Bangladesh, China, and India) nations [38]. Centralized water treatment plants have been essential to managing water supplies in highly populated areas. In centralized water treatment, reasonably high-quality water from various natural sources is treated before water is distributed and used. In contrast, in decentralized water management systems, water from local sources is collected and treated on a small scale (community level) or using a household filtration system [39,40].

The current centralized water treatment facilities cannot provide safe drinking water to millions worldwide [41]. Some areas of developing countries do not have water infrastructure or reliable water sources. In developed countries, centralized systems face several difficulties, such as reaching their capacities due to population growth, excessive energy and water use due to the aging infrastructure, and downstream re-contamination [42]. Decentralized water treatment is a suitable solution for households in rural and remote areas where the central water treatment system is unavailable, or in times of emergency, such as epidemic disease. A decentralized water system may also be more affordable due to the lower maintenance and transmission costs [43]. Various treatment methods, such as ion exchange, membrane technologies, and coagulation, are available in decentralized systems. Still, these methods' applications in small communities are limited because they usually require skilled operators, complicated maintenance, high-cost chemicals, and timely procedures [44].

The market for decentralized water treatment was USD 21.45 billion in 2020 and was projected to increase at a compound annual growth rate (CAGR) of 10.70% from 2020 to 2026, reaching USD 39.48 billion [45]. Figure 4 demonstrates a detailed segmentation of the decentralized system industry. Household filtration units (including point-of-entry (POE) and point-of-use (POU) systems) and community filtration units are two main approaches to providing clean water for communities and rural areas (Figure 5) [46]. Point-of-entry (POE) systems are installed at the location where the water enters the building and is constantly treated for the entire house. In contrast, the point-of-use (POU) systems are installed before a single outlet, such as a kitchen sink tap, to eliminate impurities in drinking water [47]. Small-scale systems or community filtration units are smaller in size than centralized systems but larger than POU or POE systems. Typically, small-scale systems treat the water used by several households or a community [48].
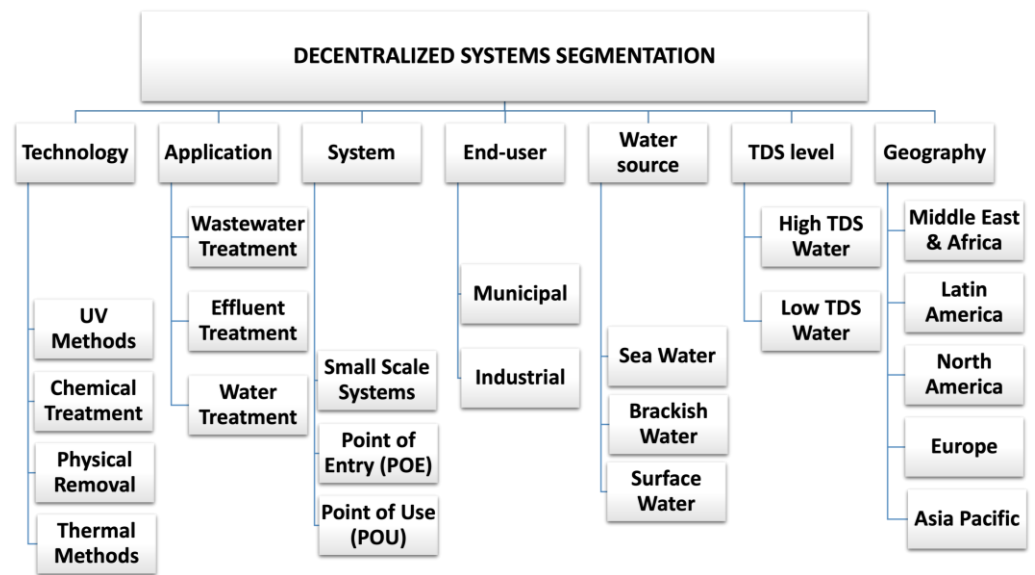
Figure 4. Detailed segmentation of decentralized treatment systems [45]. TDS: totals dissolved solids.
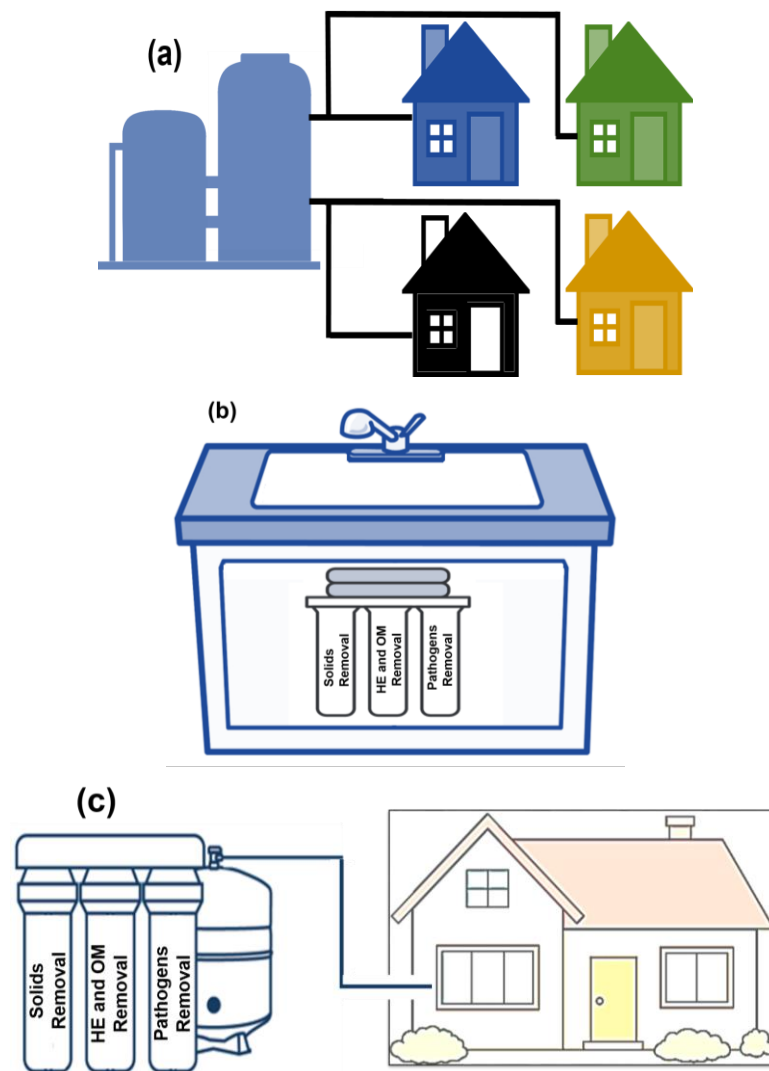
Figure 5. (**a**) Small-scale (community) water treatment system, (**b**) Point-of-use (POU) system, and (**c**) Point-of-entry (POE) system. HE: heavy metals; OM: organic matter.

2.1. Ion Exchange

Ion exchange is a chemical reaction that removes dissolved metal ions from the solution and replaces them with other similarly charged ions [49]. It has been used for a long time to soften and demineralize water and eliminate nitrate and other water treatments [50]. Figure 6 shows the schematic of calcium ion exchange (water softening) and resin regeneration.

(**a**) (**b**)
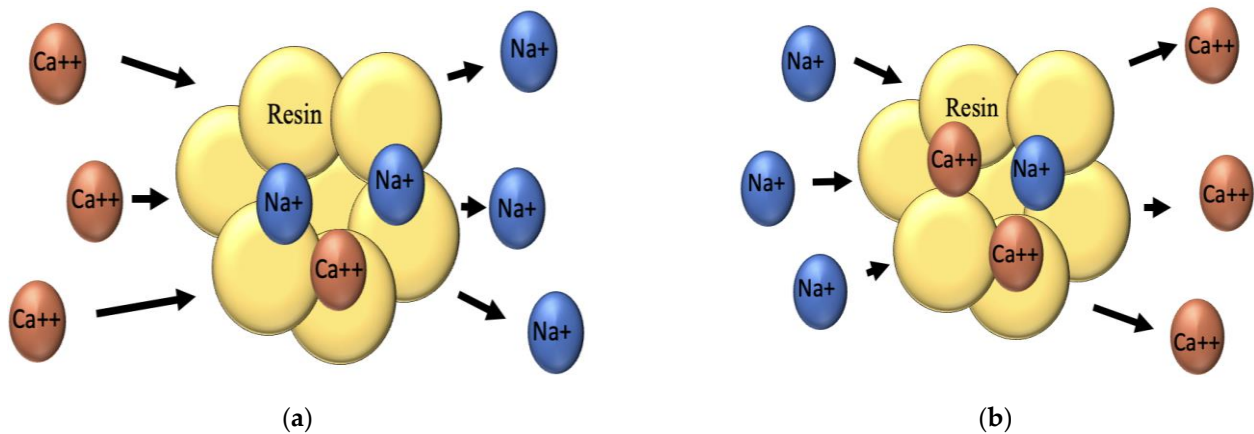
Figure 6. (**a**) Schematic of the ion-exchange process and (**b**) resin regeneration.

For As species removal, strongly basic ion exchangers are commonly used [51]. The arsenic-chloride ion-exchange reaction is as follows (EPA 2000). Where R = matrix, overbarred symbols refer to the exchanger phase. At the exchange sites, the chloride ions are replaced by As ions; thus, the exiting water contains a higher concentration of chloride and a lower concentration of As than the input water.

$$\overline{R - [N(CH_3)_3]^+ Cl^-} + H_2AsO_4^- \rightleftarrows \overline{R - [N(CH_3)_3]^+ H_2AsO_4^-} + Cl^- \tag{7}$$
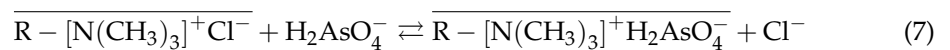
when As occupies all or a significant portion of the exchange sites, resin exhaustion occurs and should be regenerated [52]. The ion-exchange resin is regenerated using methanol or other organic solvents, an inorganic salt such as sodium chloride, a base such as sodium hydroxide, or a mix of different regenerants [53]. Ion exchange removes As species though sulfate, and to some extent nitrate anions impose significant interference. To remove arsenate species efficiently, sulfate concentrations cannot exceed 50 mg L^{-1} if filter throughputs of 750 bed-volumes between successive regenerations can be obtained; otherwise, the treatment cost-effectiveness is jeopardized because the service cycles become too short [54].

Ion exchange is not efficient for As(III) removal because it exists mostly as an uncharged ion (H$_3$AsO$_3$) in water at a pH below 9.0 [55]. Thus, As(III) must first be oxidized to As(V) prior to being removed by resin [56]. Water passes through one or more ion-exchange resin beds to remove As. Arsenate ions and a few other anions, such as sulfate, and follows the preference order for exchange; therefore, competing ions, such as total dissolved solids (TDS) and sulfate, strongly affect the efficiency of the ion-exchange process for As removal. Table 2 represents the effectiveness of various resins for As exchange under different conditions. The performance of the ion exchange depends on other process parameters such as empty bed contact time and spent brine. Various ions compete for available ion-exchange sites and can significantly impact and reduce the efficiency and economic viability of ion-exchange systems [57].

Table 2. Operating conditions and efficiencies of different resins used to remove arsenic.

Resin Material	As Concentration (mg L^{-1})	Regeneration	Removal Efficiency (RE; %) and Adsorption Capacity (AC; mg g^{-1} Resin)	Process Conditions	Ref.
Hybridized ion-exchange fibers containing dispersed hydrated ferric oxide (HFO) nanoparticles	0.1	2% NaOH + 2% NaCl In <40 bed volumes, As recovery >98%	AC: 5	pH: 4–8.5 Competing ions: Na$^+$ = 100 ppm SO$_4{}^{2-}$ = 5 ppm HCO$_3{}^-$ = 100 ppm	[58]
Polymer–clay nanocomposite ion-exchange resin based on N-methyl-D-glucamine ligand groups	60		AC: 55 (Max retention at pH 3.5–6.0, 25 °C, 24 h)	30 mg nanocomposite resin+ 5 mL As solution pH: 2–12	[59]
N-methyl-D-glucamine functionalized resins revealing gel (1JW) Expanded gel (2JW) Epidermal-like structure (2PTN	0.176		RE: 35.8 RE: 28.8 RE: 22.4	Flow rate: 5 mL min^{-1} Resin concentration: 1JW, 2 PTN: 4 g L^{-1}, 2 JW: 2 g L^{-1}	[60]
Ion-exchange fiber with amino groups (RPFA-I)	5	0.1 M NaOH + 200 mg fiber +100 mL As solution	RE: As(III): 70 RE: As(V): 93	pH: 4–12 T:25 °C	[61]
Amine-doped acrylic ion-exchange fiber	10	0.1 N HCl, 0.1 N NaOH, and ultra-pure water sequentially	RE: 83 AC: 205	pH: 3.04 T: 25 °C	[62]
Amberlite IR-400 (polystyrene DVB strong base anionic exchange resin	5–15		RE: 91–99.28	pH: 3–10 Resin dose: 100–800 mg L^{-1} Voltage: 5–20 V	[63]

Typically, the background ion concentration dictates the applicability of the ion-exchange procedure at a specific condition. For strong base anion (SBA) resins, the selectivity order is $SO_4 > NO_3 > HAsO_4 > NO_2$, $Cl > H_2AsO_4$, $HCO_3 >> Si(OH)4$, H_3AsO_4 [64]. Therefore, high sulfate and TDS levels can significantly reduce As removal efficiency [64]. When the water contains Fe(III), it forms Fe(III)-As complexes, which affect the As removal because ion-exchange resins cannot remove Fe(III)-As complexes [57]. At high sulfate concentrations, a resin bed may release previously adsorbed As(V), increasing the As concentrations in the effluent compared to the feed water. This phenomenon, which can be dangerous when toxic ions are involved, is called chromatographic peaking (dumping). To avoid this phenomenon, the resin bed should be monitored and regenerated before the onset of the peaking [57].

Ion exchange is a scalable technique used in centralized and decentralized water treatment systems, such as household treatment units [65]. However, its applicability in decentralized systems is significantly constrained due to the frequent regeneration needed [66]. Since cost is the main factor in waste management, choosing brine treatment methods depends on their technical ability and the implementation strategy, including whether they use centralized or decentralized systems [67]. Finding cheap, available, and harmless materials to use as ion exchangers is crucial to improve this technology because the high cost of operation and disposal of the toxic regeneration sludge are among the problems facing this method. Although a resin can be reused after regeneration, it must be replaced after several years [68,69]. Installing an ion-exchange system is often determined by the price of regeneration salt and waste brine disposal. For instance, regenerant salt accounted for 77% of operating costs in an As system. Capital costs could become more affordable by centralizing brine treatment even in decentralized systems [67]. In other words, a decentralized system's household cartridges can be regularly sent to a centralized regeneration facility and replaced [70]. A hazardous waste brine produced by the ion-exchange process is too saline to be released into surface water, even if the heavy metal concentration is very low in the inlet. The waste brine heavy metals levels exceed the allowable limits. As a result, waste management improvements are required to make the ion exchange an affordable and environmentally friendly method for small communities [67].

A research study showed that cations and anions in the solutions slow down heavy metals removal [71]. Due to their electrical structure, transition metals can form stable complexes with charged substances such as NH_4^+, inorganic anions, and water molecules, which typically give their solutions colors. The high stability of the complexes made of SO_4^{2-} and HPO_4^{2-} in the solution caused the poor removal of Cr^{3+}, Cu^{2+}, and Fe^{3+}. These complexes may also precipitate on resin pores and surfaces and clog them, reducing the resin's capacity for ion exchange [71,72].

2.2. Membrane Technologies

Membrane technologies are pressure-driven processes where membranes selectively allow the particles (atoms and ions) to cross them. In this case, the membrane allows water to pass through the filter and retains heavy metals. These technologies are categorized into four main groups (Figure 7): microfiltration, ultrafiltration, nanofiltration, and reverse osmosis based on particle size. Table 3 reports the results of different membranes for As removal under specific conditions. As in Table 3, the removal effectiveness depends on the type of membrane, the solute, and how those two interact. The temperature, pH, pressure, and concentration influence the rejection. The advantage of this method is that the membrane eliminates As and some dissolved minerals or even pathogenic microorganisms [73]. Another benefit of membrane technologies is that since membranes do not accumulate impurities, chemical usage is limited to cleaning them [74].
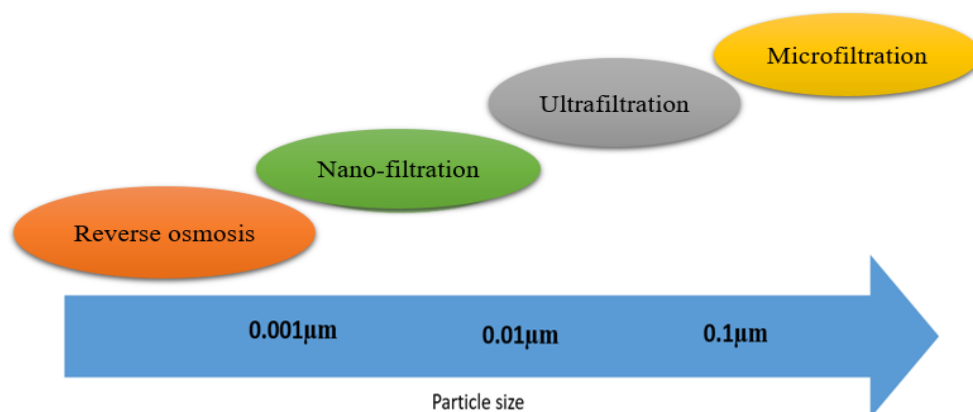
Figure 7. Applicability ranges of different membranes based on pore sizes.

Reverse osmosis (RO), ultrafiltration (UF), or microfiltration (MF) are possible options for decentralized membrane systems [75]. The most common membrane types in decentralized systems are the RO systems, mostly used to desalinate water, while MF and UF membranes are designed for disinfection. However, most membrane-based small-scale systems fail to meet all the evaluation criteria, such as performance, ease of use, and low cost [76].

Membrane-based water treatment plants are among the most efficient and clean technologies; however, they have high construction and operation costs and need high-tech maintenance and operation procedures [69]. Membrane fouling and scaling are still obstacles preventing the widespread industrial utilization of membranes. Effective pre-treatment and cleaning techniques are crucial for managing this issue [77]. There are two types of membrane cleaning: physical cleaning and chemical cleaning. The physical cleaning of membrane surfaces eliminates loosely attached substances and is typically referred to as reversible fouling. In contrast, chemical cleaning removes resistant compounds and is frequently referred to as irreversible fouling [78]. Although chemical methods are more effective, they may harm membranes [79].

2.3. Coagulation-Flocculation

Coagulation-flocculation is another standard method for As removal from water. Although these processes are sometimes used interchangeably, they are two different processes [80]. In the coagulation process, a coagulant is added to destabilize the colloid particles to start aggregation by neutralizing their charges (Figure 8) and thus the electrostatic repulsive forces [81]. Cationic coagulants lessen the negative electric charge of the colloids by providing positive charges to destabilize the non-settleable particles. Then, gentle (slow) mixing is maintained to promote the agglomeration of the new neutral colloids into larger flocs; the slow mixing process is called flocculation [80]. The pH can be adjusted in these units to increase removal efficiency. The floc size, strength, and structure may be affected by pH adjustment [82]. Aluminum sulfate ($Al_2(SO_4)_3$) and ferric chloride ($FeCl_3$) are among the common coagulants for water treatment [83]. Equations 8 and 9, respectively, show the As removal reactions when iron and aluminum are used as the coagulant [84].

The efficiency of several coagulants/flocculants under specific operating conditions is listed in Table 4. It was proven that pH has a significant effect on the performance of coagulants/flocculants. Initial concentration and coagulant dose are two other major parameters affecting coagulation performance. Flocculation is the activity of polymers to bridge flocs and form large agglomerates. Bridging happens when portions of the polymeric chains are adsorbed on some particles, causing the particles to aggregate. An anionic flocculant will be used for a suspension with a positive charge to destabilize the colloid by bridging the particles or neutralizing the charge [80].

Table 3. Overview of pressure-driven membrane processes and their characteristics.

Type	Membrane Model	Initial Concentration ($\mu g\ L^{-1}$ Unless Indicated Otherwise)	Process Conditions	Result	Ref.
RO	SWHR and BW-30 (FILMTEC)	As(V) = 50 AS(III) = 12	pH: 2.1–10.4 P: 10–35 bar	SWHR rejection %> BW-30 rejection % Final concentration: 2.86 $\mu g\ L^{-1}$	[85]
	Desal AK, General Electric Co., USApH	As(III) = 50–400	pH: 2–9 P: 0.41–0.82 MPa	Max: 90%	[86]
NF	NF-45, a fully aromatic, polyamide, thin-film composite NF membrane from FilmTec (Minnetonka, MN)	As(V) = 10–316	pH: 4–8 P: 550 and 690 kPa (80–100 psig)	60–90%	[87]
	NE 90 membrane (Woongjin Chemical, SouthKorea), a TFC negatively charged polyamidemembrane.	As(V) = 20–100	pH: 4–10	As(V): 89–96% As (III): 44–41%	[88]
UF	Negatively charged UF membrane, Osmonics (DESAL) GM	As(V)= 50–5000	pH: 2–11 T: 20–40 °C	88%	[89]
	Micellar-enhanced ultrafiltration (MEUF) (Amicon 8400, USA)	As(V) =243, 486	Cationic surfactants: hexadecylpyridinium chloride (CPC), hexadecyltrimethyl ammonium bromide (CTAB), octadecylamine acetate (ODA) and benzalkonium chloride (BC)	CPC: 96%, CTAB: 94%. BC: 57% ODA: 80%	[90]
MF	Coagulation/microfiltration: a 0.2 lm membrane disc	As(V) = 100	pH: 4.57–9.53 Coagulant: Ferric (1–7 mg L^{-1})	92.8–98.2%	[91]
	Micro-/nanostructured MnO2 spheres and microfiltration (ADVANTEC MFS Inc., pore size: 0.2 lm, diameter: 47 mm)	As(V) = 0.2 mM	pH: 2–10	>90%	[92]

RO = Reverse osmosis; NF = Nanofiltration; UF = Ultrafiltration; MF = Microfiltration.

$$Fe(OH)_3 + AsO_4^{3-}(aq) \rightarrow \left[Fe(OH)_3 * AsO_4^{3-}\right](s) \tag{8}$$

$$Al(OH)_3 + AsO_4^{3-}(aq) \rightarrow \left[Al(OH)_3 * AsO_4^{3-}\right](s) \tag{9}$$
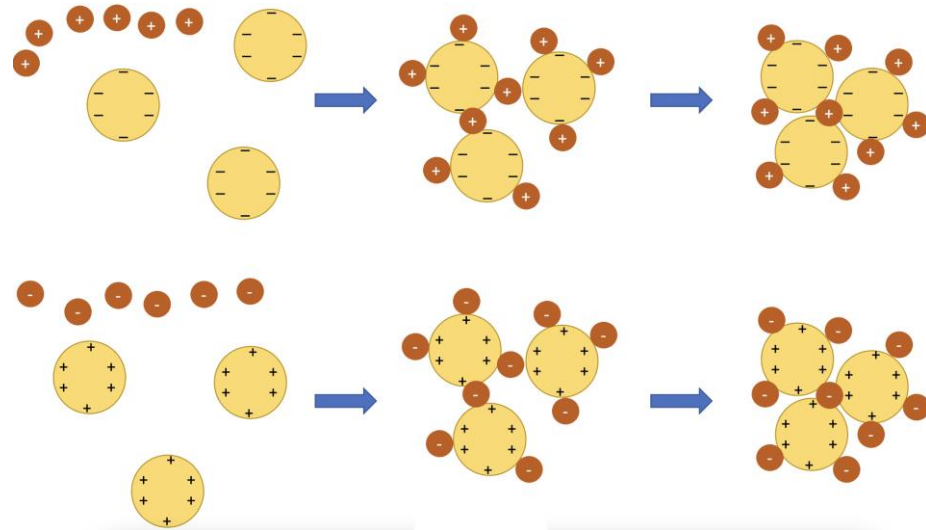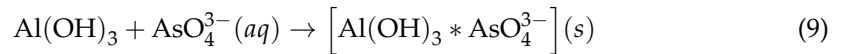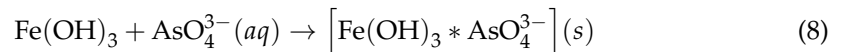
Figure 8. Mechanism of coagulation by cationic and anionic polymers.

Table 4. Coagulants/flocculants used in arsenic ion exchange, their operating conditions, and efficiencies.

Coagulant/Flocculant	Initial Concentration ($\mu g\ L^{-1}$)	pH	Coagulant Dose (mg L^{-1})/Intensity (A)	Removal Efficiency (%)	Ref.
Ferric chloride	As(V) = 50–60	7, 8	0.84–3.00	>80	[93]
Aluminum sulfate	As(V) = 10 As(V) = 500		66, 42	91	[94]
Ferric ions and coarse calcite	As(V) = 5000	5–11	100	>99	[95]
Titanium xerogel coagulant	As(III) = 1000	5–10	10	>90	[95]
Electrocoagulation (Al and Fe anode)	As(V) = 100	8.4	0.2 A	99%	[84]

Although the substances usually used in coagulation and flocculation processes are efficient and available, they produce toxic sludge in most cases. Therefore, sedimentation and filtration are needed as downstream processes after flocculation. There are still arguments on the effects of some metal coagulants and flocculants, such as aluminum and iron, on people's health and the environment [96,97]. Another problem with these plants is that they are not feasible in remote areas due to the lack of skilled workers and laboratory facilities to monitor, analyze, and control the process parameters [98].

Conventional chemical coagulation-flocculation is unsuitable for small communities because of the lack of capital to support their high operating costs, expensive installation and transportation cost of chemicals, and challenging management of the chemical sludge generated [99,100]. Electrochemical technologies offer a potentially appealing alternative for decentralized applications since they cut out the chemical distribution chain and solve the challenges of working with chemicals involved in traditional coagulation-flocculation methods [100]. In electrocoagulation, the anode is sacrificed into the water in ionic form, which occurs when a direct electric current passes through electrodes. The metal ions can create a variety of coagulated species that can either adsorb dissolved pollutants or destabilize suspended particles [101].

2.4. Oxidation

Oxidation processes are not considered independent As removal methods; they are the primary stages of other technologies. In other words, since the removal of As(III) is less effective than As(V), As removal procedures start with the oxidation of As(III) to As(V), followed by other processes such as adsorption, co-precipitation and coagulation [102]. The oxidation of As (III) to As (V) can be expressed as follows [103]:

$$H_3AsO_4 + 2H^+ + 2e^- \rightarrow H_3AsO_3 + H_2O \tag{10}$$

This process's oxidant (oxidizing agent) can be air or oxygen, ozone, chlorine, hypochlorite, chlorine dioxide, manganese compounds, and hydrogen peroxide. Table 5 presents the oxidation yields of different oxidants for arsenite oxidation. Table 5 shows that oxidation happens slowly when pure oxygen or air is used. On the other hand, ozone, chlorine, hypochlorite, chlorine dioxide, or H_2O_2 can speed up oxidation [17]. Other possible means of As oxidation utilize advanced oxidation processes (AOP) such as UV or microbiological oxidation when bacteria are present [17].

Table 5. The standard potential of different oxidants and their efficiencies in arsenite oxidation.

Oxidant	Standard Potential (V, 25 °C)	Sample (μg L^{-1})	Oxidation Yield (%) after (Time)	Ref.
Air	N/A	GW: 46–62	54 (5 days)	[104]
Pure oxygen	1.23	GW: 46–62	57 (5 days)	[104,105]
Ozone	2.07	GW: 46–62	>96 (10 min)	[104,105]
Hypochlorite	1.7	DW: 50	>80 (5 min)	[105,106]
Chlorine dioxide	1.27	DW: 50	>50 (2 days)	[105,106]
Potassium permanganate	1.23	DW: 50 300	>90 (5 min) >90 (5 min)	[105,106]
Hydrogen peroxide	1.78			

Note: GW = groundwater; DW = demineralized water.

Conventional oxidation in some treatment plants is one of the first steps because it makes the As removal process easier; however, one of the limitations of air or oxygen oxidation processes is their slow rate and moderate yield (Table 5) [17]. As a result, advanced oxidation processes (AOPs) were developed for treating As-contaminated water. The AOPs use highly reactive radical species to treat environmental waste and pollutants. The main AOPs include hydroxyl-radical-based processes, UV-photolysis-driven processes, ozonation, Fenton oxidation, electrochemical oxidation and heterogeneous photocatalysis [107,108]. The combination of various oxidation techniques such as UV, ozone, hydrogen peroxide, and TiO_2, improves the production of OH radicals. As a result, compared to using one type of oxidant, this combination typically speeds up oxidation reactions [109]. For instance, O_3/H_2O_2, O_3/UV, UV/H_2O_2, TiO_2/UV, H_2O_2/catalyst, and photo-Fenton processes are commonly used combinations in drinking water treatment [110]. AOPs are typically employed in full-scale systems or laboratories, mostly for conditions where conventional methods are not highly effective since they often need complex chemicals and light or electricity energy [111]. The major challenges of evaluating AOPs are the operational costs (energy and chemical input), sustainability (resource use and carbon footprint), and production of oxidation by-products [112]. Centralized water systems mostly rely on conventional oxidation and AOPs such as O_3/H_2O_2 and UV/H_2O_2 techniques. However, electricity-based techniques like the electrochemical production of oxidants such as chlorine and hydrogen peroxide have great potential in decentralized systems because they do not require chemical transportation [113,114]. In electrochemical oxidation, water contaminants are mostly oxidized by the anodic oxidation surface, by charge transfer on the anodic surface or interaction with the hydroxyl radical produced as a result of water oxidation [115].

Photo-Oxidation

Photocatalytic oxidation is a promising method among AOPs [116]. Generally, As(V) is less harmful than As(III) and easier to be removed; thus, oxidizing As(V) to As(III) is an effective step in the removal process [117]. Table 6 presents the results of the photo-oxidation of arsenite under different operating conditions. These studies show that in the presence of a heterogeneous catalyst such as titanium dioxide, the As(III) oxidation rate can be significantly improved. Among the catalysts used in the photo-oxidation process, TiO_2 is the most important one. The TiO_2 is important because it has high efficiency in oxidizing As(V) to As(III) due to its large surface-to-volume ratio, stable chemical properties, affordability, non-toxicity, great oxidizing power, and excellent electronic and optical properties [118,119]. The TiO_2 nanopowder can be used as suspended particles or immobilized on a surface. However, the literature revealed that the immobilization of TiO_2 leads to better results from an engineering and economic point of view. The major limitation of immobilization is that particle aggregation may cause a reduction in surface area. The main parameters that affect the TiO_2 photocatalytic performance include energy gap, particle size, specific surface area, porosity, crystallinity, and exposed surface facets [120].

Table 6. Oxidants used in the photo-oxidation of arsenite to arsenate, their operating conditions, and efficiencies.

Oxidant	As (III) Initial Concentration (mg L^{-1})	Process Conditions	Results	Ref.
Hydrogen peroxide and UVC radiation	0.2	T:20 °C IC (H_2O_2): 0–30 mg L^{-1} pH: 5.6–6.7	OY = 10% (30 min) As (III) oxidation $t_{1/2}$ = 3.5 s	[121]
TiO_2-impregnated chitosan bead (TICB)/UV light	100, 1000 and 10,000	T = 25 °C TICB: 17.5 mg chitosan + 7.5 mg TiO2 in 40 mL solution	2198 mg As(III)/g TICB and 2050 mg As(V)/g TICB	[122]
MoOx/TiO_2 (+UVA)	5	pH: 7.2	OY = 100% (120 min)	[118]
ZnO-Au nanocomposite	2	ZnO: 20 mg in 40 mL solution	ZnO: OY = 9.1%(2 h) ZnO–Au (0.5%): OY = 17% (2 h) ZnO–Au (1%): OY = 45% (2 h) ZnO–Au (2%): OY = 23% (2 h)	[123]
Few and multi-layer Ti_3C_2Tx nanosheets	0.7	pH: 7 under UVA	Multi-layerTi_3C_2Tx: 20% (90 min) Few-layer Ti_3C_2Tx:, 44% (45 min)	[119]
Dissolved Fe(III) in the presence of UV	10	Fe(II): 180 mg L^{-1} pH: 7	Complete oxidation process time: 1–6 h	[124]

OY: Oxidation yield for As (III).

3. Adsorption

Adsorption is the use of solids to eliminate substances from gaseous and liquid solutions. Activated carbon, metal hydrides, and synthetic resins are common adsorbents used in water and wastewater treatment plants [80]. The most common adsorbent categories for water treatments are presented in Figure 9. Comparing several water treatment methods for heavy metals removal (Table 7) shows that adsorption is more affordable than membrane technologies, simpler, and more secure to deal with than contaminated sludge produced by precipitation, and it is multipurpose in contrast to ion exchange [125]. The main limitation of the adsorption method is that its effectiveness is affected by the presence of other ions. Various ions compete for the adsorbent's active site, affecting the adsorption capacity [126]. For example, phosphate ions can compete with As ions due to their similar chemical structure; thus, they can significantly lower the As removal efficiency (Gallegos-Garcia et al., 2012). The presence of 10 mmol L^{-1} $H_2PO_4^{2-}$ decreased the adsorption efficiency of As(III) on zero-valent iron nanoparticles from 99.9% to 66.3% [127].
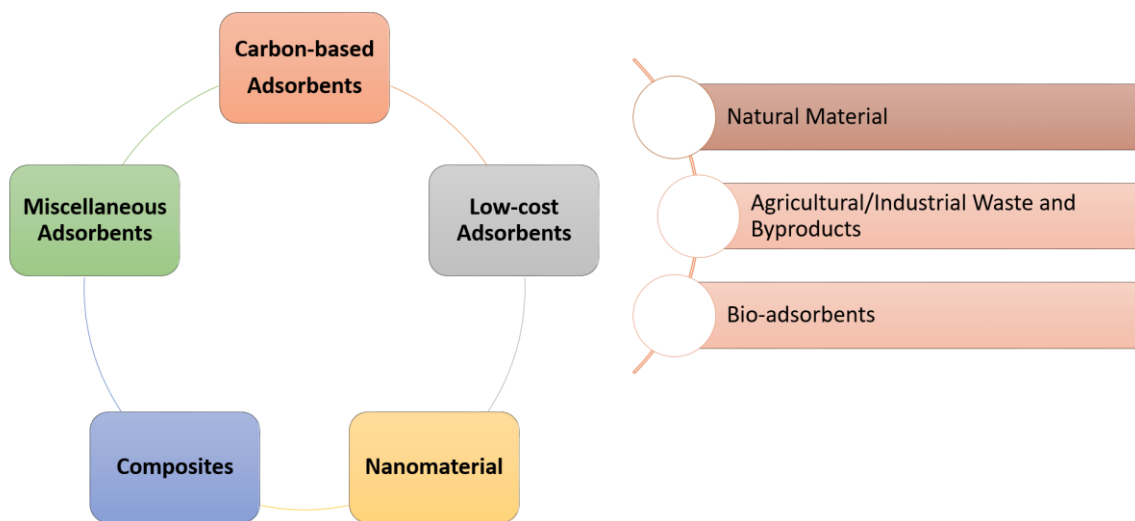
Figure 9. Classification of adsorbents for water treatment (adapted from [128]).

Figure 10 shows the different configurations previously suggested for As adsorption. Batch experiments, fixed configurations, and fluidized-bed reactors are the primary categories that are widely used. Adsorbent particles are in motion in the fluidized reactor configurations, while they are stationary in a fixed-bed reactor [129]. In batch experiments, a liquid solution containing a known amount of adsorbate is brought in contact with a given mass of adsorbent, and the adsorbate's concentration is monitored over time. [130].
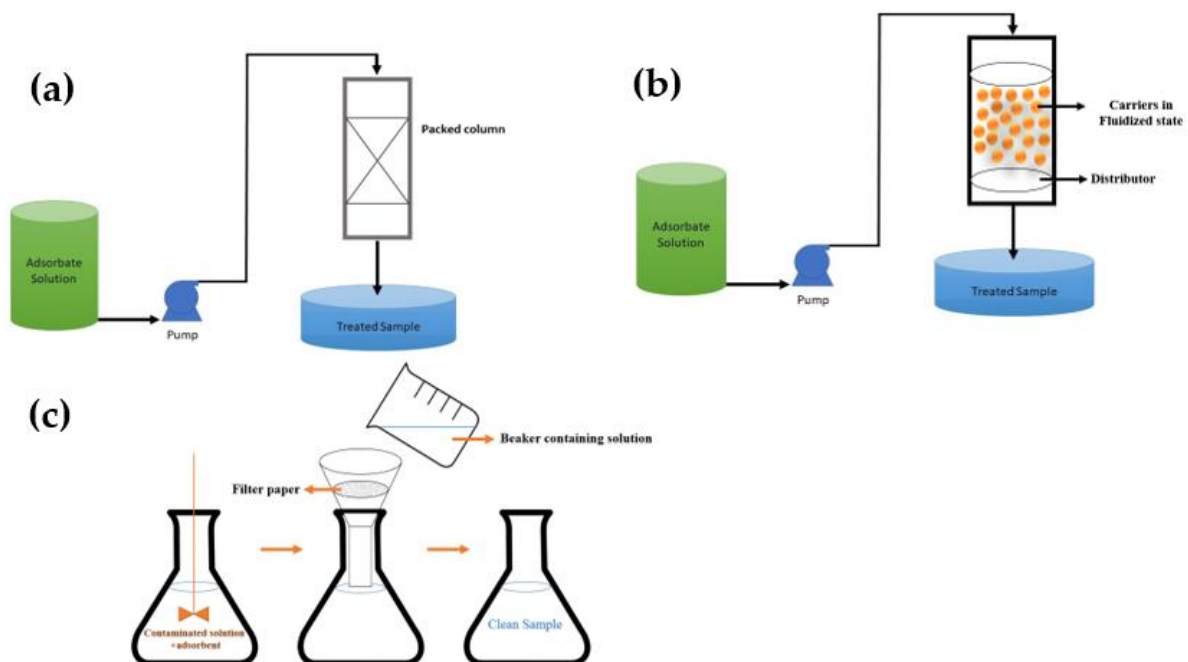
Figure 10. Different configurations for adsorption of impurities: (**a**) Packed-bed adsorber, (**b**) Fluidized-bed adsorber, and (**c**) Batch experiments.

3.1. Adsorption Kinetic

The concentration data and adsorption rates obtained from experiments should be interpreted using kinetic models such as pseudo-first-order (PFO) and pseudo-second-order (PSO). PFO (Equation (11)) and PSO (Equation (12)) models are the most common models employed in explaining the kinetic data of heavy metal removal [131].

$$\ln(q_e - q_t) = \ln q_e - k_1 t \tag{11}$$

$$\frac{t}{q_t} = \frac{1}{k_2 q_e^2} + \frac{1}{q_t}t \tag{12}$$

where q_e (mg g^{-1}) is the removal capacity of metals at equilibrium state; q_t (mg g^{-1}) refers to the removal capacity at time t (min); k_1 (min^{-1}) introduces the velocity constant of Equation (11); and k_2 (mg g^{-1} min^{-1}) is the velocity constant of Equation (12), respectively. The magnitudes of k_1 and q_e are found by plotting $ln(q_e - q_t)$ versus t. The values of k_2 and q_e are obtained by plotting t/q_t against t. Table 8 provides the kinetic parameters for the As adsorption on different adsorbents. Generally, the literature confirms that the pseudo-second-order model fits As adsorption data better than the pseudo-first-order model [132].

Table 7. Advantages and disadvantages of common treatment technologies for arsenic removal [7,71,128,133–142].

Methods	Advantages	Disadvantages
Ion exchange	. Simultaneous removal of other dissolved pollutants like sulfate . Less affected by the water pH . Specific resins available for specific ions . Relatively well-known process and widely commercially available resins	. Competing ions impact arsenic elimination . Low efficiency in highly concentrated effluent . Replacement and regeneration are required, and regeneration leads to sludge disposal problems. . Not Suitable for high-TDS. . High-cost and high-tech operation and maintenance required
Membranes	. High removal efficiency . Do not create toxic solid waste . Effective for eliminating some microorganisms and some other pollutants . Need fewer resources (labor and area) than alternative treatment methods . Eliminate further dissolved contaminants and partially disinfect the water	. Very high capital and running cost . High-tech operation and maintenance . Requires pre-treatment . Requires membrane replacements . Possibility of membrane pore fouling/biofouling resulting in lower flux, higher energy consumption, weak membrane performance and more frequent chemical cleaning . Less effective for arsenite
Coagulation /flocculation	. Ideal for waters with Fe and Mg content . Removes other suspended solids in case of surface water source . Relatively low capital cost . Relatively simple in operation . Common chemicals available	. Limited removal of As(III) . Might not remove arsenic below the allowable limits . Might need pre-oxidation which could form toxic disinfection byproducts . Depends strongly on the coagulant type and dose, solution pH, and other competing ions like phosphates or silicates
Oxidation/AOP	. Relatively simple and low-cost process . Oxidizes other impurities and kills microbes . Effective for total As removal	. In most cases, these processes are very slow . Processes remove only some of arsenic . Used as pretreatment for other processes (needs to be followed by another method) . Toxic by-product formations (organo-chlorides)
Adsorption	. High As removal efficiency, low costs, simple operation, handling, and maintenance . Relatively well-known method and commercially available adsorbents . High removal efficiency and cost efficiency . Additional chemical and sludge free. . No harmful by-products.	. Efficiency is affected by other ions such as phosphate. . Adsorbent material should be regenerated or replaced frequently as the adsorption bed becomes exhausted . Challenging recycling of conventional adsorbents (especially very small-sized powders)

3.2. Isotherm Models

Adsorption isotherm is the relation that describes the equilibrium between the quantity adsorbed to the unit mass of adsorbent and the concentration of the remaining adsorbate (pollutant) in a solution at a fixed temperature. The standard adsorption isotherm models are Langmuir and Freundlich's isotherm models [143]. The adsorbed species, adsorbate, adsorbent, and other physical and chemical characteristics of the solution, such as pH, ionic strength, and temperature, play a role in the adsorption isotherm [144]. Different isotherm models have variable model parameters since the interaction between the adsorbent and adsorbate varies [145]. Two main isotherm models, Langmuir and Freundlich, used in heavy metal adsorption, are discussed here. Based on the Langmuir isotherm model, monolayer adsorption occurs on a homogenous surface without interaction between adsorbate species. In contrast, the Freundlich isotherm is based on multilayer and non-ideal adsorption on heterogeneous surfaces [146].

3.2.1. Langmuir Isotherm

The equations describing this model are based on the assumption that the adsorbent provides homogeneous monolayer adsorption because it has sites with uniform energy for adsorption. Equation (13) is the linear form of the Langmuir model.

$$\frac{1}{q_e} = \frac{1}{bc_e q_{max}} + \frac{1}{q_{max}} \tag{13}$$

where q_e (mg g^{-1}) and q_{max} (mg g^{-1}) stand for the amount of adsorbed metal particles at a specified equilibrium and the maximum amount of the metal particles per 1 g of sorbent; and b (mg g^{-1}) is a constant that has a relation to the adsorption energy [143]. According to Figure 11, which is a graphical illustration of Equation (6), q increases sharply from zero with the filling of the adsorption sites on the monolayer as the solute concentration in the solution rises, and it peaks at a limiting surface density of q_{max} when the surface is saturated. Then, no further increase in q with increasing solution concentration is possible once the surface is saturated. However, a dynamic equilibrium is still maintained with equal solute adsorption and desorption rates [147].
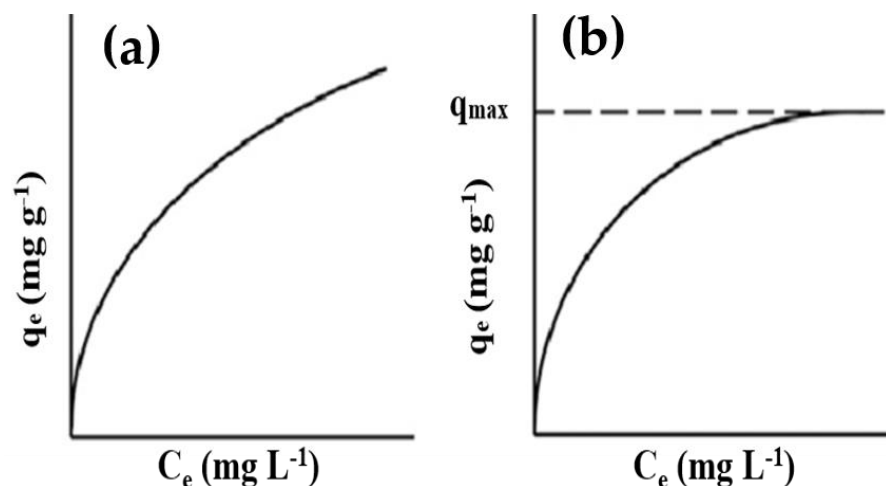
Figure 11. (**a**) Freundlich adsorption isotherm, and (**b**) Langmuir adsorption isotherm.

Table 8. Kinetic parameters for the adsorption of arsenic on different adsorbents.

Adsorbents	Pseudo 1st or 2nd Order Kinetics	C_0 (mg L^{-1})	k	q_e (µg g^{-1})	R^2	Ref.
Untreated powdered eggshell	1st	0.5	0.717 h^{-1}	30	0.944	[148]
	2nd		18.47 g mg$^{-1}\cdot$h^{-1}	724	0.999	
Dolomitic sorbents	1st	2	6.8×10^{-3} µg g^{-1} min^{-1}	652.04	0.970	[149]
	2nd		1.75×10^{-5} µg g^{-1} min^{-1}	652.04	0.975	
A MIL-53(Fe)	1st	5	0.016 min^{-1}	11,060	0.833	[150]
	2nd		0.0120 g mg^{-1} min^{-1}	5180	0.994	
Hematite nanoparticles	2nd	10	6.45 ± 3.11 g mg^{-1} h^{-1} (10–4)	2899 ± 71.1	0.997	[151]
Hematite agglomerate	2nd		6.45 ± 1.39 g mg^{-1} h^{-1} (10–4)	1689 ± 90.2	0.996	
Copper (II) oxide nanoparticles	1st	1	0.02 min^{-1}	742.48	0.94	[152]
	2nd		0.03 g mg^{-1} min^{-1}	1014.41	0.99	

3.2.2. Freundlich Isotherm

The Freundlich model is used when heterogeneous surfaces and multilayer sorption are studied. Equation 14 provides the mathematical expression of Freundlich isotherm.

$$\ln q_e = \ln k_{fe} + \left(\frac{1}{n}\right) \ln c_e \tag{14}$$

where k_f indicates the extent of adsorption, n is the non-linearity degree between solution and adsorbent, and both are constants. The k_f (mg$^{1-1/n}$ g^{-1} L$^{1/n}$) becomes higher as the surface accessibility for pollutants becomes greater [143]. The Freundlich model can be used for multilayer adsorption because it is not constrained to monolayer creation like the Langmuir isotherm model. Freundlich isotherm expression assumes that the surface is heterogeneous and active sites' distribution and energy are exponential. Figure 11 shows that the mass of adsorbate adsorbed per unit mass of adsorbent is not constant at various concentrations of the solution. The stronger binding sites will first be occupied, and the adsorption energy will begin to fall exponentially once the adsorption is complete [147]. In most metal adsorption studies, Freundlich isotherm provides a more accurate fit to the data [143] since arsenic adsorption on the adsorbents is often non-ideal multilayer adsorption on heterogeneous surfaces [153]. Table 9 details the equilibrium isotherm parameters for As adsorption.

Table 9. Equilibrium isotherm parameters for arsenic adsorption.

Adsorbent	Langmuir			Freundlich			Ref.
	q_{max} (g g^{-1})	b (L mg^{-1})	R_2	k_f (mg g^{-1})	n	R^2	
Zeolite (H-MFI-24)	0.0358	0.009	0.9566	3.52	1.11	0.9962	[154]
Zeolite (H-MFI-90)	0.0348	0.0109	0.9642	4.21	1.12	0.9993	[154]
Chitosan magnetic graphene oxide nanocomposite	0.0023	0.021	0.9605	86.640	0.514	0.9776	[155]
Watermelon rind	0.0031	1.39	0.96	1.99	0.40	0.88	[156]
Hydroxyl-eggshell	0.529	0.005	0.81	104.11	5.05	0.92	[157]
Maghemite nano-adsorbents	0.0072	17.5	0.98	13.8	1.95	0.93	[158]
Starch functionalized maghemite	0.0086	9.1	0.98	16.5	1.60	0.98	[158]

4. Characterization Techniques for Investigation of Adsorbents Properties

Understanding and identifying the various retention phenomena (adsorbent-adsorbate) and interpreting the kinetic results depend on the characterization results. Moreover, developing technical adsorption methods and conducting adsorption studies require a basic understanding of adsorbents' physical and chemical characteristics. Furthermore, the adsorbent surface characteristics are crucial in determining its sorption capacity because adsorption is a surface phenomenon [159–161]. Figure 12 presents the most common characterization techniques. Table 10 presents an overview of the characterization results of different adsorbents (proximate and ultimate analysis, specific surface area, and bulk density). Table 11 details typical examples of Fourier transform infrared spectroscopy (FTIR) and X-ray powder diffraction (XRD). Table 12 shows typical examples of scanning electron microscopy (SEM) and particle size.
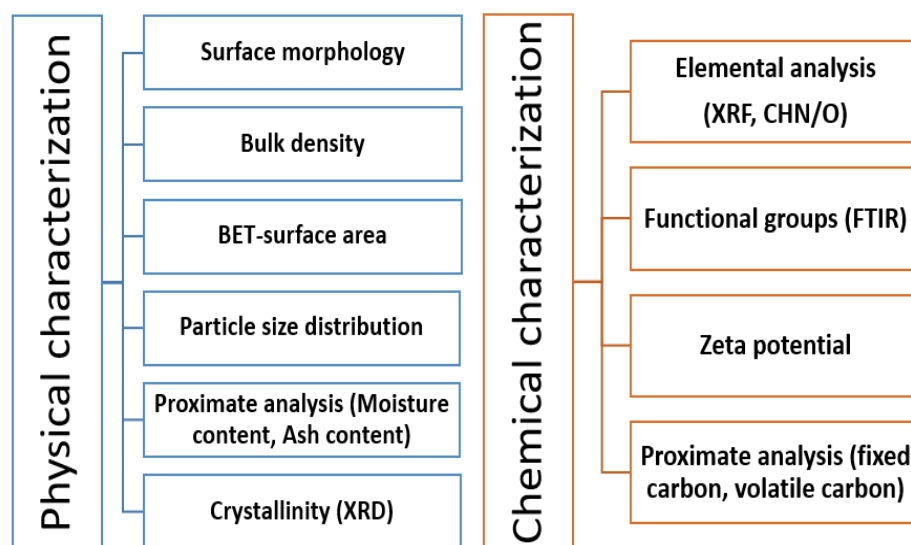
Figure 12. Overview of main characterization techniques.

4.1. Surface Morphology

Microscopic methods such as optical microscopy (OM), scanning electron microscopy (SEM), transmission electron microscopy (TEM), and atomic force microscopy (AFM) can be employed to directly observe the adsorbent morphology or topography [162]. SEM characterization, a common technique for investigating surface morphology, produces high-resolution images of a sample by applying a focused electron beam on the sample's surface and measuring the secondary or backscattered electrons. An Energy Dispersive X-ray Analyzer (SEM-EDX) is employed to determine certain elements' atomic percentages [163].

4.2. Bulk Density and Particle Size

An untapped powder sample's mass-to-volume (including void volume) ratio determines its bulk density. As a result, the powder particles' density and spatial arrangement within the powder bed affect the bulk density. After weighing the contents of a container (m) with a known volume, V, the bulk density can be determined [162].

Table 10. Proximate and ultimate analysis, specific surface area and bulk density of different adsorbents.

Adsorbents Type	Adsorbent	Proximate Analysis		Ultimate Analysis (%)		Specific Surface Area (m^2 g^{-1})	Bulk Density (g cm^{-3})	Ref.
Carbon-based	Activated carbons	Moisture Volatile Fixed carbon Ash	7.53% 15.23% 67.66% 9.58%	C H N O	68.32 3.12 2.12 26.44	720	0.43	[164,165]
Natural	Zeolites	Volatile Fixed carbon Ash	9.24% 3.94% 86.57%	SiO$_2$ Al$_2$O$_3$ K$_2$O Na$_2$O Fe$_2$O$_3$ CuO MnO Br TiO$_2$ Cl ZnO	86.1 5.79 0.65 5.08 0.039 0.009 0.064 0.04 0.012 2.22 0.005	211.97	0.068	[166,167]
Agricultural waste	Sawdust	Moisture Volatile Fixed carbon Ash	5.83% 76.44% 12.02% 5.73%	C H N O S	46.1 6.39 0.37 41 0.55	303	0.152	[168,169]
Industrial waste/byproducts	Fly ash	Volatile content Fixed carbon Ash content	3.68% 22.30% 74.00%	SiO$_2$ Al$_2$O$_3$ CaO Fe$_2$O$_3$ MgO	60.5 15.4 2.9 4.9 0.81	450	1.01	[170,171]
Biosorbent	Chitin/chitosan	Moisture Protein Fiber Ash	15.40% 14.88% 76.40% 9.40%	C H N O S	49.7 1.72 0.2 48.3 0.1	300	1.008	[172]

Table 11. Fourier transform infrared spectroscopy (FTIR) and X-ray powder diffraction (XRD) results of different adsorbents.

Adsorbent	FTIR	XRD	Ref.
Carbon-based (Activated carbons)			[173]
Natural (Zeolites)			[174]
Agricultural waste (Sawdust)			[175]
Industrial waste (Fly ash)			[176]
Biosorbent (Chitosan)			[177]

Table 12. Scanning electron microscopy (SEM) and particle size distribution results of different adsorbents.

Adsorbent	SEM	Particle Size Distribution	Ref.
Carbon-based (Activated carbons)			[173,178]
Natural (Zeolites)			[174,179]
Agricultural waste (Sawdust)			[175,180]
Industrial waste (Fly ash)			[181]
Biosorbent (Chitosan)			[177,182]
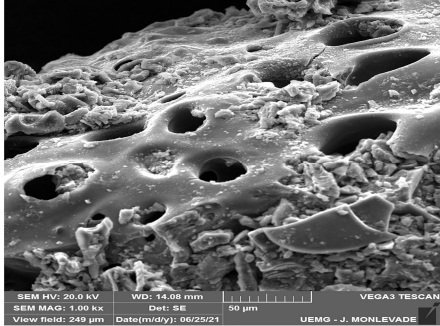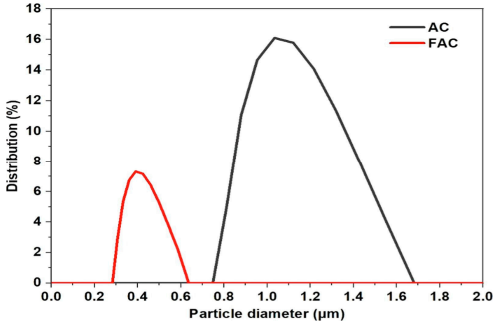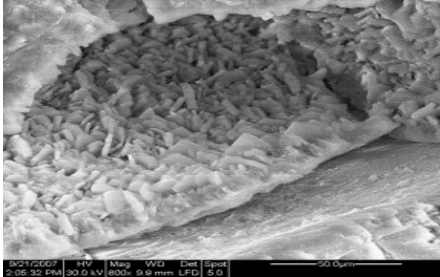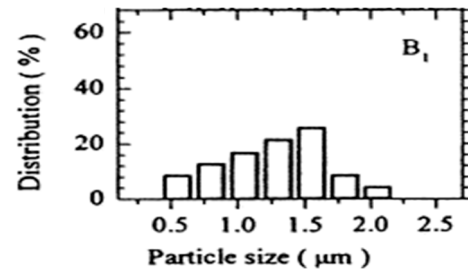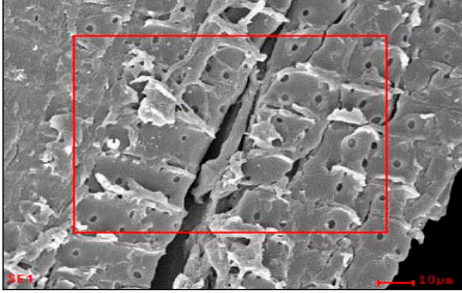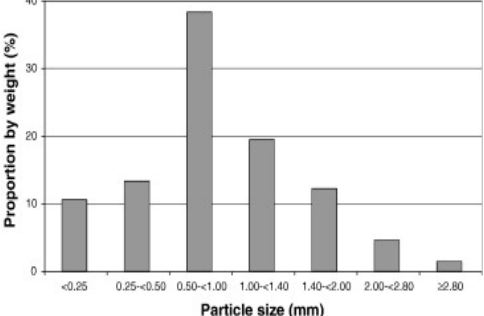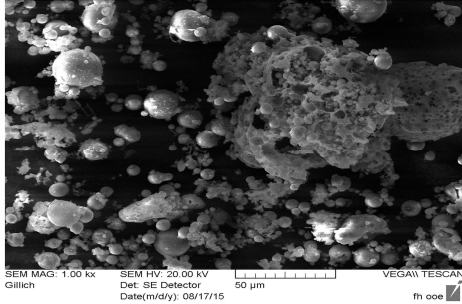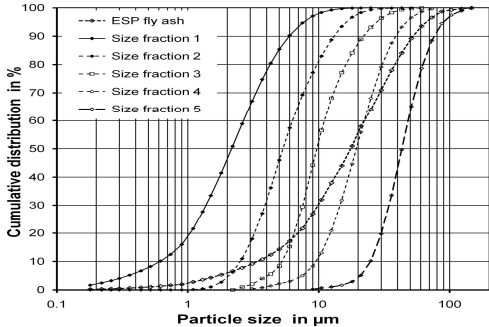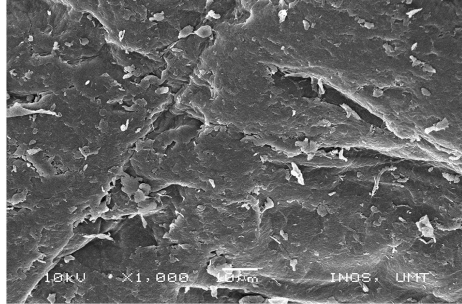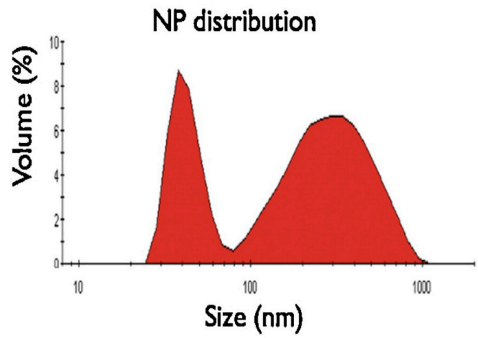
4.3. Dynamic Light Scattering (DLS)

DLS is a non-destructive, low-cost, relatively easy, and fast technique for measuring particle size distributions in colloidal suspensions and emulsions and detecting the presence of agglomerates and aggregates. The light scattered by small particles irradiated by a laser is recorded with high time resolution under a particular angle; the fluctuation of the scattering signal represents the dynamics of microstructural processes such as the Brownian motion of the particles. Particle size can be measured by analyzing the change in the scattered light intensity in a colloidal suspension. A numerical transformation of spectral measurement signals is required for this purpose [183,184].

4.4. Brunauer-Emmett-Teller (BET)-Surface Area

The BET method for determining surface area is a popular characterization method for different adsorbents. The BET theory states that surface areas can be determined from gas (typically N_2) adsorption isotherms at the boiling point of the gas. In other words, a formation of layers that consists of atoms, ions, or molecules on the surface of a substance that adsorbs gas produces van der Waals forces, which are responsible for this phenomenon. Based on this theory, the surface area and the amount of gas adsorbed on the adsorbent material are correlated [185].

4.5. Crystallinity

XRD techniques are frequently employed to identify present phases (qualitative analysis) and to calculate their corresponding quantities (quantitative analysis). X-ray scattering from atoms leads to a diffraction pattern that carries information about the atomic structure in the crystal. Amorphous materials do not show any noticeable peaks in the diffraction pattern because of the lack of periodic arrays with long-range order. The intensity (amount of X-rays recorded in a certain peak) is shown against the detector angle, *2θ*, in a diffraction pattern known as a diffractogram (Table 11). The wavelength influences the peak position in a diffraction pattern. Bragg's Law, which is the principle of XRD, explains that the incident X-rays' wavelength, the incident angle, and the distance between atoms in crystals are related [186].

4.6. Ultimate (Elemental) (XRF, CHN/O)

The ultimate analysis provides information about the elemental composition of the adsorbent [185]. X-ray fluorescence (XRF) spectroscopy is an accurate, reliable, and non-destructive analysis that is often used to determine the elemental compositions of various materials. According to the wavelength-dispersive principle, each atom emits an estimated relative quantity of X-ray photons of a certain energy or wavelength. The electron of an atom is forced out of its inner orbital by the incoming X-rays from an XRF instrument. As a result, the atom is excited, and high-energy radiation is produced (photons, protons, and electrons). The final step involves identifying emission lines and converting the line intensities to elemental concentrations [187]. The elemental analysis of some adsorbents can be derived from a CHN analyzer. Dried samples are burned in the combustion box of an elemental analyzer when conducting a CHN test. The complete oxidation of the organic substance, in the presence of ultrapure O_2 and the carrier gas (ultrapure helium), converts carbon, hydrogen, and nitrogen content into CO_2, H_2O, and N_2, respectively. The quantities of the gases are measured by changes in the products' thermal conductivity after the gases are homogenized, depressurized, and separated by analytical columns [188].

4.7. Proximate Analysis

The proximate analysis determines the solid, gaseous, and non-combustible components of an adsorbent, respectively, as fixed carbon (solid), volatile matter (gaseous), ash content (ASH), and moisture content [185]. After being heated to 110 °C in an N_2 environment, a sample loses mass, and this mass loss is used to calculate the moisture content. Except for mineral hydrates that break down beyond 110 °C, the moisture content includes

any water that may be chemically or physically bonded. The volatile matter content is equivalent to the products produced by a thermal breakdown at temperatures between 110 and 900 °C in the presence of N_2. What remains after moisture and volatile materials have been removed, minus the combustion ash, is called fixed carbon. For the combustion, the sample is maintained at 900 °C, and the environment is changed from N_2 to air, and what is left over, after burning fixed carbon at 900 °C in air, is ash [189].

4.8. Functional Groups

Fourier transform infrared spectroscopy (FTIR) can identify the functional groups in materials by producing infrared beams. The spectrum produced by infrared spectroscopy, which measures the amount of IR radiation absorbed by each bond in a molecule, is often expressed as a percentage of transmittance vs. wavenumber (cm^{-1}). The covalent bond of materials with an electric dipole absorbs energy when IR radiation interacts with it, and the bond begins to oscillate back and forth. When a molecule's dipole moment changes due to the oscillation of its bonds, IR light is absorbed by those bonds [190].

4.9. Zeta Potential (ZP)

This is an analytical method to indirectly report the surface net charge and reflect the stability of the particles. It is the electric potential at the shear/slipping plane of a moving colloid particle in an electric field, and it describes the electrochemical equilibrium between particles and liquids in solutions. The electric potential of a surface is defined as the amount of work required to move a unit of positive charge from infinity to the surface without acceleration. Extremely positive or negative ZP values represent strong repulsive forces that restrain similarly charged particles from aggregating, and as a result, the re-dispersion of the solution is guaranteed [191,192].

5. Adsorbent Performance

5.1. Removal Efficiency and Adsorption Capacity

The success of adsorption is evaluated by calculating the removal efficiency, removal capacity, and removal rate. The adsorption rate can be measured by determining the residual heavy metal after different contact times. Equation (15) calculates the adsorption efficiency [193].

$$\text{Adsorption efficiency (\%)} = \left(\frac{C_i - C_e}{C_i} \right) \times 100 \tag{15}$$

where C_i is the initial concentration, and C_e denotes the metal ion concentration in the equilibrium state. Equation (16) is employed to calculate adsorption capacity, as given below [193]:

$$\text{Adsorption capacity} \left(\text{mg g}^{-1} \right) = ((C_i - C_e) \times V)/W \tag{16}$$

where V stands for the volume of the metal solution, and W represents the mass of the adsorbent [193].

5.2. Reusability

Effective reusability refers to the ability of an adsorbent to be regenerated and utilized multiple times without considerably losing its adsorption capacity [194]. Many factors can decrease the performance of an adsorbent over time (Figure 13). These factors include incomplete adsorbate desorption, surface precipitation, active sites loss as a consequence of adsorbent wear and tear, and changes in adsorbent characteristics such as surface area, porosity and crystalline structure [195–197]. Table 13 shows examples of changes in removal efficiency or capacity after several adsorption-desorption cycles.
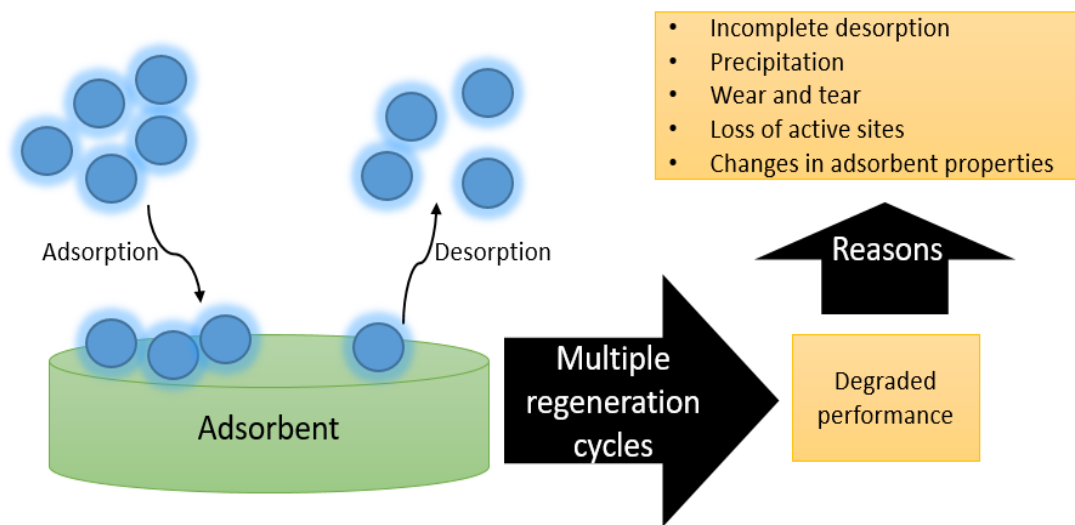
Figure 13. Effects of multiple regeneration cycles on the performance of adsorbents.

Table 13. Results of previous studies for several consecutive sorption/regeneration cycles.

Contaminant	Adsorbent	Number of Cycles	Removal Capacity (RC) or Removal Efficiency (RE) Change	Ref.
As (III) As(V)	Fe–Mn binary oxide impregnated chitosan bead	5	RC: −14% RC: −17%	[198]
As(V)	Metal-organic framework MOF-808	5	RE: 17%	[199]
As (III) As(V)	Magnetite/non-oxidative graphene composites	5	RC: −14%, RE: −22% RC: −6%, RE: −0.26	[200]
As (III)	Chitosan magnetic graphene oxide nanocomposite	5	RE: −13%	[155]
As(V)	MIL-101(Fe)	3	RE: −40%	[201]

5.3. Effects of Parameters on Adsorbent Performance

It is essential to optimize removal conditions to improve adsorbent performance. Optimization studies have traditionally been conducted by tracking the impact of one factor at a time on an experimental response, while the other variables remained constant (one variable at a time). This method does not consider the interactions between the variables being researched; this approach increases the number of experiments required to find the optimum values [202]. As a result, it is preferred to use a different approach that will be more successful and flexible for the parameter optimization of adsorption studies. One of the most used statistical tools for optimizing adsorption conditions is response surface methodology (RSM) [203]. Recent predictive polynomial equations developed in adsorption research studies to optimize operational conditions (i.e., maximum removal efficiency or maximum adsorption capacity) are summarized in Table 14. The effects of process variables (pH, temperature, contact time, initial concentration, and adsorbent dose) on heavy metal removal efficiency and the adsorption capacity of adsorbents are described in the following sections. Table 15 shows the effect of different parameters on the adsorption of As from aqueous solutions.

Table 14. Summary of previous studies on the mathematical models of arsenic removal by different adsorbents.

Method	Conditions and Factors	Models		Max Adsorption Capacity/Removal Efficiency (%)	Ref.
CCD	Adsorbate: As(V) and As(III) Adsorbent: iron-impregnated sugarcane carbon (Fe–SCC) Factors: A, C, and F	**Breakthrough time (min)**	$= 473.0 - 317.6A + 316.5C - 174.2F - 111.4\,AC - 87.0AF$ $-57.8CF + 3.7A^2 + 486.9C^2 + 38.0F^2$	AC: 147.7 µg g^{-1}	[204]
	Adsorbate: As(V) Adsorbent: mill scale-derived magnetite particles Factors: A, B, D, P	**Adsorption capacity**	$= 4.4 + 2.10A - 0.9941B + 0.3521D - 0.4235P -$ $0.7756AB + 0.1931AD - 0.1272\,BD + 0.1477BP -$ $0.33063AP - 0.0212DP - 1.2551A^2 - 0.6767B^2 +$ $0.3406D^2 - 0.1976P^2$	AC: 8.13 mg g^{-1}	[205]
	Adsorbate: As(V) Adsorbent: iron oxide immobilized graphene oxide gadolinium nanocomposite Factors: A, B, C, and D	**Removal efficiency (%)**	$= -1.760 + 0.548A + 5.014B + 184.496C + 0.291D$ $+0.017AB - 0.590AC + 0.001AD - 1.362BC - 0.002BD$ $-0.010CD - 0.015A^2 - 1.129B^2 - 111.685C^2 - 0.001D^2$	RE: 94.8%	[206]
Box–Behnken	Adsorbate: As(V) Adsorbent: metal oxide-precipitated clinoptilolite Factors: A, B, and T	**Adsorption capacity**	$= 2.583769 + 0.885829A - 0.184399B - 0.074153T$ $-0.135264\,AB + 0.005606AT + 0.002475BT$ $+0.000546T^2 - 0.008533A^2$	AC: 6.1 mg g^{-1}	[207]
	Adsorbate: As(III) and As(V) Adsorbent: CeO$_2$/Fe$_2$O$_3$/graphene nanocomposite Factors: A, B, and C	**Removal efficiency (%) (AS(III))**	$= 89.71 - 80.20A - 9.45B + 2.91C - 3.25AB + 1.24AC$ $+0.39BC - 1.73A^2 - 25.21B^2 - 0.078C^2$	As(III): 98.53% As(V): 97.26%	[208]
		Removal efficiency (%) (AS(V))	$= 66.98 - 7.63A - 27.20B + 2.77C + 0.53AB + 1.68AC$ $-0.028BC + 3.48A^2 - 8.27B^2 + 4.38C^2$		

A = Initial concentration, B = pH, C = Adsorbent dose, CCD = Central composite design; D = Contact time, F = Flow rate, P = Particle size and T = Temperature.

Table 15. Summary of studies on the effect of process parameters on arsenic removal by different adsorbents.

Adsorbent	Adsorbate	Optimum pH	Optimum Temperature (K)	Contact or Equilibrium Time (min)	Optimum As Initial Concentration (mg L^{-1})	Optimum Adsorbent Dose (g L^{-1})	Removal Efficiency (%) (Max)	Adsorption Capacity (mg g^{-1})	Ref.
Magnetic graphene oxide	Pb (II) Cr (III) Cu (II) Zn (II) Ni (II)	3–9 (Pb (II): 5 Cr (III): 6 Cu^{+2}:7 Ni (II):8)	298	10–65 (Pb (II), Cu (II), Ni (II): 25 Cr (III), Zn (II):35)	60	0.002–0.016	Pb (II): 99.97 Cr (III): 97.78 Cu (II): 96.65 Zn (II): 91.88 Ni (II): 95.28	Pb (II): 200 Cr (III):24 Cu (II):62 Zn (II):63 Ni (II):51	[209]
Carboxyl modified lignocellulose-biomass jute fiber	Pb (II) Cd (II) Cu(II)	2–6 (6)	298	0–180 (20)	200	1.0		157.21, 88.98, 43.98	[210]
Magnetic carboxymethyl chitosan nanoparticles	Pb(II), Cu(II) Zn (II)	5.2	298	2–60 (60)	100	1.0		Pb (II): 243, Cu (II): 232, Zn (II): 131	[211]
Esterified hydroxyapatite	Pb(II)	3–7 (3)	298	10–720 (60)	30−300 (100)	0.1	Pb (II): 99% < 60 ppm Pb (II): 99.99% =63 ppb)	2397	[212]
Peanut hull	Cu(II)	1.5–4 (4)	298 to 338 (298)	5–180 (60)	150- 500 (150)	0.1–1 (1)	>80%	14	[213]
Microcrystalline cellulose-based nanogel	Cd (II)	6	300	10–90 (30)	20	0.05–1 (0.5)	97%	595	[214]
Magnetic Zr-MOF	Pb (II) Cr(VI)	Pb (II) 1–7 (4) Cr(VI) 1–10 (3)	298	10–250 (Pb (II): 60 and Cr(VI): 30)	Pb (II): 10–500 (500) Cr(VI):10–1000 (1000)	1		Pb (II): 273 Cr(VI): 429	[215]

5.3.1. pH

The solution pH significantly impacts the distributions of the elements of metals, their mobilization, and the surface charge of the adsorbents during the adsorption process [216]. In a lead (Pb)-removal study, the adsorption capacity of the mussel shell increased from 43.62 mg g^{-1} to 63.49 mg g^{-1} upon an increase in pH (4–6). Low pH decreased the Ca^{2+} dissociation in the solution, and Pb(II) swaps with a limited quantity of Ca^{2+}; when the pH is high, there is more dissociation of Ca^{2+}, and Pb(II) exchanges with more Ca^{2+}, implying that the adsorption capacity increases. [217].

As(V) adsorption on the granitic material gradually reduced from pH 4 as the pH value was increased, according to a previous study [218]. The granitic material compounds with variable charges, such as Fe and Al oxyhydroxides, kaolinite-type clays, and organic matter, pose a positive charge at an acidic pH, which helps them retain H$_2$AsO and HAsO$_2$. Still, as the pH rises, they suffer from progressive deprotonation and an increase in negative charge, which can reduce As(V) adsorption [218].

The effects of pH on the removal of As (III and V) were studied to find the ideal pH for the highest adsorption of As on biochar-stabilized iron and copper oxide nanoparticles. In the pH range of 6–8, the highest adsorption of As occurs at pH 7.0, with >95% removal. The surface charge of the composite-based adsorbents and the ionization potential of the As species are both influenced by the pH of the solution. A pH between 6.5 and 7.0, which is mildly acidic to neutral, encourages the ionization of H$_3$AsO$_4$ to produce H$_3$AsO$_4$$^{2-}$, which has a negative charge, while the composite mixture acquires a mildly positive charge as a result of the conversion of Fe-OH and Cu-OH to Fe-OH^{2+} and Cu-OH^{2+}. Due to the opposite charges of the composite mixture and As (V) species, the electrostatic attraction between adsorbate and adsorbent increases, leading to higher adsorption [219].

In a pH range of 1.0–13.5, the behavior of As adsorption on octahedral TiO$_2$ nanocrystals was studied. As(III) and As(V) exhibited their highest adsorptions at pH values of 8 and 4, respectively. The smallest As (III) and As (V) adsorptions occurred at pH 12, and at higher pH levels, such as 13.0 and 13.5, their adsorptions increased once again. The primary cause of the significant adsorption of As should be the electrostatic interactions between the As species and the TiO$_2$ surface [220]. Another work assessed the effects of solution pH and ionic strength on As (III) uptake by a new nanostructured iron-copper-manganese tri-metal oxide. As the pH of the solution increases, As (III) sorption decreases. Strong repulsive forces between the produced anions of As(V) and the surface of tri-metal oxide with a negative charge may be the reason for the relatively low adsorption of As(III) at high pH levels [221].

The impact of pH has been investigated (CMGO) in As (III) removal by a chitosan magnetic graphene oxide nanocomposite. The removal efficiency improved by increasing the pH from an acidic to a neutral pH; at an alkaline pH, it dropped. The maximum removal and adsorption capacities were attained at pH 7.3. The pH of the point zero charge (pH$_{pzc}$) of the nanocomposite was about 6.8. As a result, the surface of the adsorbent will be negatively charged at pH levels greater than pH$_{pzc}$ and positively charged at pH levels lower than pH$_{pzc}$. Thus, the surface of the CMGO is negatively charged, where the maximum As (III) was found. Since As (III) usually exists in the nonionic state (H$_3$AsO$_3$) at pH levels below 9.2, surface complexation rather than electrostatic interactions govern the adsorption of As(III) [155].

5.3.2. Temperature

The endothermic process experiences an increase in sorption capacity with increasing temperature, and the exothermic process exhibits a reduction in sorption capacity with increasing temperature [222]. As temperature has little effect on the adsorbent's ability to adsorb heavy metal, room temperature is frequently used in this kind of study [223].

Mussel shell powder was added to a Pb (II) solution, and the sample was stirred until equilibrium was achieved in the range of 293–308 K, in order to investigate the impact of temperature on the adsorption performance of the adsorbent. According to the results, as

the temperature was increased from 293 to 308 K, the *qe* of the calcined shell powder was improved from 53.86 to 65.41 mg g^{-1}. This may be due to increased molecular mobility at higher temperatures, which increases the likelihood that Pb (II) will come into contact with the adsorption sites [217]. As (V) removal effectiveness and modified saxaul ash removal effectiveness increased with temperature from 293 to 323 K. By increasing the temperature, the viscosity of the solution was reduced. The increased removal efficiency was also caused by increasing the release of adsorbent molecules in the pores of adsorbent particles and through the external boundary layer [224].

In the adsorption of lead and As ions by activated carbon from Tamarix leaves, the adsorption efficiency decreased upon an increase in the temperature between 25 and 55 °C, because heavy metal ions have a strong tendency to leave the adsorbent surface and return to the solution as the temperature goes up [225]. According to the findings of a different investigation, as the temperature increased from 25 to 45 °C, the percentage of As removed by co-modified bentonite with manganese oxides and poly (dimethyl diallyl ammonium chloride) increased gradually from 87% to 91%. This might be caused by an increase in the mobility of As species or by the adsorbate faster diffusion rate through the pores due to a reduction in the viscosity of the solution [226].

5.3.3. Contact Time

Since it influences the operation's economic viability and adsorption kinetics, it is crucial to determine the ideal contact time for the adsorption process [227]. A Pb (II) solution (100 mg L^{-1}) was mixed with shell powder (0.02 g), the pH was adjusted to 6, and the adsorption process was carried out at 25°C for 10–540 min. The results demonstrated the existence of more active sites that caused the calcined sample's adsorption capacity to grow quickly, 360 min after the process began. Due to the gradual saturation of the powdered calcined mussel shell, a further extension of the adsorption duration led to a marginal increase in the adsorption capacity. [217].

In another study, with increasing contact time, the effectiveness of removing cadmium increased from 56 to 78%, chromium from 90 to 94%, and lead from 93 to 96% [18]. The green mussel shell adsorbed more metal ions as the agitation time increased. After a certain amount of time, the adsorbent surface area slowly exhausts, reducing the adsorption capacity. According to the results, the equilibrium adsorption capacities for these metals were 2.1, 2.6, and 2.7 mg g^{-1}, obtained after 8 h (h). The uptake trend increased and then became constant after 8 h [228].

An experiment was conducted for 48 h with initial concentrations of 100, 500, and 1000 g L^{-1} of As (III) and 50 mg L^{-1} of nanoparticles to examine the influence of the contact time evaporation of As (III) and As (V) by Fe/Cu nanoparticles. The findings showed that most of the reaction occurs within the first hour [127]. According to the findings of an investigation on As (III) sorption (As(III) removal by a nanostructured iron-copper-manganese tri-metal oxide), the removal rate was rapid within the first 2 h, and over 85% of the equilibrium uptake capacity was achieved. Afterward, As(III) sorption began to slow down, and sorption equilibrium was attained after about 24 h [221]. Arsenic was quickly absorbed into the Fe-modified biochar and Cu-modified biochar adsorbent during the first 5–40 min, increasing significantly after that. The process continued at quite a slow rate until the equilibrium was achieved after 60 min. After 60 min of stirring, there was no noticeable change in the amount of As that was adsorbing; hence, 60 min was regarded as an effective equilibrium contact period for 95.3% As removal efficiency [219].

Furthermore, the impact of contact time on lead and As ion adsorption by activated carbon prepared from Tamarix leaves was examined for 5–120 min. After 60 and 40 min for lead and As, respectively, the adsorption efficiency stabilized, revealing that the adsorbent's active sites had been saturated [225]. Modified saxaul ash was used to remove As (V) from water-based solutions, and the As removal increased with longer contact times. The absorption rate was high in the first 30 min and equilibrium time was 60 min; changing As initial concentration did not affect the amount of time to reach equilibrium [224].

In general, the quantity of adsorption sites in the adsorbent structure is what causes the rapid adsorption process in the initial stages of the process. As a result of the ions occupying these sites, the efficiency starts to decline progressively, but after a period, no changes in the adsorption efficiencies are noticed. The occupation of the remaining unoccupied sites becomes more challenging as the contact time increases because of the gradual occupancy of the vacant sites and the ions-liquid phase repulsive interactions [225].

5.3.4. Initial Concentration

Increasing the initial metal ion concentration in a solution usually enhances the adsorption uptake [229]. A research study showed that as a function of equilibrium As and initial concentration, As adsorption on mussel shell ash increases linearly [230]. Another study showed that the adsorption capacity of Pb (II) on the calcined shell powder gradually increased from 14.72 to 57.79 mg g^{-1} as the starting lead concentration increased from 20 to 100 mg L^{-1}. Lower Pb (II) concentrations prevented the adsorbent from reaching saturation, whereas larger concentrations caused the accessible adsorption sites on the surface of the calcined shell powder to gradually fill up and attain saturation [217].

Batch mode investigations on the adsorption of heavy metals on the green mussel shell-derived adsorbent revealed that with an increase in the initial concentration from 1 to 20 mg L^{-1}, the removal efficiency of cadmium, chromium, and lead was changed from 80 to 59%, 28 to 92% and 79 to 95%, respectively. The pattern may be justified because a higher initial concentration of ions increases the adsorption capacity temporarily, but as the process progresses, an increasing amount of ions come into contact with fewer active sites on the adsorbent surface. [228]. Investigations were conducted on the removal efficiency of As by co-modified bentonite with manganese oxides and poly (dimethyl diallyl ammonium chloride) as a function of initial As concentrations between 0.25 and 2.00 mg L^{-1}. The removal efficiency of As was initially high, reaching 90% (initial concentration =0.25 mg L^{-1}), then constant for values between 0.25 and 0.5 mg L^{-1}, then gradually declined with increasing concentration, and finally, the decrease was rapid for the initial concentration higher than 1.5 mg L^{-1} [226]. In another study, 2 mg of nanofibers was fixed at a neutral pH by conducting the adsorption at various concentrations from 10 ppb to 10 ppm. The highest absorption of the porous carbon nanofibers was at 1 ppm concentration [231].

In the adsorption of lead and As by zeolite modified with copper oxide and iron oxide, initial concentrations of 20 to 100 mg L^{-1} did not significantly change the removal efficiency [232]. Changes in lead concentration between 1 mg L^{-1} and 180 mg L^{-1} were used to maximize removal efficiency by Bentonite clay. It was observed that lead removal efficiency increases initially upon an increase in the initial concentration. From 35 mg L^{-1}, the lead removal efficiency slightly declines. Adsorption reduces once the saturation level is reached since no more ions can be absorbed [233]. The reduction in the removal percentage at higher concentrations is likely because of the adsorbent's limited available active sites and the additional heavy metal ions that compete for these sites, which become more saturated as metal ion concentration increases. [232].

5.3.5. Adsorbent Dose

Adsorbent dose affects adsorption surface area and the number of exchangeable sites on the adsorbent's surface. If interference from active sites interacts after a specific dose limit, adsorption may stay the same or even decrease [234]. The effect of the mussel shell adsorbent dose (0.01–0.05 g) on the adsorption of Pb(II) was studied. The results showed that the removal rate increased from 41.21% to 65.08% as the adsorbent dose increased, while the q_e of the adsorbent steadily reduced from 82.42 to 26.03 mg g^{-1} [217]. This might be explained by taking into account the greater number of adsorption sites provided by increasing the shell powder concentration [228]. The authors decided that 1.0 mg mL^{-1} was the ideal adsorbent concentration for further testing [217].

The presence of larger concentrations of green mussel shell increased cadmium, chromium and lead removal efficiency from 50% to 67%, 70% to 93%, and 51% to 97%,

respectively. [228]. The percentage of As(III) adsorption rose with the increase in adsorbent dose, as the results of As removal by iron oxide/nano-porous carbon magnetic composite showed that 1.8 g L^{-1} of adsorbent removed the maximum percentage of As (about 75%). After that, an equilibrium was reached, and subsequent additions did not affect the percentage of adsorption [235]. The impact of the adsorbent dose on the As (III) adsorption was examined by adjusting the concentration of chitosan magnetic graphene oxide nanocomposite (CMGO) in the solution between 1 and 5 g L^{-1}. As the adsorbent dosage was increased from 1 to 5 g L^{-1}, the removal efficiency improved, but the adsorption capacity dropped [155].

According to the investigation of the effect of Fe/Cu nanoparticle dose (10–100 mg L^{-1}) on the removal of As (III) and As (V), the removal percentage increased with increasing adsorbent dose. However, the rate of increase in As removal was less noticeable when the dose of nanoparticles was increased from 50 to 100 mg L^{-1} [127]. The highest removal of As was determined to be nearly 98% at the adsorbent (co-modified bentonite with manganese oxides and poly (dimethyl diallyl ammonium chloride)) dosage of 15 mg/70 mL, according to the results of another experiment. The removal of As rose slowly with increasing adsorbent dosage. After a dosage of 15 mg/70 mL, the As removal percentage did not change noticeably [226]. The optimum quantity of clay for lead removal was identified for an initial metal concentration of 50 mg L^{-1} at a pH of 6 by adjusting the clay amount from 0.1 g to 0.9 g. It was found that as the clay dose increases, the adsorption efficiency increases. This is because the adsorbent's surface area increases. The optimum clay concentration for removing lead (Pb) was 0.3 g/50 mL [233].

Generally, increasing the number of adsorbent particles generates bigger surface areas and more accessible active sites, which in turn increase the adsorption capacity. Obviously, a higher adsorbent dose adsorbs more ions. In contrast, the decrease in the percentage of adsorption with a higher adsorbent dosage after a certain amount may be caused by the loss in adsorbent surface area due to the accumulation of adsorbent particles or the low quantity of ions in the solution in comparison to the accessible vacant sites, or interference between the high adsorbent dosage and active sites [232].

6. Arsenic Adsorbents

Some known adsorbents used to remove As are hydrous titanium dioxide (TiO$_2$)m [27], iron oxides/hydroxides [28], zeolites [29], activated carbon [225], and alumina [30]. Nanoparticles such as gold [32], cupric oxide [33], metal oxide nanomaterials [236], impregnated granulated activated carbon [237], and nanostructured Fe(III)– Cr(III) mixed oxides [35] have also been used in As removal. The literature showed that nanomaterials can be efficient adsorbents for heavy metal removal. Due to the toxic nature of As, scientists are seriously working on developing new adsorbents, which should be more rapid and cost-effective than reported methods. Table 16 provides examples of the efficiency of different adsorbents under different process conditions.

6.1. Low-Cost Adsorbents

Although commercial adsorbents such as activated carbon [238], activated alumina [30], and iron oxide-based [28] sorbents have shown high efficiency in removing As, finding economically feasible adsorbents and locally available solutions is still strongly desired. Nowadays, researchers investigate the application of natural materials, including soils [239], rocks [240], hydroxylapatite and struvite [241], zeolites [29], industrial wastes [242], polymer resins [243], and biosorbents [244]. Recent studies used low-cost adsorbents such as iron oxide-coated fungal biomass [245], methylated yeast biomass [246], residue rice polish [247], crab shells [248], modified coconut coir pith [249], cotton-based adsorbents [250], bone char [251], shrimp wastes [252], and modified sawdust [253]. The leading low-cost adsorbents used in recent studies can be classified as industrial waste, animal waste, natural materials, bio-adsorbent, and agricultural waste [5]. Table 17 provides an example of each category in specific conditions.

6.1.1. Industrial Waste (Fly Ash-Based Adsorbents)

The presence of toxic elements in fly ash makes this powdery material toxic; therefore, fly ash disposal is a challenging process [254]. Researchers have studied the application of waste material such as fly ash in different processes since the utilization of fly ash, rather than its disposal, has environmental and economic benefits. Fly ash can be efficiently used as a low-cost adsorbent of heavy metal and organic pollutants from water solutions and flue gas. Bagasse fly ash ($3 \, g \, L^{-1}$) at pH 7 and 20.0 °C removed 95.0 and 89.5% of As(V) and As(III) from water, respectively, after 50 min, with an initial concentration of $50 \, g \, L^{-1}$ [170]. Another adsorbent for As (V) removal was synthesized using special iron-abundant fly ash. The adsorption capacity of the adsorbent was $19.46 \, mg \, g^{-1}$, and removal efficiency was above 99% [255]. In another study, a low-cost adsorbent was developed to remove As from Bell Island's (NL, Canada) well water using modified fly ash from the Corner Brook Pulp and Paper (CBPP) mill. For local well water, the highest adsorption capacity was $35.6 \, \mu g \, g^{-1}$ and $1428.6 \, \mu g \, g^{-1}$ for local well water and synthetic water, respectively [256].

Coal, as a source of energy in electric power generation, produces tons of fly ash worldwide. Coal fly ash (CFA) is 65–95% of the total ash generated by burning coal. Some coals contain high ash content (30–50%), while others have a low ash content, of the order of 10–15% [257–259]. The type of coal that is burned (anthracite, bituminous, sub-bituminous, and lignite) and the way it is handled and stored affect the coal fly ash chemical properties. The main components of fly ash are generally carbon, silica, alumina, iron oxide, and calcium. Using fly ash in heavy metal adsorbents not only prevents environmental problems caused by this contaminant but also is a convincing way to remove heavy metal pollutants from water and wastewater streams [260].

Burning biomass is another source of fly ash that causes environmental problems; however, in contrast to coal ash, there are no toxic metals in fly ash produced after burning biomass. The composition of this type of fly ash depends on the type of the original biomass. The combustion method determines the crystallinity and mineralogy of this fly ash.

In general, Ca, Na, Si, P, and silicon and alkali metals, in some cases, are the inorganic elements that form biomass fly ash. Biomass fuels have higher concentrations and amounts of inorganic material variation than coal. Therefore, depending on the origin of the biomass and production factors such as weather and storage conditions, there are various compositions of biomass fly ash [261–263]. Due to this variation, there are not sufficient records of the utilization of biomass fly ash in contrast to coal fly ash. However, several studies have demonstrated the applications of biomass fly ash as an adsorbent [264], raw material for ceramics [265], cement [266], and concrete additive [267]. Table 18 provides the chemical composition of several types of fly ash.

6.1.2. Animal Waste (Fisheries Waste-Based Adsorbents)

Crab shell has been used to prepare an adsorbent to remove heavy metal ions (Pb, Cd, Cu, Cr) from solutions. The preparation procedure included separating the shell and meat by boiling or steaming, washing, and drying the shell, and finally pulverizing the dried shell. Compared to conventional methods, crab shells showed a higher removal rate than cation exchange resin (CER), zeolite, powdered activated carbon, and granular activated carbon for Pb, Cd, and Cr. In contrast, the capacity of the crab shell was less than CER for Cu [4]. In another study, calcined mussel shell showed an adsorption capacity of 102.04 $mg \, g^{-1}$ for lead removal, proving that calcined mussel shell is a promising adsorbent for heavy metals [217].

Table 16. Different adsorbents used in arsenic removal, their operating conditions, and efficiencies for arsenic removal.

Adsorbent	Conditions	RE (%) and/or AC (mg g^{-1})	Ref.
Activated alumina	pH: 7.6, IC (As(III)) = 1 mg L^{-1} Contact time: 0–6 h	RE: 96.2 As(III) Rapid removal	[268]
Manganese oxide	pH:7.9 IC: <1 mg L^{-1}	AC: (As (V)): 0.172	[269]
Porous resin loaded with crystalline hydrous zirconium oxide	IC: 0–5 mmol L^{-1} pH4.5 for As(V), pH: 8.0 for As(III)	Equilibrium time: ≥6 h AC (As(V)): 79.42, AC (As(III)): 53.94	[270]
Iron-oxide-impregnated activated carbon	Adsorbent concentrations 0–0.2 g L^{-1} pH: 7 IC (As(V)): 1 mg L^{-1}	AC: 4.5	[271]
Titanium dioxide-loaded Amberlite XAD-7 resin	pH (As(v)): 1–5, pH (As(III)): 5–10 Contact time (As(v)): 6 h Contact time (As(III)): 2 h	AC (As(V)): 9.74 AC (As(III)): 4.72	[272]

RE = Removal efficiency; AC = Adsorption capacity (mg (As) g^{-1} (Adsorbent)); IC = Initial concentration.

Table 17. The results of using some low-cost adsorbents in arsenic removal.

Adsorbate	Adsorbent	pH	Temperature (°C)	Contact Time (h)	As IC (mg L^{-1})	Adsorbent Dose (g L^{-1})	Max RE (%)	Max AC (mg g^{-1})	Ref.
As(III) As(V)	Industrial waste (fly ash)	7.3	20	24	1	0.5	87.6 99.6	-	[256]
As(V)	Animal waste (mussel shell)	~10	-	24	0.5–100	100	96	-	[230]
As(V)	Agricultural waste (1: natural orange peel 2: charred orange peel)	6.5	20	24	200	4	68 98	32.7 60.9	[273]
As(III)	Natural materials (Fe–Mn binary oxides-loaded zeolite)	7.0	25	3	2 mg L^{-1}	0.5	99	-	
As(III) As(V)	Biosorbent (modified chitosan beads)	7.0	25	36	5–60	1	-	54.2 39.1	[198]

RE = Removal efficiency; AC = Adsorption capacity (mg (As) g^{-1} (Adsorbent)); IC = Initial concentration.

Fish scales are another available waste that is abundant and easy to prepare as an adsorbent. Fish scales were used to investigate their efficiency in removing lead (II) and zinc (II) ions [274,275]. In a study, fish scales were used in batch adsorption experiments. The results proved the potential of fish scales for lead (II) and zinc (II) removal with a maximum removal efficiency of 81.97% and 80.37%, respectively [276].

Fish bones have been used to remove copper and cobalt from wastewater. The results revealed that the contact time for equilibrium is 270 min for Cu (II) and 300 min for Co (II). By increasing the initial metal concentration from 50 ppm to 300 ppm, the removal efficiency dropped from almost 40% to nearly 25% [143].

Table 18. Chemical composition of coal and biomass fly ash [277–279].

Fly Ash Type	SiO_2	CaO	Al_2O_3	Fe_2O_3	K_2O	MgO	Na_2O	P_2O_5	TiO_2
Coal	54.08	3.27	26.38	6.12	1.64	1.55	0.51	0.80	1.44
Biomass	36.03	27.41	8.33	4.12	4.92	3.56	0.87	3.21	0.94
Biomass	44.41	23.84	10.80	3.63	3.99	3.76	1.27	2.02	1.05
Biomass	20.38	40.13	8.20	17.40	2.41	3.26	0.43	3.20	0.42
Biomass	37.43	10.96	12.97	9.74	3.21	2.30	1.50	1.61	0.91

6.1.3. Natural Materials (Zeolites)

HDTMA-Br and HDTMA-Cl as surfactants were employed to modify two natural zeolites (clinoptilolite and phillipsite). These developed adsorbents were synthesized and evaluated as adsorbents for As(V) removal from wastewater. Results revealed that As(V) removal has a fast adsorption rate and follows a pseudo-second-order kinetic model, with 100% removal occurring in all samples in 2 h [280]. In another study, the adsorption capacity of zeolite (Z, micrometric size), nanomagnetite (Mt), and a nanomagnetite-zeolite composite (MtZ) were found to be 0.3, 4.7 and 6.2 mg g^{-1} for the adsorption of arsenate in hydroponic tomato cultures, respectively [281]. The application of 2D zeolitic imidazolate framework-67 porous nanosheets (ZIF-67-NS) was evaluated as a potential adsorbent for As(III) removal from water. In contrast to its 3D bulk-type counterpart, ZIF-67-NS showed much better adsorption capacity (516 mg g^{-1}) and faster absorption kinetics (2 h) (ZIF-67-NB). After three cycles, ZIF-67-NS was effectively regenerable, with minimal adsorption capacity loss [282].

6.1.4. Bio-Adsorbent (Chitin/Chitosan)

Silica-stabilized hybrid chitosan microspheres were used to remove As from water. When compared to chitosan beads alone, hybrid beads have a higher As(V) adsorption efficiency because the addition of magnetite (Fe_3O_4) nanoparticles increases the beads' surface area. Furthermore, the hybrid and chitosan beads' adsorption capacities were 1.699 and 0.082 mg g^{-1}, respectively [283]. Fe-Mn binary oxide was impregnated into chitosan beads to produce a sorbent known as Fe-Mn binary oxide impregnated chitosan bead (FMCB). The highest adsorption capacities for As(V) and As(III) were 39.1 and 54.2 mg g^{-1}, respectively. NaOH solution could be employed to effectively regenerate and reuse the As-loaded FMCB [198]. In another study, chitin was pyrolyzed and treated with nitric acid to increase surface area. Then, Ca(OH)2 was loaded onto the char to develop a new type of biomaterial to eliminate As. According to the kinetic experiments, an adsorbent dosage of 0.4 g L^{-1} and a concentration of 10 mg L^{-1} produced an optimal equilibrium time of 2 h. The highest removal efficiency was around 99.8% with 0.4 g L^{-1} of adsorbent [284].

6.1.5. Agricultural Waste (Fruit Peels)

Column-scale laboratory experiments were conducted using synthetic solutions and groundwater to determine the As removal efficiency by orange peel and banana peel. In

As-contaminated groundwater of 5, 10, and 50 μg L^{-1} after 1 h, the removal efficiency of both adsorbents was 100%, 100%, and 90%, respectively. In synthetic As-spiked water of 10, 50, and 100 μg L^{-1}, the removal efficiency was 50%, 90%, and 90%, respectively [285]. Batch sorption studies were used to compare the biosorption capacities of natural orange peel (NOP) and charred orange peel (COP) for As(V) removal in aqueous environments. The largest amount of As(V) adsorption occurred at pH 6.5, and COP removed As(V) by 98%, which was higher than that obtained by NOP (68%) at the optimal adsorbent dose of 4 g L^{-1} [273]. The peel (PAC-500) and pulp (PPAC-500) of the Citrus limmeta fruit were used to develop activated carbon with magnetic characteristics at 500 °C. The PAC-500 has a higher As (III) adsorption capacity (714.3 g g^{-1}) than the PPAC-500 (526.316 g g^{-1}). For As (V) removal, PAC-500 and PPAC-500 showed an adsorption capability of 2000 g g^{-1}. Concentrations < 300 g L^{-1} were completely removed by PAC-500 and PPAC-500 [286].

7. Application of Adsorption in Drinking Water Treatment Systems

Adsorption is regarded as the most economically advantageous method for removing As for small communities because of its high removal and energy efficiency, ease of design and operation, and minimum disposal cost and toxicity. As can be removed from water using commercial adsorbents such as activated carbon. However, its relatively high cost might exclude its use in rural areas [41]. Numerous adsorbents have been developed over recent years; however, few options are efficient, affordable, or easy to install, particularly in developing nations [105]. Another challenge is that removing fine powder adsorbents from the water after adsorption is not easy. Additionally, fine powders may block the filters and cause hydraulic issues in columns, increasing the energy and maintenance costs [41]. Granulating the adsorbents and using them in fixed-bed filters represents a common solution to this issue; however, these treatments significantly reduce the active sites available for As and raise the price of adsorbents' production [105,287]. When fine particles or micro-sized fractions (<250 μm) are used in a fluidized-bed reactor for As removal, a downstream membrane reactor is required to separate the adsorbent [287]. The necessity to regenerate and reuse adsorbents to lower costs adds another difficulty. The regenerating process requires strong basic solutions, which challenge the maintenance of the reactors and the treatment of basic waste [105]. As a result, these important issues must be solved to promote adsorption in decentralized systems. More research and engineering investigations are required to successfully employ adsorption in the treatment of community drinking water supplies, since most adsorption studies are limited to laboratory-scale experiments. Table 19 includes several pilot-size (small-scale) investigations of As removal by different treatment methods.

Table 19. Arsenic removal efficiency by different methods (pilot scale).

	Removal Agent	Flowrate (m^3 d^{-1}) /Volume	Initial Concentration (μg L^{-1})	Removal (%)/Final Concentration (μg L^{-1})	Other Available Data	Ref.
Adsorption	ZVI adsorption–aeration	0.14–1.4	130	90–95	Operation life: 30 days Initial ZVI loading = 500 g	[288]
	Laterite	5	220–300	86.0	Mn: 96.9%, Cd: 79.6%, Zn: 52.9%, and Pb: 38.7%.	[289]
	GFH-based adsorbent	96–3840	12–28	>80	Hydraulic EBCT: 3–10 min pH = 7–8	[290]
	ZVI two-steps system	1.44	100–130	77–96	Adsorption capacity: 20.5 mgAs/gFe Neutral pH	[291]
	TiO$_2$-based adsorption	52	32	91	Initial fluorides: 2.8 mg L^{-1}	[292]
	Mixes of Berea red sand and ZVIs	0.006–0.290	13,000–17,000	100	Porosity: 38–60% Void ratio (e): 0.6–1.5 Specific gravity: 4.3–7 g cm^{-3}	[293]
Ion Exchange	Arsenex II (SBA type II)	2943	16.7	<10 μg L^{-1}	Empty-bed contact time: (2.6 min) Regeneration frequency: 1.7 day	[48]
	A300E (SBA type II)	1362	49.7	<10 μg L^{-1}	Empty-bed contact time: (4.8 min) Regeneration frequency: 1.7 day	[48]
	npXtra system (Arsenex)	1.47	15–68	0 μg L^{-1}	pH = 6.8	[294]
	npXtra system (Arsenex)	0.71	27–47	4.5 μg L^{-1}	pH = 7.8	[294]
	npXtra system (Arsenex)	1.18	173	6 μg L^{-1}	pH = 7.1	[294]
Membrane	POE RO	4.5	18.1	>99	Sediment filter pore size: 5 μm	[48]
	POU RO	0.13	57.8	>99	Sediment filter pore size: 20 μm	[48]
	POU RO	variable	14.34	85.5	261 samples (100 mL)	[295]
	Softener + RO	variable	9.76	19	261 samples (100 mL)	[295]
Coagulation	Naturally occurring Fe + oxidizing agent (KMnO$_4$)	Jar test (1L) simulating groundwater of the Bengal Delta	1000 500	50 μg L^{-1}: (Fe/As < 13) 10 μg L^{-1}: (Fe/As > 13)	pH = 6.0–7.5	[296]
	Iron electrocoagulation (FeEC)	reactor volume:100 L	153.2	<10 μg L^{-1}	Current: 5.8 A Charge dose: 100 C/L Alum: 7.5 mg L^{-1}	[297]

Table 19. *Cont.*

	Removal Agent	Flowrate ($m^3\ d^{-1}$) /Volume	Initial Concentration ($\mu g\ L^{-1}$)	Removal (%)/Final Concentration ($\mu g\ L^{-1}$)	Other Available Data	Ref.
	SuMeWa⏐SYSTEM + chlorine as oxidant	1.44	300	96	pH= 5.56–7.05	[298]
	Iron electrocoagulation (FeEC)	1.87	118	30 $\mu g\ L^{-1}$ (<5 min) 20 $\mu g\ L^{-1}$ (>5 min)	Retention time: 19 s Charge dose: 233 C L^{-1} Alum: 5 mg L^{-1}	[299]
Oxidation	Solar-driven inline-electrolytic oxidation followed by co-precipitation and filtration	1.2–1.44	187 202 195 165	80 88 76 94	In situ chlorine production using water chloride, Fe > 99%, MN: 96%, PO$_4$: 72%, NH$_4$: 84%	[300]
	Oxidation with sodium hypochlorite (0.33 mg L^{-1}) followed by filtration	840	12	95	Laboratory scale result: removing As from 18 to 2 $\mu g\ L^{-1}$	[301]
	Bio-oxidation (immobilized acid othiobacillus ferrooxidans bacteria) followed by adsorptive filtration (granulated activated carbon)	0.004	1000 to 30,000	>50 (after oxidation)	Final concentration: 0.2 mg L^{-1} (after adsorptive filtration)	[302]

8. Conclusions

Water contamination with toxic heavy metals, such as arsenic, is one of the most significant environmental issues worldwide. Arsenic must be removed from drinking water because it has many negative impacts, including neurotoxicity and carcinogenicity. Many methods can be used to remove arsenic from water. In the present review paper, various As removal methods with a particular focus on adsorption have been reviewed. The reviewed literature confirms the application of oxidation, ion exchange, coagulation-flocculation, adsorption, etc., in heavy metal removal from drinking water. However, technical and financial challenges affect the feasibility of these techniques for small communities' decentralized systems. In other words, the simplicity, affordability, and availability of the material, equipment, and skilled operators are the major factors that should be considered to find an ideal solution for small communities. With these considerations, adsorption is a very appealing option for decentralized systems of arsenic removal because of the ease of installation and use and also the low-cost and straightforward operational process.

Common adsorbents such as commercial activated carbon, nanomaterials, composites and miscellaneous adsorbents have been used in heavy metal removal from water sources. However, cost-effective adsorbents such as agricultural, industrial or animal waste, natural materials, and bio-adsorbent should be employed to keep costs low and increase the effectiveness of heavy metal removal. In most adsorption studies, physical characteristics of conventional or cost-effective adsorbents have been analyzed through techniques such as SEM, DLS, XRD, BET-surface area, etc., while the common methods such as XRF, CHN/O, FT-IR, zeta potential, etc., were widely used for chemical characterization. It should be noted that there are some considerations that should be taken because adsorption effectiveness depends on various factors, including the initial concentration of arsenic ions, pH levels, adsorbent dose, contact time, and temperature. In terms of kinetic and isotherm modelling, it seems that the pseudo-second-order model and Freundlich isotherm provide a more accurate fit to the arsenic adsorption data.

The research knowledge gaps should be filled through further investigations on arsenic removal in water by adsorption. First, more studies should focus on the bench-scale and large-scale application of arsenic adsorption from drinking water supplies, including surface and groundwater. Moreover, since financial resources are usually limited in small communities, cost-effectiveness and cost-benefit studies need to be conducted in greater detail. Furthermore, the adsorbent removal effectiveness and capacity should be improved to be able to use low-cost adsorbents for industrial purposes and at a large scale, as alternatives for commercial adsorbents. For this purpose, it is necessary to carry out more research on the impact of surface modification on removal efficiency. Additionally, the applicability of the integrated systems, such as photocatalytic-adsorption or adsorption-membrane, and other possible combinations of different methods in decentralized water treatment systems should be examined, to improve efficiency and overcome the drawbacks of each particular technique. Finally, to save time and cost, more modelling studies, particularly multi-scale modelling, are required to predict removal performance before running numerous experiments.

Author Contributions: Conceptualization, N.M.C.S. and C.B.; literature review, R.S.N., N.M.C.S. and B.A.; analysis of the literature data, R.S.N., N.M.C.S., S.Z. and A.A.-n.; writing—original draft preparation, R.S.N., N.M.C.S., S.Z., A.A.-n., B.A. and P.C.; writing—review and editing, R.S.N., N.M.C.S., C.B., S.Z., B.A., A.A.-n. and P.C.; visualization, R.S.N.; funding acquisition, N.M.C.S. and C.B. All authors have read and agreed to the published version of the manuscript.

Institutional Review Board Statement: Not applicable.

Informed Consent Statement: Not applicable.

Data Availability Statement: Data sharing is not applicable.

Conflicts of Interest: The authors declare no conflict of interest. The funders had no role in the design of the study; in the collection, analyses, or interpretation of data; in the writing of the manuscript; or in the decision to publish the results.

References

1. Li, Z.; Ma, Z.; van der Kuijp, T.J.; Yuan, Z.; Huang, L. A Review of Soil Heavy Metal Pollution from Mines in China: Pollution and Health Risk Assessment. *Sci. Total Environ.* **2014**, 468–469. [CrossRef]
2. Tchounwou, P.B.; Yedjou, C.G.; Patlolla, A.K.; Sutton, D.J. *Heavy Metal Toxicity and the Environment*. EXS 2012, 101. Available online: https://sci-hub.mksa.top/10.1007/978-3-7643-8340-4_6 (accessed on 13 December 2022).
3. Karcioglu, O.; Arslan, B. *Poisoning in the Modern World: New Tricks for an Old Dog?* BoD–Books on Demand: Norderstedt, Germany, 2019; ISBN 1838807853. [CrossRef]
4. An, H.K.; Park, B.Y.; Kim, D.S. Crab Shell for the Removal of Heavy Metals from Aqueous Solution. *Water Res.* **2001**, *35*. [CrossRef] [PubMed]
5. Chakraborty, R.; Asthana, A.; Singh, A.K.; Jain, B.; Susan, A.B.H. Adsorption of Heavy Metal Ions by Various Low-Cost Adsorbents: A Review. *Int. J. Environ. Anal. Chem.* **2022**, *102*, 342–379. [CrossRef]
6. Lata, S.; Samadder, S.R. Removal of Arsenic from Water Using Nano Adsorbents and Challenges: A Review. *J. Environ. Manag.* **2016**, *166*, 387–406. [CrossRef]
7. Shaji, E.; Santosh, M.; Sarath, K.V.; Prakash, P.; Deepchand, V.; Divya, B. V Arsenic Contamination of Groundwater: A Global Synopsis with Focus on the Indian Peninsula. *Geosci. Front.* **2021**, *12*, 101079. [CrossRef]
8. Otgon, N.; Zhang, G.; Yang, C. Arsenic Removal from Waste Water by Ozone Oxidation Combined with Ferric Precipitation. *Mong. J. Chem.* **2016**, *17*, 18–22.
9. Al-Ali, F.; Barrow, T.; Duan, L.; Jefferson, A.; Louis, S.; Luke, K.; Major, K.; Smoker, S.; Walker, S.; Yacobozzi, M. Vertebral Artery Ostium Atherosclerotic Plaque as a Potential Source of Posterior Circulation Ischemic Stroke: Result from Borgess Medical Center Vertebral Artery Ostium Stenting Registry. *Stroke* **2011**, *42*, 2544–2549. [CrossRef] [PubMed]
10. Moon, K.; Guallar, E.; Navas-Acien, A. Arsenic Exposure and Cardiovascular Disease: An Updated Systematic Review. *Curr. Atheroscler. Rep.* **2012**, *14*, 542–555. [CrossRef]
11. Moon, K.A.; Guallar, E.; Umans, J.G.; Devereux, R.B.; Best, L.G.; Francesconi, K.A.; Goessler, W.; Pollak, J.; Silbergeld, E.K.; Howard, B. V Association between Exposure to Low to Moderate Arsenic Levels and Incident Cardiovascular Disease: A Prospective Cohort Study. *Ann. Intern. Med.* **2013**, *159*, 649–659. [CrossRef]
12. Kunrath, J.; Gurzau, E.; Gurzau, A.; Goessler, W.; Gelmann, E.R.; Thach, T.-T.; Mccarty, K.M.; Yeckel, C.W. Blood Pressure Hyperreactivity: An Early Cardiovascular Risk in Normotensive Men Exposed to Low-to-Moderate Inorganic Arsenic in Drinking Water. *J. Hypertens.* **2013**, *31*, 361. [CrossRef]
13. Mazumder, D.N.G. Effect of Chronic Intake of Arsenic-Contaminated Water on Liver. Toxicol. *Appl. Pharmacol.* **2005**, *206*, 169–175. [CrossRef]
14. Viraraghavan, T.; Subramanian, K.S.; Aruldoss, J.A. Arsenic in Drinking Water—Problems and Solutions. *Water Sci. Technol.* **1999**, *40*, 69–76. [CrossRef]
15. Smedley, P.L.; Kinniburgh, D.G. A Review of the Source, Behaviour and Distribution of Arsenic in Natural Waters. *Appl. Geochem.* **2002**, *17*, 517–568. [CrossRef]
16. Gong, Z.; Lu, X.; Ma, M.; Watt, C.; Le, X.C. Arsenic Speciation Analysis. *Talanta* **2002**, *58*, 77–96. [CrossRef]
17. Bissen, M.; Frimmel, F.H. Arsenic—A Review. Part II: Oxidation of Arsenic and Its Removal in Water Treatment. *Acta Hydrochim. Hydrobiol.* **2003**, *31*, 97–107. [CrossRef]
18. Flora, S.J.S. Arsenic: Chemistry, Occurrence, and Exposure. In *Handbook of Arsenic Toxicology*; Elsevier: Amsterdam, The Netherlands, 2015; pp. 1–49.
19. O'Day, P.A. Chemistry and Mineralogy of Arsenic. *Elements* **2006**, *2*, 77–83. [CrossRef]
20. Mohanty, D. Conventional as Well as Emerging Arsenic Removal Technologies—A Critical Review. *Water Air Soil Pollut.* **2017**, *228*, 1–21. [CrossRef]
21. Huang, H.-H. The Eh-PH Diagram and Its Advances. *Metals* **2016**, *6*, 23. [CrossRef]
22. Aghaei, E.; Wang, Z.; Tadesse, B.; Tabelin, C.B.; Quadir, Z.; Alorro, R.D. Performance Evaluation of Fe-Al Bimetallic Particles for the Removal of Potentially Toxic Elements from Combined Acid Mine Drainage-Effluents from Refractory Gold Ore Processing. *Minerals* **2021**, *11*, 590. [CrossRef]
23. Rakhunde, R.; Jasudkar, D.; Deshpande, L.; Juneja, H.D.; Labhasetwar, P. Health Effects and Significance of Arsenic Speciation in Water. *Int. J. Environ. Sci. Res.* **2012**, *1*, 92–96.
24. Asere, T.G.; Stevens, C.V.; Du Laing, G. Use of (Modified) Natural Adsorbents for Arsenic Remediation: A Review. *Sci. Total Environ.* **2019**, *676*, 706–720. [CrossRef]
25. Mondal, M.K.; Garg, R. A Comprehensive Review on Removal of Arsenic Using Activated Carbon Prepared from Easily Available Waste Materials. Environ. *Sci. Pollut. Res.* **2017**, *24*, 13295–13306. [CrossRef] [PubMed]

26. Mazumder, D.G.; Dasgupta, U.B. Chronic Arsenic Toxicity: Studies in West Bengal, India. *Kaohsiung J. Med. Sci.* **2011**, *27*, 360–370. [CrossRef] [PubMed]

27. Guan, X.; Du, J.; Meng, X.; Sun, Y.; Sun, B.; Hu, Q. Application of Titanium Dioxide in Arsenic Removal from Water: A Review. *J. Hazard. Mater.* **2012**, *215*, 1–16. [CrossRef] [PubMed]

28. Hao, L.; Liu, M.; Wang, N.; Li, G. A Critical Review on Arsenic Removal from Water Using Iron-Based Adsorbents. *RSC Adv.* **2018**, *8*, 39545–39560. [CrossRef]

29. Shevade, S.S. Utility of Zeolites in Arsenic Removal from Water. In Proceedings of the Abstracts of Papers of the American Chemical Society 1155 16th St, Nw, Washington, DC, USA, 7–11 September 2003; Volume 226, pp. U589–U590.

30. Camacho, L.M.; Ponnusamy, S.; Campos, I.; Davis, T.A.; Deng, S. Evaluation of Novel Modified Activated Alumina as Adsorbent for Arsenic Removal. In *Handbook of Arsenic Toxicology*; Elsevier: Amsterdam, The Netherlands, 2015; pp. 121–136.

31. Habuda-Stanić, M.; Nujić, M. Arsenic Removal by Nanoparticles: A Review. *Environ. Sci. Pollut. Res.* **2015**, *22*, 8094–8123. [CrossRef]

32. Hua, J. Synthesis and Characterization of Gold Nanoparticles (AuNPs) and ZnO Decorated Zirconia as a Potential Adsorbent for Enhanced Arsenic Removal from Aqueous Solution. *J. Mol. Struct.* **2021**, *1228*, 129482. [CrossRef]

33. Reddy, K.J.; McDonald, K.J.; King, H. A Novel Arsenic Removal Process for Water Using Cupric Oxide Nanoparticles. *J. Colloid Interface Sci.* **2013**, *397*, 96–102. [CrossRef]

34. Kalaruban, M.; Loganathan, P.; Nguyen, T.V.; Nur, T.; Johir, M.A.H.; Nguyen, T.H.; Trinh, M.V.; Vigneswaran, S. Iron-Impregnated Granular Activated Carbon for Arsenic Removal: Application to Practical Column Filters. *J. Environ. Manag.* **2019**, *239*, 235–243. [CrossRef]

35. Basu, T.; Ghosh, U.C. Influence of Groundwater Occurring Ions on the Kinetics of As (III) Adsorption Reaction with Synthetic Nanostructured Fe (III)–Cr (III) Mixed Oxide. *Desalination* **2011**, *266*, 25–32. [CrossRef]

36. Balouch, A.; Jagirani, M.S.; Mustafai, F.A.; Tunio, A.; Sabir, S.; Mahar, A.M.; Rajar, K.; Shah, M.T.; Samoon, M.K. Arsenic Remediation by Synthetic and Natural Adsorbents. *Pak. J. Anal. Environ. Chem.* **2017**, *18*, 18–36.

37. Bhowmik, T.; Sarkar, S.; Bhattacharya, A.; Mukherjee, A. A Review of Arsenic Mitigation Strategies in Community Water Supply with Insights from South Asia: Options, Opportunities and Constraints. *Environ. Sci. Water Res. Technol.* **2022**, *8*, 2491–2520. [CrossRef]

38. Adeloju, S.B.; Khan, S.; Patti, A.F. Arsenic Contamination of Groundwater and Its Implications for Drinking Water Quality and Human Health in Under-Developed Countries and Remote Communities—A Review. *Appl. Sci.* **2021**, *11*, 1926. [CrossRef]

39. Gikas, P.; Tchobanoglous, G. The Role of Satellite and Decentralized Strategies in Water Resources Management. *J. Environ. Manag.* **2009**, *90*, 144–152. [CrossRef] [PubMed]

40. Zaharia, C. Decentralized Wastewater Treatment Systems: Efficiency and Its Estimated Impact against Onsite Natural Water Pollution Status. A Romanian Case Study. *Process Saf. Environ. Prot.* **2017**, *108*, 74–88. [CrossRef]

41. Nguyen, T.H.; Tran, H.N.; Vu, H.A.; Trinh, M.V.; Nguyen, T.V.; Loganathan, P.; Vigneswaran, S.; Nguyen, T.M.; Vu, D.L.; Nguyen, T.H.H. Laterite as a Low-Cost Adsorbent in a Sustainable Decentralized Filtration System to Remove Arsenic from Groundwater in Vietnam. *Sci. Total Environ.* **2020**, *699*, 134267. [CrossRef] [PubMed]

42. Qu, X.; Brame, J.; Li, Q.; Alvarez, P.J.J. Nanotechnology for a Safe and Sustainable Water Supply: Enabling Integrated Water Treatment and Reuse. *Acc. Chem. Res.* **2013**, *46*, 834–843. [CrossRef]

43. Le, D.Q.; Pham, T.T.; Pham, H.G.; Nguyen, M.K. Evaluation of Iron-Rich Adsorbent to Remove Arsenic from Groundwater in Decentralized Water Supply Treatment. *Vietnam. J. Sci. Technol. Eng.* **2018**, *60*, 78–81. [CrossRef]

44. Nanseu-Njiki, C.P.; Gwenzi, W.; Pengou, M.; Rahman, M.A.; Noubactep, C. Fe0/H2O Filtration Systems for Decentralized Safe Drinking Water: Where to from Here? *Water* **2019**, *11*, 429. [CrossRef]

45. Decentralized Water Treatment Market | Size, Growth | 2021-26. Available online: https://www.arizton.com/market-reports/decentralized-water-treatment-market (accessed on 13 December 2022).

46. Kabir, F.; Chowdhury, S. Arsenic Removal Methods for Drinking Water in the Developing Countries: Technological Developments and Research Needs. *Environ. Sci. Pollut. Res.* **2017**, *24*, 24102–24120. [CrossRef]

47. Nalbandian, M.J.; Kim, S.; Gonzalez, H.; Myung, N.V.; Cwiertny, D.M. Recent Advances and Remaining Barriers to the Development of Electrospun Nanofiber and Nanofiber Composites for Point-of-Use and Point-of-Entry Water Treatment Systems. *J. Hazard. Mater. Adv.* **2022**, *8*, 100204. [CrossRef]

48. Chen, A.S.C.; Wang, L.; Sorg, T.J.; Lytle, D.A. Removing Arsenic and Co-Occurring Contaminants from Drinking Water by Full-Scale Ion Exchange and Point-of-Use/Point-of-Entry Reverse Osmosis Systems. *Water Res.* **2020**, *172*, 115455. [CrossRef]

49. Sarode, S.; Upadhyay, P.; Khosa, M.A.; Mak, T.; Shakir, A.; Song, S.; Ullah, A. Overview of Wastewater Treatment Methods with Special Focus on Biopolymer Chitin-Chitosan. *Int. J. Biol. Macromol.* **2019**, *121*, 1086–1100. [CrossRef]

50. Al-Asheh, S.; Aidan, A. A Comprehensive Method of Ion Exchange Resins Regeneration and Its Optimization for Water Treatment. In *Promising Techniques for Wastewater Treatment and Water Quality Assessment*; IntechOpen, 2020; ISBN 1838819010. [CrossRef]

51. Zakhar, R.; Derco, J.; Cacho, F. An Overview of Main Arsenic Removal Technologies. *Acta Chim. Slovaca* **2018**, *11*, 107–113. [CrossRef]

52. Kartinen, E.O., Jr.; Martin, C.J. An Overview of Arsenic Removal Processes. *Desalination* **1995**, *103*, 79–88. [CrossRef]

53. Dixit, F.; Dutta, R.; Barbeau, B.; Berube, P.; Mohseni, M. PFAS Removal by Ion Exchange Resins: A Review. *Chemosphere* **2021**, *272*, 129777. [CrossRef]

54. Höll, W.H. Mechanisms of Arsenic Removal from Water. Environ. *Geochem. Health* **2010**, *32*, 287–290. [CrossRef]
55. Petrusevski, B.; Sharma, S.; Schippers, J.C.; Shordt, K. Arsenic in Drinking Water. Delft IRC Int. *Water Sanit. Cent.* **2007**, *17*, 36–44.
56. Fox, K.R. Field Experience With Point-of-Use Treatment Systems for Arsenic Removal. *J.-Am. Water Work Assoc.* **1989**, *81*, 94–101. [CrossRef]
57. Wang, L.; Chen, A.; Fields, K. *Arsenic Removal from Drinking Water by Ion Exchange and Activated Alumina Plants*; Environmental Protection Agency: Cincinnati, OH, USA, 2000.
58. Greenleaf, J.E.; Lin, J.C.; Sengupta, A.K. Two Novel Applications of Ion Exchange Fibers: Arsenic Removal and Chemical-Free Softening of Hard Water. *Environ. Prog.* **2006**, *25*. [CrossRef]
59. Urbano, B.F.; Rivas, B.L.; Martinez, F.; Alexandratos, S.D. Water-Insoluble Polymer-Clay Nanocomposite Ion Exchange Resin Based on N-Methyl-d-Glucamine Ligand Groups for Arsenic Removal. *React. Funct. Polym.* **2012**, *72*. [CrossRef]
60. Çermikli, E.; Şen, F.; Altıok, E.; Wolska, J.; Cyganowski, P.; Kabay, N.; Bryjak, M.; Arda, M.; Yüksel, M. Performances of Novel Chelating Ion Exchange Resins for Boron and Arsenic Removal from Saline Geothermal Water Using Adsorption-Membrane. *Filtr. Hybrid Process. Desalination* **2020**, *491*, 114504. [CrossRef]
61. Zhang, X.; Jiang, K.; Tian, Z.; Huang, W.; Zhao, L. Removal of Arsenic in Water by an Ion-exchange Fiber with Amino Groups. *J. Appl. Polym. Sci.* **2008**, *110*, 3934–3940. [CrossRef]
62. Lee, C.-G.; Alvarez, P.J.J.; Nam, A.; Park, S.-J.; Do, T.; Choi, U.-S.; Lee, S.-H. Arsenic (V) Removal Using an Amine-Doped Acrylic Ion Exchange Fiber: Kinetic, Equilibrium, and Regeneration Studies. *J. Hazard. Mater.* **2017**, *325*, 223–229. [CrossRef]
63. Rathi, B.S.; Kumar, P.S.; Ponprasath, R.; Rohan, K.; Jahnavi, N. An Effective Separation of Toxic Arsenic from Aquatic Environment Using Electrochemical Ion Exchange Process. *J. Hazard. Mater.* **2021**, *412*, 125240. [CrossRef] [PubMed]
64. Ghurye, G.L.; Clifford, D.A.; Tripp, A.R. Combined Arsenic and Nitrate Removal by Ion Exchange. *J.-Am. Water Work. Assoc.* **1999**, *91*, 85–96. [CrossRef]
65. Amini, A.; Kim, Y.; Zhang, J.; Boyer, T.; Zhang, Q. Environmental and Economic Sustainability of Ion Exchange Drinking Water Treatment for Organics Removal. *J. Clean. Prod.* **2015**, *104*, 413–421. [CrossRef]
66. Edgar, M.; Boyer, T.H. Nitrate Adsorption and Desorption during Biological Ion Exchange. *Sep. Purif. Technol.* **2022**, *285*, 120363. [CrossRef]
67. Korak, J.A.; Mungan, A.L.; Watts, L.T. Critical Review of Waste Brine Management Strategies for Drinking Water Treatment Using Strong Base Ion Exchange. *J. Hazard. Mater.* **2022**, *441*, 129473. [CrossRef]
68. Gaikwad, R.W.; Sapkal, V.S.; Sapkal, R.S. Ion Exchange System Design for Removal of Heavy Metals from Acid Mine Drainage Wastewater. *Acta Montan. Slovaca* **2010**, *15*, 298.
69. Mohan, D.; Pittman Jr, C.U. Arsenic Removal from Water/Wastewater Using Adsorbents—A Critical Review. *J. Hazard. Mater.* **2007**, *142*, 1–53. [CrossRef]
70. Tarpeh, W.A.; Udert, K.M.; Nelson, K.L. Comparing Ion Exchange Adsorbents for Nitrogen Recovery from Source-Separated Urine. *Environ. Sci. Technol.* **2017**, *51*, 2373–2381. [CrossRef] [PubMed]
71. Inglezakis, V.J.; Zorpas, A.A.; Loizidou, M.D.; Grigoropoulou, H.P. The Effect of Competitive Cations and Anions on Ion Exchange of Heavy Metals. *Sep. Purif. Technol.* **2005**, *46*, 202–207. [CrossRef]
72. Inglezakis, V.J.; Zorpas, A.A.; Loizidou, M.D.; Grigoropoulou, H.P. Simultaneous Removal of Metals Cu^{2+}, Fe^{3+} and Cr^{3+} with Anions SO_4^{2-} and HPO_4^{2-} Using Clinoptilolite. *Microporous Mesoporous Mater.* **2003**, *61*, 167–171. [CrossRef]
73. Shih, M.-C. An Overview of Arsenic Removal by Pressure-Drivenmembrane Processes. *Desalination* **2005**, *172*, 85–97. [CrossRef]
74. Askenaizer, D. Drinking Water Quality and Treatment. *Encycl. Phys. Sci. Technol.* **2003**, *3*, 651–751.
75. Liu, X.; Ren, Z.; Ngo, H.H.; He, X.; Desmond, P.; Ding, A. Membrane Technology for Rainwater Treatment and Reuse: A Mini Review. *Water Cycle* **2021**, *2*, 51–63. [CrossRef]
76. Peter-Varbanets, M.; Zurbrügg, C.; Swartz, C.; Pronk, W. Decentralized Systems for Potable Water and the Potential of Membrane Technology. *Water Res.* **2009**, *43*, 245–265. [CrossRef]
77. Abdel-Karim, A.; Leaper, S.; Skuse, C.; Zaragoza, G.; Gryta, M.; Gorgojo, P. Membrane Cleaning and Pretreatments in Membrane Distillation–a Review. *Chem. Eng. J.* **2021**, *422*, 129696. [CrossRef]
78. Wang, Z.; Ma, J.; Tang, C.Y.; Kimura, K.; Wang, Q.; Han, X. Membrane Cleaning in Membrane Bioreactors: A Review. *J. Memb. Sci.* **2014**, *468*, 276–307. [CrossRef]
79. Peters, C.D.; Rantissi, T.; Gitis, V.; Hankins, N.P. Retention of Natural Organic Matter by Ultrafiltration and the Mitigation of Membrane Fouling through Pre-Treatment, Membrane Enhancement, and Cleaning-A Review. *J. Water Process Eng.* **2021**, *44*, 102374. [CrossRef]
80. Choong, T.S.Y.; Chuah, T.G.; Robiah, Y.; Koay, F.L.G.; Azni, I. Arsenic Toxicity, Health Hazards and Removal Techniques from Water: An Overview. *Desalination* **2007**, *217*, 139–166. [CrossRef]
81. Sonal, S.; Mishra, B.K. Role of Coagulation/Flocculation Technology for the Treatment of Dye Wastewater: Trend and Future Aspects. In *Water Pollution and Management Practices*; Springer: Berlin/Heidelberg, Germany, 2021; pp. 303–331.
82. Naceradska, J.; Pivokonska, L.; Pivokonsky, M. On the Importance of PH Value in Coagulation. *J. Water Supply Res. Technol.* **2019**, *68*, 222–230. [CrossRef]
83. Ranjbar, F.; Karrabi, M.; Danesh, S.; Gheibi, M. Improvement of Wastewater Sludge Dewatering Using Ferric Chloride, Aluminum Sulfate, and Calcium Oxide (Experimental Investigation and Descriptive Statistical Analysis). *Water Environ. Res.* **2021**, *93*, 1138–1149. [CrossRef]

84. Mendoza-Chávez, C.E.; Carabin, A.; Dirany, A.; Drogui, P.; Buelna, G.; Meza-Montenegro, M.M.; Ulloa-Mercado, R.G.; Diaz-Tenorio, L.M.; Leyva-Soto, L.A.; Gortáres-Moroyoqui, P. Statistical Optimization of Arsenic Removal from Synthetic Water by Electrocoagulation System and Its Application with Real Arsenic-Polluted Groundwater. *Environ. Technol.* **2021**, *42*, 3463–3474. [CrossRef] [PubMed]

85. Akin, I.; Arslan, G.; Tor, A.; Cengeloglu, Y.; Ersoz, M. Removal of Arsenate [As (V)] and Arsenite [As (III)] from Water by SWHR and BW-30 Reverse Osmosis. *Desalination* **2011**, *281*, 88–92. [CrossRef]

86. Chang, F.; Liu, W.; Wang, X. Comparison of Polyamide Nanofiltration and Low-Pressure Reverse Osmosis Membranes on As (III) Rejection under Various Operational Conditions. *Desalination* **2014**, *334*, 10–16. [CrossRef]

87. Vrijenhoek, E.M.; Waypa, J.J. Arsenic Removal from Drinking Water by a "Loose" Nanofiltration Membrane. *Desalination* **2000**, *130*, 265–277. [CrossRef]

88. Nguyen, C.M.; Bang, S.; Cho, J.; Kim, K.-W. Performance and Mechanism of Arsenic Removal from Water by a Nanofiltration Membrane. *Desalination* **2009**, *245*, 82–94. [CrossRef]

89. Brandhuber, P.; Amy, G. Arsenic Removal by a Charged Ultrafiltration Membrane—Influences of Membrane Operating Conditions and Water Quality on Arsenic Rejection. *Desalination* **2001**, *140*, 1–14. [CrossRef]

90. Iqbal, J.; Kim, H.-J.; Yang, J.-S.; Baek, K.; Yang, J.-W. Removal of Arsenic from Groundwater by Micellar-Enhanced Ultrafiltration (MEUF). *Chemosphere* **2007**, *66*, 970–976. [PubMed]

91. Zhang, G.; Li, X.; Wu, S.; Gu, P. Effect of Source Water Quality on Arsenic (V) Removal from Drinking Water by Coagulation/Microfiltration. Environ. *Earth Sci.* **2012**, *66*, 1269–1277. [CrossRef]

92. Zhang, T.; Sun, D.D. Removal of Arsenic from Water Using Multifunctional Micro-/Nano-Structured MnO2 Spheres and Microfiltration. *Chem. Eng. J.* **2013**, *225*, 271–279. [CrossRef]

93. Laky, D.; Licskó, I. Arsenic Removal by Ferric-Chloride Coagulation–Effect of Phosphate, Bicarbonate and Silicate. *Water Sci. Technol.* **2011**, *64*, 1046–1055. [CrossRef]

94. Baskan, M.B.; Pala, A. A Statistical Experiment Design Approach for Arsenic Removal by Coagulation Process Using Aluminum Sulfate. *Desalination* **2010**, *254*, 42–48. [CrossRef]

95. Song, S.; Lopez-Valdivieso, A.; Hernandez-Campos, D.J.; Peng, C.; Monroy-Fernandez, M.G.; Razo-Soto, I. Arsenic Removal from High-Arsenic Water by Enhanced Coagulation with Ferric Ions and Coarse Calcite. *Water Res.* **2006**, *40*, 364–372. [CrossRef] [PubMed]

96. Lichtfouse, E.; Morin-Crini, N.; Fourmentin, M.; Zemmouri, H.; do Carmo Nascimento, I.O.; Queiroz, L.M.; Tadza, M.Y.M.; Picos-Corrales, L.A.; Pei, H.; Wilson, L.D. Chitosan for Direct Bioflocculation of Wastewater. *Environ. Chem. Lett.* **2019**, *17*, 1603–1621. [CrossRef]

97. Sieliechi, J.M.; Kayem, G.J.; Sandu, I. Effect of Water Treatment Residuals (Aluminum and Iron Ions) on Human Health and Drinking Water Distribution Systems. *Int. J. Conserv. Sci.* **2010**, *1*, 175–182.

98. Muruganandam, L.; Kumar, M.P.S.; Jena, A.; Gulla, S.; Godhwani, B. Treatment of Waste Water by Coagulation and Flocculation Using Biomaterials. *IOP Conf. Ser. Mater. Sci. Eng.* **2017**, *263*, 032006. [CrossRef]

99. Jeon, S.-B.; Kim, S.; Park, S.-J.; Seol, M.-L.; Kim, D.; Chang, Y.K.; Choi, Y.-K. Self-Powered Electro-Coagulation System Driven by a Wind Energy Harvesting Triboelectric Nanogenerator for Decentralized Water Treatment. *Nano Energy* **2016**, *28*, 288–295. [CrossRef]

100. McBeath, S.T.; English, J.T.; Wilkinson, D.P.; Graham, N.J.D. Circumneutral Electrosynthesis of Ferrate Oxidant: An Emerging Technology for Small, Remote and Decentralised Water Treatment Applications. *Curr. Opin. Electrochem.* **2021**, *27*, 100680. [CrossRef]

101. Holt, P.K.; Barton, G.W.; Mitchell, C.A. The Future for Electrocoagulation as a Localised Water Treatment Technology. *Chemosphere* **2005**, *59*, 355–367. [CrossRef] [PubMed]

102. Lee, Y.; Um, I.; Yoon, J. Arsenic (III) Oxidation by Iron (VI)(Ferrate) and Subsequent Removal of Arsenic (V) by Iron (III) Coagulation. *Environ. Sci. Technol.* **2003**, *37*, 5750–5756. [CrossRef] [PubMed]

103. Sharma, V.K.; Dutta, P.K.; Ray, A.K. Review of Kinetics of Chemical and Photocatalytical Oxidation of Arsenic (III) as Influenced by PH. *J. Environ. Sci. Health Part A* **2007**, *42*, 997–1004. [CrossRef] [PubMed]

104. Kim, M.-J.; Nriagu, J. Oxidation of Arsenite in Groundwater Using Ozone and Oxygen. *Sci. Total Environ.* **2000**, *247*, 71–79. [CrossRef] [PubMed]

105. Liu, R.; Qu, J. Review on Heterogeneous Oxidation and Adsorption for Arsenic Removal from Drinking Water. *J. Environ. Sci.* **2021**, *110*, 178–188. [CrossRef]

106. Sorlini, S.; Gialdini, F. Conventional Oxidation Treatments for the Removal of Arsenic with Chlorine Dioxide, Hypochlorite, Potassium Permanganate and Monochloramine. *Water Res.* **2010**, *44*, 5653–5659. [CrossRef]

107. Ike, I.A.; Linden, K.G.; Orbell, J.D.; Duke, M. Critical Review of the Science and Sustainability of Persulphate Advanced Oxidation Processes. *Chem. Eng. J.* **2018**, *338*, 651–669. [CrossRef]

108. Du, J.; Zhang, B.; Li, J.; Lai, B. Decontamination of Heavy Metal Complexes by Advanced Oxidation Processes: A Review. *Chin. Chem. Lett.* **2020**, *31*, 2575–2582. [CrossRef]

109. Mohammed, H.A.; Ali, S.A.K.; Basheer, M.I. Heavy Metal Ions Removal Using Advanced Oxidation (UV/H_2O_2) Technique. *IOP Conf. Ser. Mater. Sci. Eng.* **2020**, *870*, 12026. [CrossRef]

110. Matilainen, A.; Sillanpää, M. Removal of Natural Organic Matter from Drinking Water by Advanced Oxidation Processes. *Chemosphere* **2010**, *80*, 351–365. [CrossRef] [PubMed]

111. Hodges, B.C.; Cates, E.L.; Kim, J.-H. Challenges and Prospects of Advanced Oxidation Water Treatment Processes Using Catalytic Nanomaterials. *Nat. Nanotechnol.* **2018**, *13*, 642–650. [CrossRef] [PubMed]

112. Miklos, D.B.; Remy, C.; Jekel, M.; Linden, K.G.; Drewes, J.E.; Hübner, U. Evaluation of Advanced Oxidation Processes for Water and Wastewater Treatment–A Critical Review. *Water Res.* **2018**, *139*, 118–131. [CrossRef]

113. von Gunten, U. Oxidation Processes in Water Treatment: Are We on Track? *Environ. Sci. Technol.* **2018**, *52*, 5062–5075. [CrossRef] [PubMed]

114. Zhang, Y.; Wang, H.; Li, Y.; Wang, B.; Huang, J.; Deng, S.; Yu, G.; Wang, Y. Removal of Micropollutants by an Electrochemically Driven UV/Chlorine Process for Decentralized Water Treatment. *Water Res.* **2020**, *183*, 116115. [CrossRef]

115. Gurung, K.; Ncibi, M.C.; Shestakova, M.; Sillanpää, M. Removal of Carbamazepine from MBR Effluent by Electrochemical Oxidation (EO) Using a Ti/Ta2O5-SnO2 Electrode. *Appl. Catal. B Environ.* **2018**, *221*, 329–338. [CrossRef]

116. Oturan, M.A.; Aaron, J.-J. Advanced Oxidation Processes in Water/Wastewater Treatment: Principles and Applications. A Review. *Crit. Rev. Environ. Sci. Technol.* **2014**, *44*, 2577–2641. [CrossRef]

117. Yu, X.-Y.; Luo, T.; Jia, Y.; Zhang, Y.-X.; Liu, J.-H.; Huang, X.-J. Porous Hierarchically Micro-/Nanostructured MgO: Morphology Control and Their Excellent Performance in As (III) and As (V) Removal. *J. Phys. Chem. C* **2011**, *115*, 22242–22250. [CrossRef]

118. Iervolino, G.; Vaiano, V.; Rizzo, L.; Sarno, G.; Farina, A.; Sannino, D. Removal of Arsenic from Drinking Water by Photo-catalytic Oxidation on MoOx/TiO2 and Adsorption on Γ-Al2O3. *J. Chem. Technol. Biotechnol.* **2016**, *91*, 88–95. [CrossRef]

119. Rosales, M.; Garcia, A.; Fuenzalida, V.M.; Espinoza-González, R.; Song, G.; Wang, B.; Yu, J.; Gracia, F.; Rosenkranz, A. Unprecedented Arsenic Photo-Oxidation Behavior of Few-and Multi-Layer Ti3C2Tx Nano-Sheets. *Appl. Mater. Today* **2020**, *20*, 100769. [CrossRef]

120. Ray, S.; Lalman, J.A. Fabrication and Characterization of an Immobilized Titanium Dioxide (TiO$_2$) Nanofiber Photocatalyst. Mater. *Today Proc.* **2016**, *3*, 1582–1591.

121. Lescano, M.; Zalazar, C.; Cassano, A.; Brandi, R. Kinetic Modeling of Arsenic (III) Oxidation in Water Employing the UV/H$_2$O$_2$ Process. *Chem. Eng. J.* **2012**, *211*, 360–368. [CrossRef]

122. Miller, S.M.; Zimmerman, J.B. Novel, Bio-Based, Photoactive Arsenic Sorbent: TiO2-Impregnated Chitosan Bead. *Water Res.* **2010**, *44*, 5722–5729. [CrossRef] [PubMed]

123. Huang, M.; Feng, W.; Xu, W.; Liu, P. An in Situ Gold-Decorated 3D Branched ZnO Nanocomposite and Its Enhanced Absorption and Photo-Oxidation Performance for Removing Arsenic from Water. *RSC Adv.* **2016**, *6*, 112877–112884. [CrossRef]

124. Zaw, M.; Emett, M.T. Arsenic Removal from Water Using Advanced Oxidation Processes. *Toxicol. Lett.* **2002**, *133*, 113–118. [CrossRef]

125. Gallegos-Garcia, M.; Ramírez-Muñiz, K.; Song, S. Arsenic Removal from Water by Adsorption Using Iron Oxide Minerals as Adsorbents: A Review. *Miner. Process. Extr. Metall. Rev.* **2012**, *33*, 301–315. [CrossRef]

126. Siddiqui, S.I.; Chaudhry, S.A. Iron Oxide and Its Modified Forms as an Adsorbent for Arsenic Removal: A Comprehensive Recent Advancement. *Process Saf. Environ. Prot.* **2017**, *111*, 592–626. [CrossRef]

127. Babaee, Y.; Mulligan, C.N.; Rahaman, M.S. Removal of Arsenic (III) and Arsenic (V) from Aqueous Solutions through Adsorption by Fe/Cu Nanoparticles. *J. Chem. Technol. Biotechnol.* **2018**, *93*, 63–71. [CrossRef]

128. Elwakeel, K.Z.; Elgarahy, A.M.; Khan, Z.A.; Almughamisi, M.S.; Al-Bogami, A.S. Perspectives Regarding Metal/Mineral-Incorporating Materials for Water Purification: With Special Focus on Cr (vi) Removal. *Mater. Adv.* **2020**, *1*, 1546–1574. [CrossRef]

129. Dhoke, C.; Zaabout, A.; Cloete, S.; Amini, S. Review on Reactor Configurations for Adsorption-Based CO$_2$ Capture. *Ind. Eng. Chem. Res.* **2021**, *60*, 3779–3798. [CrossRef]

130. Brandani, S. Kinetics of Liquid Phase Batch Adsorption Experiments. *Adsorption* **2021**, *27*, 353–368. [CrossRef]

131. Revellame, E.D.; Fortela, D.L.; Sharp, W.; Hernandez, R.; Zappi, M.E. Adsorption Kinetic Modeling Using Pseudo-First Order and Pseudo-Second Order Rate Laws: A Review. *Clean. Eng. Technol.* **2020**, *1*, 100032. [CrossRef]

132. Núñez, D.; Serrano, J.A.; Mancisidor, A.; Elgueta, E.; Varaprasad, K.; Oyarzún, P.; Cáceres, R.; Ide, W.; Rivas, B.L. Heavy Metal Removal from Aqueous Systems Using Hydroxyapatite Nanocrystals Derived from Clam Shells. *RSC Adv.* **2019**, *9*. [CrossRef]

133. Jasrotia, S.; Kansal, A.; Kishore, V.V.N. Application of Solar Energy for Water Supply and Sanitation in Arsenic Affected Rural Areas: A Study for Kaudikasa Village, India. *J. Clean. Prod.* **2013**, *60*, 102–106. [CrossRef]

134. Baigorria, E.; Cano, L.; Alvarez, V.A. Nanoclays as Eco-Friendly Adsorbents of Arsenic for Water Purification. In *Handbook of Nanomaterials and Nanocomposites for Energy and Environmental Applications*; Springer: Cham, Switzerland, 2021; pp. 455–470.

135. Ahmed, M.F. An Overview of Arsenic Removal Technologies in Bangladesh and India. In Proceedings of the BUET-UNU International Workshop on Technologies for Arsenic Removal from Drinking Water, Citeseer, Dhaka, Bengal, 5 May 2001; pp. 5–7.

136. Alka, S.; Shahir, S.; Ibrahim, N.; Ndejiko, M.J.; Vo, D.-V.N.; Abd Manan, F. Arsenic Removal Technologies and Future Trends: A Mini Review. *J. Clean. Prod.* **2021**, *278*, 123805. [CrossRef]

137. Zhang, W.; Cheng, W.; Ziemann, E.; Be'er, A.; Lu, X.; Elimelech, M.; Bernstein, R. Functionalization of Ultrafiltration Membrane with Polyampholyte Hydrogel and Graphene Oxide to Achieve Dual Antifouling and Antibacterial Properties. *J. Memb. Sci.* **2018**, *565*, 293–302. [CrossRef]

138. Zhang, W.; Huang, H.; Bernstein, R. Zwitterionic Hydrogel Modified Reduced Graphene Oxide/ZnO Nanocomposite Blended Membrane with High Antifouling and Antibiofouling Performances. *J. Colloid Interface Sci.* **2022**, *613*, 426–434. [CrossRef]

139. Zhang, W.; Yang, Y.; Ziemann, E.; Be'Er, A.; Bashouti, M.Y.; Elimelech, M.; Bernstein, R. One-Step Sonochemical Synthesis of a Reduced Graphene Oxide–ZnO Nanocomposite with Antibacterial and Antibiofouling Properties. *Environ. Sci. Nano* **2019**, *6*, 3080–3090. [CrossRef]

140. Zhang, W.; Yang, Z.; Kaufman, Y.; Bernstein, R. Surface and Anti-Fouling Properties of a Polyampholyte Hydrogel Grafted onto a Polyethersulfone Membrane. *J. Colloid Interface Sci.* **2018**, *517*, 155–165. [CrossRef]

141. Cheng, W.; Lu, X.; Kaneda, M.; Zhang, W.; Bernstein, R.; Ma, J.; Elimelech, M. Graphene Oxide-Functionalized Membranes: The Importance of Nanosheet Surface Exposure for Biofouling Resistance. *Environ. Sci. Technol.* **2019**, *54*, 517–526. [CrossRef] [PubMed]

142. Zhang, Y.; Yang, K.; Fang, Y.; Ding, J.; Zhang, H. Removal of Phosphate from Wastewater with a Recyclable La-Based Particulate Adsorbent in a Small-Scale Reactor. *Water* **2022**, *14*, 2326. [CrossRef]

143. Rezk, R.A.; Galmed, A.H.; Abdelkreem, M.; Abdel Ghany, N.A.; Harith, M.A. Detachment of Cu (II) and Co (II) Ions from Synthetic Wastewater via Adsorption on Lates Niloticus Fish Bones Using LIBS and XRF. *J. Adv. Res.* **2018**, *14*. [CrossRef]

144. Yan, X.-F.; Fan, X.-R.; Wang, Q.; Shen, Y. An Adsorption Isotherm Model for Adsorption Performance of Silver-Loaded Activated Carbon. *Therm. Sci.* **2017**, *21*, 1645–1649. [CrossRef]

145. Awad, A.M.; Shaikh, S.M.R.; Jalab, R.; Gulied, M.H.; Nasser, M.S.; Benamor, A.; Adham, S. Adsorption of Organic Pollutants by Natural and Modified Clays: A Comprehensive Review. *Sep. Purif. Technol.* **2019**, *228*, 115719. [CrossRef]

146. Ma, M.-D.; Wu, H.; Deng, Z.-Y.; Zhao, X. Arsenic Removal from Water by Nanometer Iron Oxide Coated Single-Wall Carbon Nanotubes. *J. Mol. Liq.* **2018**, *259*, 369–375. [CrossRef]

147. Latour, R.A. The Langmuir Isotherm: A Commonly Applied but Misleading Approach for the Analysis of Protein Adsorption Behavior. *J. Biomed. Mater. Res. Part A* **2015**, *103*, 949–958. [CrossRef]

148. Oke, I.A.; Olarinoye, N.O.; Adewusi, S.R.A. Adsorption Kinetics for Arsenic Removal from Aqueous Solutions by Untreated Powdered Eggshell. *Adsorption* **2008**, *14*, 73–83. [CrossRef]

149. Salameh, Y.; Al-Lagtah, N.; Ahmad, M.N.M.; Allen, S.J.; Walker, G.M. Kinetic and Thermodynamic Investigations on Arsenic Adsorption onto Dolomitic Sorbents. *Chem. Eng. J.* **2010**, *160*, 440–446. [CrossRef]

150. Vu, T.A.; Le, G.H.; Dao, C.D.; Dang, L.Q.; Nguyen, K.T.; Nguyen, Q.K.; Dang, P.T.; Tran, H.T.K.; Duong, Q.T.; Nguyen, T. V Arsenic Removal from Aqueous Solutions by Adsorption Using Novel MIL-53 (Fe) as a Highly Efficient Adsorbent. *Rsc Adv.* **2015**, *5*, 5261–5268. [CrossRef]

151. Dickson, D.; Liu, G.; Cai, Y. Adsorption Kinetics and Isotherms of Arsenite and Arsenate on Hematite Nanoparticles and Aggregates. *J. Environ. Manag.* **2017**, *186*, 261–267. [CrossRef]

152. Goswami, A.; Raul, P.K.; Purkait, M.K. Arsenic Adsorption Using Copper (II) Oxide Nanoparticles. *Chem. Eng. Res. Des.* **2012**, *90*, 1387–1396. [CrossRef]

153. Mohan, D.; Dey, S.; Dwivedi, S.B.; Shukla, S.P. Adsorption of Arsenic Using Low Cost Adsorbents: Guava Leaf Biomass, Mango Bark and Bagasse. *Curr. Sci.* **2019**, *117*, 649–661. [CrossRef]

154. Chutia, P.; Kato, S.; Kojima, T.; Satokawa, S. Arsenic Adsorption from Aqueous Solution on Synthetic Zeolites. *J. Hazard. Mater.* **2009**, *162*, 440–447. [CrossRef]

155. Sherlala, A.I.A.; Raman, A.A.A.; Bello, M.M.; Buthiyappan, A. Adsorption of Arsenic Using Chitosan Magnetic Graphene Oxide Nanocomposite. *J. Environ. Manag.* **2019**, *246*, 547–556. [CrossRef]

156. Shakoor, M.B.; Niazi, N.K.; Bibi, I.; Shahid, M.; Sharif, F.; Bashir, S.; Shaheen, S.M.; Wang, H.; Tsang, D.C.W.; Ok, Y.S. Arsenic Removal by Natural and Chemically Modified Water Melon Rind in Aqueous Solutions and Groundwater. *Sci. Total Environ.* **2018**, *645*, 1444–1455. [CrossRef]

157. Ribeiro, I.C.A.; Vasques, I.C.F.; Teodoro, J.C.; Guerra, M.B.B.; da Silva Carneiro, J.S.; Melo, L.C.A.; Guilherme, L.R.G. Fast and Effective Arsenic Removal from Aqueous Solutions by a Novel Low-Cost Eggshell Byproduct. *Sci. Total Environ.* **2021**, *783*, 147022. [CrossRef]

158. Siddiqui, S.I.; Singh, P.N.; Tara, N.; Pal, S.; Chaudhry, S.A.; Sinha, I. Arsenic Removal from Water by Starch Functionalized Maghemite Nano-Adsorbents: Thermodynamics and Kinetics Investigations. *Colloid Interface Sci. Commun.* **2020**, *36*, 100263. [CrossRef]

159. Bläker, C.; Muthmann, J.; Pasel, C.; Bathen, D. Characterization of Activated Carbon Adsorbents–State of the Art and Novel Approaches. *ChemBioEng Rev.* **2019**, *6*, 119–138. [CrossRef]

160. Sihem, A.; Lehocine, M.B.; Miniai, H.A. Preparation and Characterisation of an Natural Adsorbent Used for Elimination of Pollutants in Wastewater. *Energy Procedia* **2012**, *18*, 1145–1151. [CrossRef]

161. Kumar, A.S.K.; Jiang, S.-J. Preparation and Characterization of Exfoliated Graphene Oxide–L-Cystine as an Effective Adsorbent of Hg (II) Adsorption. *RSC Adv.* **2015**, *5*, 6294–6304. [CrossRef]

162. Al-Maadeed, M.A.A.; Ponnamma, D.; Carignano, M.A. *Polymer Science and Innovative Applications: Materials, Techniques, and Future Developments*; Elsevier: Amsterdam, The Netherlands, 2020; ISBN 0128173033.

163. Bakdach, W.M.M.; Haiba, M.; Hadad, R. Changes in Surface Morphology, Chemical and Mechanical Properties of Clear Aligners during Intraoral Usage: A Systematic Review and Meta-Analysis. *Int. Orthod.* **2022**, *20*, 100610. [CrossRef]

164. Wirasnita, R.; Hadibarata, T.; Yusoff, A.R.M.; Lazim, Z.M. Preparation and Characterization of Activated Carbon from Oil Palm Empty Fruit Bunch Wastes Using Zinc Chloride. *J. Teknol.* **2015**, *74*, 77–81. [CrossRef]

165. Hidayu, A.R.; Mohamad, N.F.; Matali, S.; Sharifah, A. Characterization of Activated Carbon Prepared from Oil Palm Empty Fruit Bunch Using BET and FT-IR Techniques. *Procedia Eng.* **2013**, *68*, 379–384. [CrossRef]

166. Quan, C.; Chu, H.; Zhou, Y.; Su, S.; Su, R.; Gao, N. Amine-Modified Silica Zeolite from Coal Gangue for CO_2 Capture. *Fuel* **2022**, *322*, 124184. [CrossRef]

167. Hung, C.; Bai, H.; Karthik, M. Ordered Mesoporous Silica Particles and Si-MCM-41 for the Adsorption of Acetone: A Comparative Study. *Sep. Purif. Technol.* **2009**, *64*, 265–272. [CrossRef]

168. Mierzwa-Hersztek, M.; Gondek, K.; Jewiarz, M.; Dziedzic, K. Assessment of Energy Parameters of Biomass and Biochars, Leachability of Heavy Metals and Phytotoxicity of Their Ashes. *J. Mater. Cycles Waste Manag.* **2019**, *21*, 786–800. [CrossRef]

169. Chatterjee, R.; Sajjadi, B.; Chen, W.-Y.; Mattern, D.L.; Hammer, N.; Raman, V.; Dorris, A. Effect of Pyrolysis Temperature on Physicochemical Properties and Acoustic-Based Amination of Biochar for Efficient CO2 Adsorption. *Front. Energy Res.* **2020**, *8*, 85. [CrossRef]

170. Ali, I.; Al-Othman, Z.A.; Alwarthan, A.; Asim, M.; Khan, T.A. Removal of Arsenic Species from Water by Batch and Column Operations on Bagasse Fly Ash. *Environ. Sci. Pollut. Res.* **2014**, *21*, 3218–3229. [CrossRef]

171. Balsamo, M.; Di Natale, F.; Erto, A.; Lancia, A.; Montagnaro, F.; Santoro, L. Arsenate Removal from Synthetic Wastewater by Adsorption onto Fly Ash. *Desalination* **2010**, *263*, 58–63. [CrossRef]

172. Olafadehan, O.A.; Abhulimen, K.E.; Adeleke, A.I.; Njoku, C.V.; Amoo, K.O. Production and Characterization of Derived Composite Biosorbents from Animal Bone. *Afr. J. Pure Appl. Chem.* **2019**, *13*, 12–26. [CrossRef]

173. de Souza, C.C.; de Souza, L.Z.M.; Yılmaz, M.; de Oliveira, M.A.; da Silva Bezerra, A.C.; da Silva, E.F.; Dumont, M.R.; Machado, A.R.T. Activated Carbon of Coriandrum Sativum for Adsorption of Methylene Blue: Equilibrium and Kinetic Modeling. *Clean. Mater.* **2022**, *3*, 100052. [CrossRef]

174. Elaiopoulos, K.; Perraki, T.; Grigoropoulou, E. Monitoring the Effect of Hydrothermal Treatments on the Structure of a Natural Zeolite through a Combined XRD, FTIR, XRF, SEM and N2-Porosimetry Analysis. *Microporous Mesoporous Mater.* **2010**, *134*, 29–43. [CrossRef]

175. Hao, L.; Zheng, T.; Jiang, J.; Zhang, G.; Wang, P. Removal of As (III) and As (V) from Water Using Iron Doped Amino Functionalized Sawdust: Characterization, Adsorptive Performance and UF Membrane Separation. *Chem. Eng. J.* **2016**, *292*, 163–173. [CrossRef]

176. Wang, C.; Liu, K.; Huang, D.; Chen, Q.; Tu, M.; Wu, K.; Shui, Z. Utilization of Fly Ash as Building Material Admixture: Basic Properties and Heavy Metal Leaching. *Case Stud. Constr. Mater.* **2022**, *17*, e01422. [CrossRef]

177. Iber, B.T.; Torsabo, D.; Chik, C.E.N.C.E.; Wahab, F.; Abdullah, S.R.S.; Hassan, H.A.; Kasan, N.A. The Impact of Re-Ordering the Conventional Chemical Steps on the Production and Characterization of Natural Chitosan from Biowaste of Black Tiger Shrimp, Penaeus Monodon. *J. Sea Res.* **2022**, *190*, 102306. [CrossRef]

178. Tauk, M.; Bechelany, M.; Lagerge, S.; Sistat, P.; Habchi, R.; Cretin, M.; Zaviska, F. Influence of Particle Size Distribution on Carbon-Based Flowable Electrode Viscosity and Desalination Efficiency in Flow Electrode Capacitive Deionization. *Sep. Purif. Technol.* **2022**, *306 Pt A*, 122666. [CrossRef]

179. Zaiku, X.; Qingling, C.; Bo, C.; Chengfang, Z. Influence of Alkalinity on Particle Size Distribution and Crystalline Structure in Synthesis of Zeolite Beta. *Cryst. Eng.* **2001**, *4*, 359–372. [CrossRef]

180. Bergström, D.; Israelsson, S.; Öhman, M.; Dahlqvist, S.-A.; Gref, R.; Boman, C.; Wästerlund, I. Effects of Raw Material Particle Size Distribution on the Characteristics of Scots Pine Sawdust Fuel Pellets. *Fuel Process. Technol.* **2008**, *89*, 1324–1329. [CrossRef]

181. Lanzerstorfer, C. Fly Ash from Coal Combustion: Dependence of the Concentration of Various Elements on the Particle Size. *Fuel* **2018**, *228*, 263–271. [CrossRef]

182. Rampino, A.; Borgogna, M.; Blasi, P.; Bellich, B.; Cesàro, A. Chitosan Nanoparticles: Preparation, Size Evolution and Stability. *Int. J. Pharm.* **2013**, *455*, 219–228. [CrossRef]

183. Babick, F. Dynamic Light Scattering (DLS). In *Characterization of Nanoparticles*; Elsevier: Amsterdam, The Netherlands, 2020; pp. 137–172.

184. Souza, T.G.F.; Ciminelli, V.S.T.; Mohallem, N.D.S. A Comparison of TEM and DLS Methods to Characterize Size Distribution of Ceramic Nanoparticles. *J. Phys. Conf. Ser.* **2016**, *733*, 12039. [CrossRef]

185. Ambroz, F.; Macdonald, T.J.; Martis, V.; Parkin, I.P. Evaluation of the BET Theory for the Characterization of Meso and Microporous MOFs. *Small Methods* **2018**, *2*, 1800173. [CrossRef]

186. Epp, J. X-ray Diffraction (XRD) Techniques for Materials Characterization. In *Materials Characterization Using Nondestructive Evaluation (Nde) Methods*; Elsevier: Amsterdam, The Netherlands, 2016; pp. 81–124.

187. Oyedotun, T.D.T. X-ray Fluorescence (XRF) in the Investigation of the Composition of Earth Materials: A Review and an Overview. *Geol. Ecol. Landsc.* **2018**, *2*, 148–154. [CrossRef]

188. Ghosh, U.; Chakraborty, S. Pharmaceutical and Phytochemical Evaluation of a Novel Anti–White Spot Syndrome Virus Drug Derived from Terrestrial Plants. *Int. J. Nat. Prod. Res.* **2013**, *3*, 92–101.

189. Donahue, C.J.; Rais, E.A. Proximate Analysis of Coal. *J. Chem. Educ.* **2009**, *86*, 222. [CrossRef]

190. Khan, S.A.; Khan, S.B.; Khan, L.U.; Farooq, A.; Akhtar, K.; Asiri, A.M. Fourier Transform Infrared Spectroscopy: Fundamentals and Application in Functional Groups and Nanomaterials Characterization. In *Handbook of Materials Characterization*; Springer: Berlin/Heidelberg, Germany, 2018; pp. 317–344.

191. Bhattacharjee, S. DLS and Zeta Potential–What They Are and What They Are Not? *J. Control. Release* **2016**, *235*, 337–351. [CrossRef]

192. Lunardi, C.N.; Gomes, A.J.; Rocha, F.S.; De Tommaso, J.; Patience, G.S. Experimental Methods in Chemical Engineering: Zeta Potential. *Can. J. Chem. Eng.* **2021**, *99*, 627–639. [CrossRef]

193. Lim, H.K.; Teng, T.T.; Ibrahim, M.H.; Ahmad, A.; Chee, H.T. Adsorption and Removal of Zinc (II) from Aqueous Solution Using Powdered Fish Bones. *APCBEE Procedia* **2012**, *1*. [CrossRef]

194. Kumar, P.S.; Ejerssa, W.W.; Wegener, C.C.; Korving, L.; Dugulan, A.I.; Temmink, H.; van Loosdrecht, M.C.M.; Witkamp, G.-J. Understanding and Improving the Reusability of Phosphate Adsorbents for Wastewater Effluent Polishing. *Water Res.* **2018**, *145*, 365–374. [CrossRef]

195. Cabrera, F.; De Arambarri, P.; Madrid, L.; Toga, C.G. Desorption of Phosphate from Iron Oxides in Relation to Equilibrium PH and Porosity. *Geoderma* **1981**, *26*, 203–216. [CrossRef]

196. Chitrakar, R.; Tezuka, S.; Sonoda, A.; Sakane, K.; Ooi, K.; Hirotsu, T. Phosphate Adsorption on Synthetic Goethite and Akaganeite. *J. Colloid Interface Sci.* **2006**, *298*, 602–608. [CrossRef] [PubMed]

197. Kunaschk, M.; Schmalz, V.; Dietrich, N.; Dittmar, T.; Worch, E. Novel Regeneration Method for Phosphate Loaded Granular Ferric (Hydr) Oxide–a Contribution to Phosphorus Recycling. *Water Res.* **2015**, *71*, 219–226. [CrossRef]

198. Qi, J.; Zhang, G.; Li, H. Efficient Removal of Arsenic from Water Using a Granular Adsorbent: Fe–Mn Binary Oxide Impregnated Chitosan Bead. *Bioresour. Technol.* **2015**, *193*, 243–249. [CrossRef]

199. Li, Z.-Q.; Yang, J.-C.; Sui, K.-W.; Yin, N. Facile Synthesis of Metal-Organic Framework MOF-808 for Arsenic Removal. *Mater. Lett.* **2015**, *160*, 412–414. [CrossRef]

200. Yoon, Y.; Zheng, M.; Ahn, Y.-T.; Park, W.K.; Yang, W.S.; Kang, J.-W. Synthesis of Magnetite/Non-Oxidative Graphene Composites and Their Application for Arsenic Removal. *Sep. Purif. Technol.* **2017**, *178*, 40–48. [CrossRef]

201. Li, Z.; Liu, X.; Jin, W.; Hu, Q.; Zhao, Y. Adsorption Behavior of Arsenicals on MIL-101 (Fe): The Role of Arsenic Chemical Structures. *J. Colloid Interface Sci.* **2019**, *554*, 692–704. [CrossRef]

202. Bezerra, M.A.; Santelli, R.E.; Oliveira, E.P.; Villar, L.S.; Escaleira, L.A. Response Surface Methodology (RSM) as a Tool for Optimization in Analytical Chemistry. *Talanta* **2008**, *76*, 965–977. [CrossRef] [PubMed]

203. Bashir, M.J.K.; Amr, S.S.A.; Aziz, S.Q.; Aun, N.C.; Sethupathi, S. Wastewater Treatment Processes Optimization Using Response Surface Methodology (RSM) Compared with Conventional Methods: Review and Comparative Study. *Middle-East J. Sci. Res.* **2015**, *23*, 244–252.

204. Roy, P.; Mondal, N.K.; Das, K. Modeling of the Adsorptive Removal of Arsenic: A Statistical Approach. *J. Environ. Chem. Eng.* **2014**, *2*, 585–597. [CrossRef]

205. Phearom, S.; Shahid, M.K.; Choi, Y.-G. Optimization of Arsenic Adsorption by Mill Scale–Derived Magnetite Particles Using Response Surface Methodology. *J. Hazard. Toxic Radioact. Waste* **2021**, *25*, 4021022. [CrossRef]

206. Lingamdinne, L.P.; Choi, J.-S.; Choi, Y.-L.; Chang, Y.-Y.; Yang, J.-K.; Karri, R.R.; Koduru, J.R. Process Modeling and Optimization of an Iron Oxide Immobilized Graphene Oxide Gadolinium Nanocomposite for Arsenic Adsorption. *J. Mol. Liq.* **2020**, *299*, 112261. [CrossRef]

207. Simsek, E.B.; Özdemir, E.; Beker, U. Process Optimization for Arsenic Adsorption onto Natural Zeolite Incorporating Metal Oxides by Response Surface Methodology. *Water Air Soil Pollut.* **2013**, *224*, 1–14. [CrossRef]

208. Sahu, U.K.; Mahapatra, S.S.; Patel, R.K. Application of Box–Behnken Design in Response Surface Methodology for Adsorptive Removal of Arsenic from Aqueous Solution Using CeO_2/Fe_2O_3/Graphene Nanocomposite. Mater. *Chem. Phys.* **2018**, *207*, 233–242. [CrossRef]

209. Farooq, M.U.; Jalees, M.I. Application of Magnetic Graphene Oxide for Water Purification: Heavy Metals Removal and Disinfection. *J. Water Process Eng.* **2020**, *33*, 101044.

210. Du, Z.; Zheng, T.; Wang, P.; Hao, L.; Wang, Y. Fast Microwave-Assisted Preparation of a Low-Cost and Recyclable Carboxyl Modified Lignocellulose-Biomass Jute Fiber for Enhanced Heavy Metal Removal from Water. *Bioresour. Technol.* **2016**, *201*, 41–49. [CrossRef]

211. Charpentier, T.V.J.; Neville, A.; Lanigan, J.L.; Barker, R.; Smith, M.J.; Richardson, T. Preparation of Magnetic Carboxymethylchitosan Nanoparticles for Adsorption of Heavy Metal Ions. *ACS Omega* **2016**, *1*, 77–83. [CrossRef]

212. Wang, M.; Zhang, K.; Wu, M.; Wu, Q.; Liu, J.; Yang, J.; Zhang, J. Unexpectedly High Adsorption Capacity of Esterified Hydroxyapatite for Heavy Metal Removal. *Langmuir* **2019**, *35*, 16111–16119. [CrossRef]

213. Ali, R.M.; Hamad, H.A.; Hussein, M.M.; Malash, G.F. Potential of Using Green Adsorbent of Heavy Metal Removal from Aqueous Solutions: Adsorption Kinetics, Isotherm, Thermodynamic, Mechanism and Economic Analysis. *Ecol. Eng.* **2016**, *91*, 317–332. [CrossRef]

214. El-Naggar, M.E.; Radwan, E.K.; El-Wakeel, S.T.; Kafafy, H.; Gad-Allah, T.A.; El-Kalliny, A.S.; Shaheen, T.I. Synthesis, Characterization and Adsorption Properties of Microcrystalline Cellulose Based Nanogel for Dyes and Heavy Metals Removal. *Int. J. Biol. Macromol.* **2018**, *113*, 248–258. [CrossRef]

215. Wang, C.; Xiong, C.; He, Y.; Yang, C.; Li, X.; Zheng, J.; Wang, S. Facile Preparation of Magnetic Zr-MOF for Adsorption of Pb (II) and Cr (VI) from Water: Adsorption Characteristics and Mechanisms. *Chem. Eng. J.* **2021**, *415*, 128923. [CrossRef]

216. Tahmasebpoor, M.; Hosseini Nami, S.; Khatamian, M.; Sanaei, L. Arsenate Removal from Contaminated Water Using Fe2O3-Clinoptilolite Powder and Granule. *Environ. Technol.* **2022**, *43*, 116–130. [CrossRef]

217. Wang, Q.; Jiang, F.; Ouyang, X.-K.; Yang, L.-Y.; Wang, Y. Adsorption of Pb (II) from Aqueous Solution by Mussel Shell-Based Adsorbent: Preparation, Characterization, and Adsorption Performance. *Materials* **2021**, *14*, 741. [CrossRef] [PubMed]

218. Seco-Reigosa, N.; Cutillas-Barreiro, L.; Nóvoa-Muñoz, J.C.; Arias-Estévez, M.; Álvarez-Rodríguez, E.; Fernández-Sanjurjo, M.J.; Núñez-Delgado, A. Adsorption, Desorption and Fractionation of As (V) on Untreated and Mussel Shell-Treated Granitic Material. *Solid Earth* **2015**, *6*, 337–346. [CrossRef]

219. Priyadarshni, N.; Nath, P.; Chanda, N. Sustainable Removal of Arsenate, Arsenite and Bacterial Contamination from Water Using Biochar Stabilized Iron and Copper Oxide Nanoparticles and Associated Mechanism of the Remediation Process. *J. Water Process Eng.* **2020**, *37*, 101495. [CrossRef]

220. Wei, Z.; Liang, K.; Wu, Y.; Zou, Y.; Zuo, J.; Arriagada, D.C.; Pan, Z.; Hu, G. The Effect of PH on the Adsorption of Arsenic (III) and Arsenic (V) at the TiO2 Anatase [1 0 1]. *Surface. J. Colloid Interface Sci.* **2016**, *462*, 252–259. [CrossRef]

221. Zhang, G.; Liu, Y.; Wang, J.; Li, H. Efficient Arsenic (III) Removal from Aqueous Solution by a Novel Nanostructured Iron-Copper-Manganese Trimetal Oxide. *J. Mol. Liq.* **2020**, *309*, 112993. [CrossRef]

222. Afroze, S.; Sen, T.K. A Review on Heavy Metal Ions and Dye Adsorption from Water by Agricultural Solid Waste Adsorbents. *Water Air Soil Pollut.* **2018**, *229*, 1–50. [CrossRef]

223. Fernández-López, J.A.; Angosto, J.M.; Roca, M.J.; Miñarro, M.D. Taguchi Design-Based Enhancement of Heavy Metals Bioremoval by Agroindustrial Waste Biomass from Artichoke. *Sci. Total Environ.* **2019**, *653*, 55–63. [CrossRef]

224. Rahdar, S.; Taghavi, M.; Khaksefidi, R.; Ahmadi, S. Adsorption of Arsenic (V) from Aqueous Solution Using Modified Saxaul Ash: Isotherm and Thermodynamic Study. *Appl. Water Sci.* **2019**, *9*, 1–9. [CrossRef]

225. Koohzad, E.; Jafari, D.; Esmaeili, H. Adsorption of Lead and Arsenic Ions from Aqueous Solution by Activated Carbon Prepared from Tamarix Leaves. *ChemistrySelect* **2019**, *4*, 12356–12367. [CrossRef]

226. Hua, J. Adsorption of Low-Concentration Arsenic from Water by Co-Modified Bentonite with Manganese Oxides and Poly (Dimethyldiallylammonium Chloride). *J. Environ. Chem. Eng.* **2018**, *6*, 156–168. [CrossRef]

227. Iftekhar, S.; Ramasamy, D.L.; Srivastava, V.; Asif, M.B.; Sillanpää, M. Understanding the Factors Affecting the Adsorption of Lanthanum Using Different Adsorbents: A Critical Review. *Chemosphere* **2018**, *204*, 413–430. [CrossRef]

228. Rahman, N.A.A.; Said, M.I.M.; Azman, S. Carbonized Green Mussel Shell as Heavy Metal Removal. *Malays. J. Civ. Eng.* **2017**, *29*, 56–68.

229. Hilal, N.M.; Ahmed, I.A.; El-Sayed, R.E. Activated and Nonactivated Date Pits Adsorbents for the Removal of Copper (II) and Cadmium (II) from Aqueous Solutions. *Int. Sch. Res. Not.* **2012**, *2012*, 985853. [CrossRef]

230. Seco-Reigosa, N.; Peña-Rodríguez, S.; Nóvoa-Muñoz, J.C.; Arias-Estévez, M.; Fernández-Sanjurjo, M.J.; Álvarez-Rodríguez, E.; Núñez-Delgado, A. Arsenic, Chromium and Mercury Removal Using Mussel Shell Ash or a Sludge/Ashes Waste Mixture. *Environ. Sci. Pollut. Res.* **2013**, *20*, 2670–2678. [CrossRef]

231. Mahar, F.K.; He, L.; Wei, K.; Mehdi, M.; Zhu, M.; Gu, J.; Zhang, K.; Khatri, Z.; Kim, I. Rapid Adsorption of Lead Ions Using Porous Carbon Nanofibers. *Chemosphere* **2019**, *225*, 360–367. [CrossRef]

232. Alswat, A.A.; Ahmad, M.B.; Saleh, T.A. Zeolite Modified with Copper Oxide and Iron Oxide for Lead and Arsenic Adsorption from Aqueous Solutions. *J. Water Supply Res. Technol.* **2016**, *65*, 465–479. [CrossRef]

233. Khan, M.R.; Hegde, R.A.; Shabiimam, M.A. Adsorption of Lead by Bentonite Clay. *Int. J. Sci. Res. Manag.* **2017**, *5*, 5800–5804.

234. Othmani, A.; Magdouli, S.; Kumar, P.S.; Kapoor, A.; Chellam, P.V.; Gökkuş, Ö. Agricultural Waste Materials for Adsorptive Removal of Phenols, Chromium (VI) and Cadmium (II) from Wastewater: A Review. *Environ. Res.* **2022**, *204*, 111916. [CrossRef] [PubMed]

235. Joshi, S.; Sharma, M.; Kumari, A.; Shrestha, S.; Shrestha, B. Arsenic Removal from Water by Adsorption onto Iron Oxide/Nano-Porous Carbon Magnetic Composite. *Appl. Sci.* **2019**, *9*, 3732. [CrossRef]

236. Hristovski, K.; Baumgardner, A.; Westerhoff, P. Selecting Metal Oxide Nanomaterials for Arsenic Removal in Fixed Bed Columns: From Nanopowders to Aggregated Nanoparticle Media. *J. Hazard. Mater.* **2007**, *147*, 265–274. [CrossRef]

237. Chang, Q.; Lin, W.; Ying, W. Preparation of Iron-Impregnated Granular Activated Carbon for Arsenic Removal from Drinking Water. *J. Hazard. Mater.* **2010**, *184*, 515–522. [CrossRef] [PubMed]

238. Karnib, M.; Kabbani, A.; Holail, H.; Olama, Z. Heavy Metals Removal Using Activated Carbon, Silica and Silica Activated Carbon Composite. *Energy Procedia* **2014**, *50*, 113–120. [CrossRef]

239. Mondal, R.; Mondal, S.; Kurada, K.V.; Bhattacharjee, S.; Sengupta, S.; Mondal, M.; Karmakar, S.; De, S.; Griffiths, I.M. Modelling the Transport and Adsorption Dynamics of Arsenic in a Soil Bed Filter. *Chem. Eng. Sci.* **2019**, *210*, 115205. [CrossRef]

240. Maji, S.K.; Kao, Y.-H.; Wang, Y.-B.; Liu, C.-W. Dynamic Column Adsorption of As on Iron-Oxide-Coated Natural Rock (IOCNR) and Sludge Management. *Desalin. Water Treat.* **2015**, *55*, 2171–2182. [CrossRef]

241. Rouff, A.A.; Ma, N.; Kustka, A.B. Adsorption of Arsenic with Struvite and Hydroxylapatite in Phosphate-Bearing Solutions. *Chemosphere* **2016**, *146*, 574–581. [CrossRef]

242. Sosa, A.; Armienta, M.A.; Aguayo, A.; Cruz, O. Evaluation of the Influence of Main Groundwater Ions on Arsenic Removal by Limestones through Column Experiments. *Sci. Total Environ.* **2020**, *727*, 138459. [CrossRef] [PubMed]

243. Önnby, L.; Pakade, V.; Mattiasson, B.; Kirsebom, H. Polymer Composite Adsorbents Using Particles of Molecularly Imprinted Polymers or Aluminium Oxide Nanoparticles for Treatment of Arsenic Contaminated Waters. *Water Res.* **2012**, *46*, 4111–4120. [CrossRef]

244. Shakoor, M.B.; Niazi, N.K.; Bibi, I.; Shahid, M.; Saqib, Z.A.; Nawaz, M.F.; Shaheen, S.M.; Wang, H.; Tsang, D.C.W.; Bundschuh, J. Exploring the Arsenic Removal Potential of Various Biosorbents from Water. *Environ. Int.* **2019**, *123*, 567–579. [CrossRef]

245. Pokhrel, D.; Viraraghavan, T. Arsenic Removal from an Aqueous Solution by a Modified Fungal Biomass. *Water Res.* **2006**, *40*, 549–552. [CrossRef]

246. Seki, H.; Suzuki, A.; Maruyama, H. Biosorption of Chromium (VI) and Arsenic (V) onto Methylated Yeast Biomass. *J. Colloid Interface Sci.* **2005**, *281*, 261–266. [CrossRef]

247. Ranjan, D.; Talat, M.; Hasan, S.H. Biosorption of Arsenic from Aqueous Solution Using Agricultural Residue 'Rice Polish'. *J. Hazard. Mater.* **2009**, *166*, 1050–1059. [CrossRef] [PubMed]

248. Sumaila, A.; Ndamitso, M.M.; Iyaka, Y.A.; Abdulkareem, A.S.; Tijani, J.O.; Idris, M.O. Extraction and Characterization of Chitosan from Crab Shells: Kinetic and Thermodynamic Studies of Arsenic and Copper Adsorption from Electroplating Wastewater. *Iraqi J. Sci.* **2020**, *61*, 2156–2171.

249. Bahar, M.M.; Mahbub, K.R.; Naidu, R.; Megharaj, M. As (V) Removal from Aqueous Solution Using a Low-Cost Adsorbent Coir Pith Ash: Equilibrium and Kinetic Study. *Environ. Technol. Innov.* **2018**, *9*, 198–209. [CrossRef]

250. Akpomie, K.G.; Conradie, J. Advances in Application of Cotton-Based Adsorbents for Heavy Metals Trapping, Surface Modifications and Future Perspectives. *Ecotoxicol. Environ. Saf.* **2020**, *201*, 110825. [CrossRef]

251. Alkurdi, S.S.A.; Al-Juboori, R.A.; Bundschuh, J.; Bowtell, L.; McKnight, S. Effect of Pyrolysis Conditions on Bone Char Characterization and Its Ability for Arsenic and Fluoride Removal. *Environ. Pollut.* **2020**, *262*, 114221. [CrossRef] [PubMed]

252. Dehghani, M.H.; Maroosi, M.; Heidarinejad, Z. Experimental Dataset on Adsorption of Arsenic from Aqueous Solution Using Chitosan Extracted from Shrimp Waste; Optimization by Response Surface Methodology with Central Composite Design. *Data Brief* **2018**, *20*, 1415–1421. [CrossRef]

253. Yang, J.; Liang, X.; Jiang, N.; Huang, Z.; Mou, F.; Zu, Y.; Li, Y. Adsorption Characteristics of Modified Eucalyptus Sawdust for Cadmium and Arsenic and Its Potential for Soil Remediation. *Bull. Environ. Contam. Toxicol.* **2022**, *108*, 1056–1063. [CrossRef] [PubMed]

254. Gadore, V.; Ahmaruzzaman, M. Tailored Fly Ash Materials: A Recent Progress of Their Properties and Applications for Remediation of Organic and Inorganic Contaminants from Water. *J. Water Process Eng.* **2021**, *41*, 101910. [CrossRef]

255. Li, Y.; Zhang, F.-S.; Xiu, F.-R. Arsenic (V) Removal from Aqueous System Using Adsorbent Developed from a High Iron-Containing Fly Ash. *Sci. Total Environ.* **2009**, *407*, 5780–5786. [CrossRef]

256. Shadbahr, J.; Husain, T. Affordable and Efficient Adsorbent for Arsenic Removal from Rural Water Supply Systems in Newfoundland. *Sci. Total Environ.* **2019**, *660*, 158–168. [CrossRef] [PubMed]

257. Mushtaq, F.; Zahid, M.; Bhatti, I.A.; Nasir, S.; Hussain, T. Possible Applications of Coal Fly Ash in Wastewater Treatment. *J. Environ. Manag.* **2019**, *240*, 27–46. [CrossRef] [PubMed]

258. Dwivedi, A.; Jain, M.K. Fly Ash–Waste Management and Overview: A Review. *Recent Res. Sci. Technol.* **2014**, *6*, 30–35.

259. Tiwari, M.K.; Bajpai, S.; Dewangan, U.K. Fly Ash Utilization: A Brief Review in Indian Context. *Int. Res. J. Eng. Technol.* **2016**, *3*, 949–956.

260. Ayanda, O.S.; Fatoki, O.S.; Adekola, F.A.; Ximba, B.J. Characterization of Fly Ash Generated from Matla Power Station in Mpumalanga, South Africa. *E-J. Chem.* **2012**, *9*, 1788–1795. [CrossRef]

261. Bridgeman, T.G.; Darvell, L.I.; Jones, J.M.; Williams, P.T.; Fahmi, R.; Bridgwater, A.V.; Barraclough, T.; Shield, I.; Yates, N.; Thain, S.C. Influence of Particle Size on the Analytical and Chemical Properties of Two Energy Crops. *Fuel* **2007**, *86*, 60–72. [CrossRef]

262. Masiá, A.A.T.; Buhre, B.J.P.; Gupta, R.P.; Wall, T.F. Use of TMA to Predict Deposition Behaviour of Biomass Fuels. *Fuel* **2007**, *86*, 2446–2456. [CrossRef]

263. Wiselogel, A.E.; Agblevor, F.A.; Johnson, D.K.; Deutch, S.; Fennell, J.A.; Sanderson, M.A. Compositional Changes during Storage of Large Round Switchgrass Bales. *Bioresour. Technol.* **1996**, *56*, 103–109. [CrossRef]

264. Ahmaruzzaman, M. A Review on the Utilization of Fly Ash. *Prog. Energy Combust. Sci.* **2010**, *36*, 327–363. [CrossRef]

265. Kizinievic, O.; Kizinievic, V. Utilisation of Wood Ash from Biomass for the Production of Ceramic Products. *Constr. Build. Mater.* **2016**, *127*, 264–273. [CrossRef]

266. Wang, L.; Chen, L.; Tsang, D.C.W.; Guo, B.; Yang, J.; Shen, Z.; Hou, D.; Ok, Y.S.; Poon, C.S. Biochar as Green Additives in Cement-Based Composites with Carbon Dioxide Curing. *J. Clean. Prod.* **2020**, *258*, 120678. [CrossRef]

267. Popławski, J.; Lelusz, M. Utility Assessment of Biomass Fly-Ash for Production of Concrete Products. *Tech. Trans.* **2017**, *114*, 129–142.

268. Singh, T.S.; Pant, K.K. Equilibrium, Kinetics and Thermodynamic Studies for Adsorption of As (III) on Activated Alumina. *Sep. Purif. Technol.* **2004**, *36*, 139–147. [CrossRef]

269. Ouvrard, S.; Simonnot, M.-O.; Sardin, M. Reactive Behavior of Natural Manganese Oxides toward the Adsorption of Phosphate and Arsenate. *Ind. Eng. Chem. Res.* **2002**, *41*, 2785–2791. [CrossRef]

270. Suzuki, T.M.; Bomani, J.O.; Matsunaga, H.; Yokoyama, T. Preparation of Porous Resin Loaded with Crystalline Hydrous Zirconium Oxide and Its Application to the Removal of Arsenic. React. *Funct. Polym.* **2000**, *43*, 165–172. [CrossRef]

271. Vaughan Jr, R.L.; Reed, B.E. Modeling As (V) Removal by a Iron Oxide Impregnated Activated Carbon Using the Surface Complexation Approach. *Water Res.* **2005**, *39*, 1005–1014. [CrossRef]

272. Balaji, T.; Matsunaga, H. Adsorption Characteristics of As (III) and As (V) with Titanium Dioxide Loaded Amberlite XAD-7 Resin. *Anal. Sci.* **2002**, *18*, 1345–1349. [CrossRef] [PubMed]

273. Abid, M.; Niazi, N.K.; Bibi, I.; Farooqi, A.; Ok, Y.S.; Kunhikrishnan, A.; Ali, F.; Ali, S.; Igalavithana, A.D.; Arshad, M. Arsenic (V) Biosorption by Charred Orange Peel in Aqueous Environments. *Int. J. Phytoremed.* **2016**, *18*, 442–449. [CrossRef] [PubMed]

274. Othman, N.; Abd-Kadir, A.; Zayadi, N. Waste Fish Scale as Cost Effective Adsorbent in Removing Zinc and Ferum Ion in Wastewater. *J. Eng. Appl. Sci.* **2016**, *11*, 1584–1592.

275. Onwordi, C.T.; Uche, C.C.; Ameh, A.E.; Petrik, L.F. Comparative Study of the Adsorption Capacity of Lead (II) Ions onto Bean Husk and Fish Scale from Aqueous Solution. *J. Water Reuse Desalin.* **2019**, *9*, 249–262. [CrossRef]

276. Stevens, M.G.F.; Batlokwa, B.S. Environmentally Friendly and Cheap Removal of Lead (II) and Zinc (II) from Wastewater with Fish Scales Waste Remains. *Int. J. Chem.* **2017**, *9*. [CrossRef]

277. Teixeira, E.R.; Camões, A.; Branco, F.G.; Aguiar, J.B.; Fangueiro, R. Recycling of Biomass and Coal Fly Ash as Cement Replacement Material and Its Effect on Hydration and Carbonation of Concrete. *Waste Manag.* **2019**, *94*, 39–48. [CrossRef] [PubMed]

278. Liang, G.; Li, Y.; Yang, C.; Zi, C.; Zhang, Y.; Hu, X.; Zhao, W. Production of Biosilica Nanoparticles from Biomass Power Plant Fly Ash. *Waste Manag.* **2020**, *105*, 8–17. [CrossRef]

279. Sarkkinen, M.; Kujala, K.; Kemppainen, K.; Gehör, S. Effect of Biomass Fly Ashes as Road Stabilisation Binder. *Road Mater. Pavement Des.* **2018**, *19*, 239–251. [CrossRef]

280. de Gennaro, B.; Aprea, P.; Liguori, B.; Galzerano, B.; Peluso, A.; Caputo, D. Zeolite-Rich Composite Materials for Environmental Remediation: Arsenic Removal from Water. *Appl. Sci.* **2020**, *10*, 6938. [CrossRef]

281. Pizarro, C.; Escudey, M.; Caroca, E.; Pavez, C.; Zúñiga, G.E. Evaluation of Zeolite, Nanomagnetite, and Nanomagnetite-Zeolite Composite Materials as Arsenic (V) Adsorbents in Hydroponic Tomato Cultures. *Sci. Total Environ.* **2021**, *751*, 141623. [CrossRef]

282. Zhao, P.; Jian, M.; Xu, R.; Zhang, Q.; Xiang, C.; Liu, R.; Zhang, X.; Liu, H. Removal of Arsenic (III) from Water by 2D Zeolitic Imidazolate Framework-67 Nanosheets. *Environ. Sci. Nano* **2020**, *7*, 3616–3626. [CrossRef]

283. Malwal, D.; Gopinath, P. Silica Stabilized Magnetic-Chitosan Beads for Removal of Arsenic from Water. *Colloid Interface Sci. Commun.* **2017**, *19*, 14–19. [CrossRef]

284. Yang, Z.; Yan, G.; Song, Z.; Zhang, J.; Wang, C.; Yu, Z.; Bai, Z.; Zhuang, G.; Liang, F. Study on Adsorption of as (Iii) by a New Bio-Material from Chitin Pyrolysis. *Water* **2021**, *13*, 2944. [CrossRef]

285. Tabassum, R.A.; Shahid, M.; Niazi, N.K.; Dumat, C.; Zhang, Y.; Imran, M.; Bakhat, H.F.; Hussain, I.; Khalid, S. Arsenic Removal from Aqueous Solutions and Groundwater Using Agricultural Biowastes-Derived Biosorbents and Biochar: A Column-Scale Investigation. *Int. J. Phytoremed.* **2019**, *21*, 509–518. [CrossRef]

286. Verma, L.; Siddique, M.A.; Singh, J.; Bharagava, R.N. As (III) and As (V) Removal by Using Iron Impregnated Biosorbents Derived from Waste Biomass of Citrus Limmeta (Peel and Pulp) from the Aqueous Solution and Ground Water. *J. Environ. Manag.* **2019**, *250*, 109452. [CrossRef]

287. Usman, M.; Katsoyiannis, I.; Rodrigues, J.H.; Ernst, M. Arsenate Removal from Drinking Water Using By-Products from Conventional Iron Oxyhydroxides Production as Adsorbents Coupled with Submerged Microfiltration Unit. Environ. *Sci. Pollut. Res.* **2021**, *28*, 59063–59075. [CrossRef]

288. Litter, M.I.; Ingallinella, A.M.; Olmos, V.; Savio, M.; Difeo, G.; Botto, L.; Torres, E.M.F.; Taylor, S.; Frangie, S.; Herkovits, J. Arsenic in Argentina: Technologies for Arsenic Removal from Groundwater Sources, Investment Costs and Waste Management Practices. *Sci. Total Environ.* **2019**, *690*, 778–789. [CrossRef] [PubMed]

289. Nguyen, H.T.H.; Nguyen, B.Q.; Duong, T.T.; Bui, A.T.K.; Nguyen, H.T.A.; Cao, H.T.; Mai, N.T.; Nguyen, K.M.; Pham, T.T.; Kim, K.-W. Pilot-Scale Removal of Arsenic and Heavy Metals from Mining Wastewater Using Adsorption Combined with Constructed Wetland. *Minerals* **2019**, *9*, 379. [CrossRef]

290. Driehaus, W. Arsenic Removal-Experience with the GEH®Process in Germany. Water Sci. Technol. *Water Supply* **2002**, *2*, 275–280. [CrossRef]

291. Casentini, B.; Falcione, F.T.; Amalfitano, S.; Fazi, S.; Rossetti, S. Arsenic Removal by Discontinuous ZVI Two Steps System for Drinking Water Production at Household Scale. *Water Res.* **2016**, *106*, 135–145. [CrossRef] [PubMed]

292. Sorlini, S.; Gialdini, F.; Collivignarelli, M.C. Survey on Full-Scale Drinking Water Treatment Plants for Arsenic Removal in Italy. *Water Pract. Technol.* **2014**, *9*, 42–51. [CrossRef]

293. Trois, C.; Cibati, A. South African Sands as a Low Cost Alternative Solution for Arsenic Removal from Industrial Effluents in Permeable Reactive Barriers: Column Tests. *Chem. Eng. J.* **2015**, *259*, 981–989. [CrossRef]

294. Möller, T.; Sylvester, P.; Shepard, D.; Morassi, E. Arsenic in Groundwater in New England—Point-of-Entry and Point-of-Use Treatment of Private Wells. *Desalination* **2009**, *243*, 293–304. [CrossRef]

295. Slotnick, M.J.; Meliker, J.R.; Nriagu, J.O. Effects of Time and Point-of-Use Devices on Arsenic Levels in Southeastern Michigan Drinking Water, USA. *Sci. Total Environ.* **2006**, *369*, 42–50. [CrossRef]

296. Sharma, A.K.; Sorlini, S.; Crotti, B.M.; Collivignarelli, M.C.; Tjell, J.C.; Abbà, A. Enhancing Arsenic Removal from Groundwater at Household Level with Naturally Occurring Iron. *Rev. Ambient. Água* **2016**, *11*, 486–498. [CrossRef]

297. Glade, S.; Bandaru, S.R.S.; Nahata, M.; Majmudar, J.; Gadgil, A. Adapting a Drinking Water Treatment Technology for Arsenic Removal to the Context of a Small, Low-Income California Community. *Water Res.* **2021**, *204*, 117595. [CrossRef] [PubMed]

298. Feistel, U.; Otter, P.; Kunz, S.; Grischek, T.; Feller, J. Field Tests of a Small Pilot Plant for the Removal of Arsenic in Groundwater Using Coagulation and Filtering. *J. Water Process Eng.* **2016**, *14*, 77–85. [CrossRef]

299. Bandaru, S.R.S.; van Genuchten, C.M.; Kumar, A.; Glade, S.; Hernandez, D.; Nahata, M.; Gadgil, A. Rapid and Efficient Arsenic Removal by Iron Electrocoagulation Enabled with in Situ Generation of Hydrogen Peroxide. Environ. *Sci. Technol.* **2020**, *54*, 6094–6103. [CrossRef] [PubMed]

300. Otter, P.; Malakar, P.; Jana, B.B.; Grischek, T.; Benz, F.; Goldmaier, A.; Feistel, U.; Jana, J.; Lahiri, S.; Alvarez, J.A. Arsenic Removal from Groundwater by Solar Driven Inline-Electrolytic Induced Co-Precipitation and Filtration—A Long Term Field Test Conducted in West Bengal. *Int. J. Environ. Res. Public Health* **2017**, *14*, 1167. [CrossRef]

301. Duarte, A.A.L.S.; Cardoso, S.J.A.; Alçada, A.J. Emerging and Innovative Techniques for Arsenic Removal Applied to a Small Water Supply System. *Sustainability* **2009**, *1*, 1288–1304. [CrossRef]

302. Kamde, K.; Dahake, R.; Pandey, R.A.; Bansiwal, A. Integrated Bio-Oxidation and Adsorptive Filtration Reactor for Removal of Arsenic from Wastewater. *Environ. Technol.* **2019**, *40*, 1337–1348. [CrossRef]